Analysis of the Function of NF-κB Activation *in vivo*

Inaugural-Dissertation
zur
Erlangung des Doktorgrades
der Mathematisch-Naturwissenschaftlichen Fakultät
der Universität zu Köln

vorgelegt von
Marc Schmidt-Supprian
aus Rotterdam

Köln 2002

Berichterstatter: Prof. Dr. Klaus Rajewsky

Prof. Dr. Jürgen Dohmen

Tag der mündlichen Prüfung: _____

Für Alheide und Reinhard

TABLE OF CONTENTS

1 INTRODUCTION

The immune system has evolved to protect organisms against invasion by foreign pathogens. In vertebrates immune responses are mediated by cells of the innate immune system, such as macrophages, neutrophils and dendritic cells, and by B and T cells of the adaptive immune response. Cells react to changes in their environment by production of new proteins. Changes, such as appearance of pathogens are detected at the cell membrane by specific receptors, whereas the mRNA needed for *de novo* synthesis of proteins is generated in the nucleus. Information therefore has to be transmitted from the cell membrane to the nucleus, in a process called signal transduction. Typical signal transduction pathways are initiated through cross-linking of receptors located in the cell membrane. This leads to recruitment and modification of intermediate “messengers”, mostly proteins and lipids, which transmit the signal from the receptor ultimately to transcription factors. Activated transcription factors in turn initiate transcription from promoters of their target genes, which leads to the production of new proteins to combat the pathogen.

1.1 The NF-κB Transcription Factor Family

The transcription factor family NF-κB regulates the expression of genes controlling cell survival and proliferation, immune and stress responses, and inflammatory reactions (reviewed in (Baldwin, 1996; Ghosh and Karin, 2002; Ghosh et al., 1998; Li and Verma, 2002; Silverman and Maniatis, 2001)). In mammals the NF-κB protein family contains five different Rel proteins: p65/RelA, c-Rel/Rel, RelB, p50/NF-κB1 and p52/NF-κB2; the latter two are generated through proteolytic processing of their respective precursor molecules p105 (p50) and p100 (p52). Rel proteins form various hetero- or homodimeric complexes, which in most resting cells are kept inactive sequestered to the ankyrin repeats of inhibitory molecules termed IκBs (Ghosh et al., 1998) (Figure 1). The precursors of NF-κB1 and NF-κB2 also contain ankyrin repeats and therefore can act as inhibitors of Rel proteins (Solan et al., 2002). Upon exposure to a wide variety of stimuli including proinflammatory cytokines (such as TNF and IL-1), bacterial lipopolysaccharide (LPS) and viral infection, IκB proteins are phosphorylated on two conserved serine residues. This triggers subsequent

ubiquitination and proteasomal degradation of the IκBs (reviewed in (Karin and Ben-Neriah, 2000; Verma et al., 1995)). Degradation of IκB releases NF-κB dimers, which then accumulate in the nucleus where they activate transcription of NF-κB target genes, including genes encoding proinflammatory cytokines and chemokines, cell-adhesion molecules and anti-apoptotic proteins (Karin and Ben-Neriah, 2000) (Figure 1). Recent studies show, however, that after liberation from IκB NF-κB/Rel proteins have to undergo several modifications such as phosphorylation and acetylation in order to activate transcription (Ghosh and Karin, 2002). Deficiency for the enzyme glycogen-synthase 3β (GSK-3β) in mice leads to a defect in NF-κB-dependent gene transcription despite normal induction of NF-κB DNA-binding (Hoeflich et al., 2000). It seems therefore that NF-κB activation is regulated by GSK-3β at the level of the transcriptional complex, most likely through the phosphorylation of RelA (Schwabe and Brenner, 2002). Other kinases, such as PI3-K (Sizemore et al., 1999), TBK (T2K) (Bonnard et al., 2000), ζPKC (Leitges et al., 2001) and PKA (Zhong et al., 1998) have also been implicated in the transactivation of Rel subunits by phosphorylation (Figure 1).

1.2 The IκB Kinase Complex

Induced phosphorylation of IκB is mediated by the IκB-kinase (IKK) signalsome, a high molecular weight kinase complex (700 – 900 kD) that contains two catalytic subunits named IKK1and IKK2 (or IKKα and IKKβ) (reviewed in (Israel, 2000; Karin, 1999)) and a regulatory subunit termed NEMO, IKKγ or IKKAP (Mercurio et al., 1999; Rothwarf et al., 1998; Yamaoka et al., 1998) (Figure 1). The exact stochiometry of the components of the IKK complex is still unknown and might vary between different cell-types and depend on the activation status of the cell. IκB-kinase activity is also found in lysates from activated cells in form of a complex with an apparent molecular weight of 300 kD. This complex corresponds to dimers of IKK1 and 2, making it reasonable to assume that the predominant 700 – 900 kD IKK complex consists of a dimer of IKK1/2 dimers brought together by several NEMO-proteins. It has been shown, however, that IKK1 and 2 are also active as homodimers (Rothwarf et al., 1998). IKK1 and IKK2 are highly homologous kinases, consisting of an N-terminal kinase domain, a helix-loop-helix (HLH) and a leucine zipper (LZ). The kinase

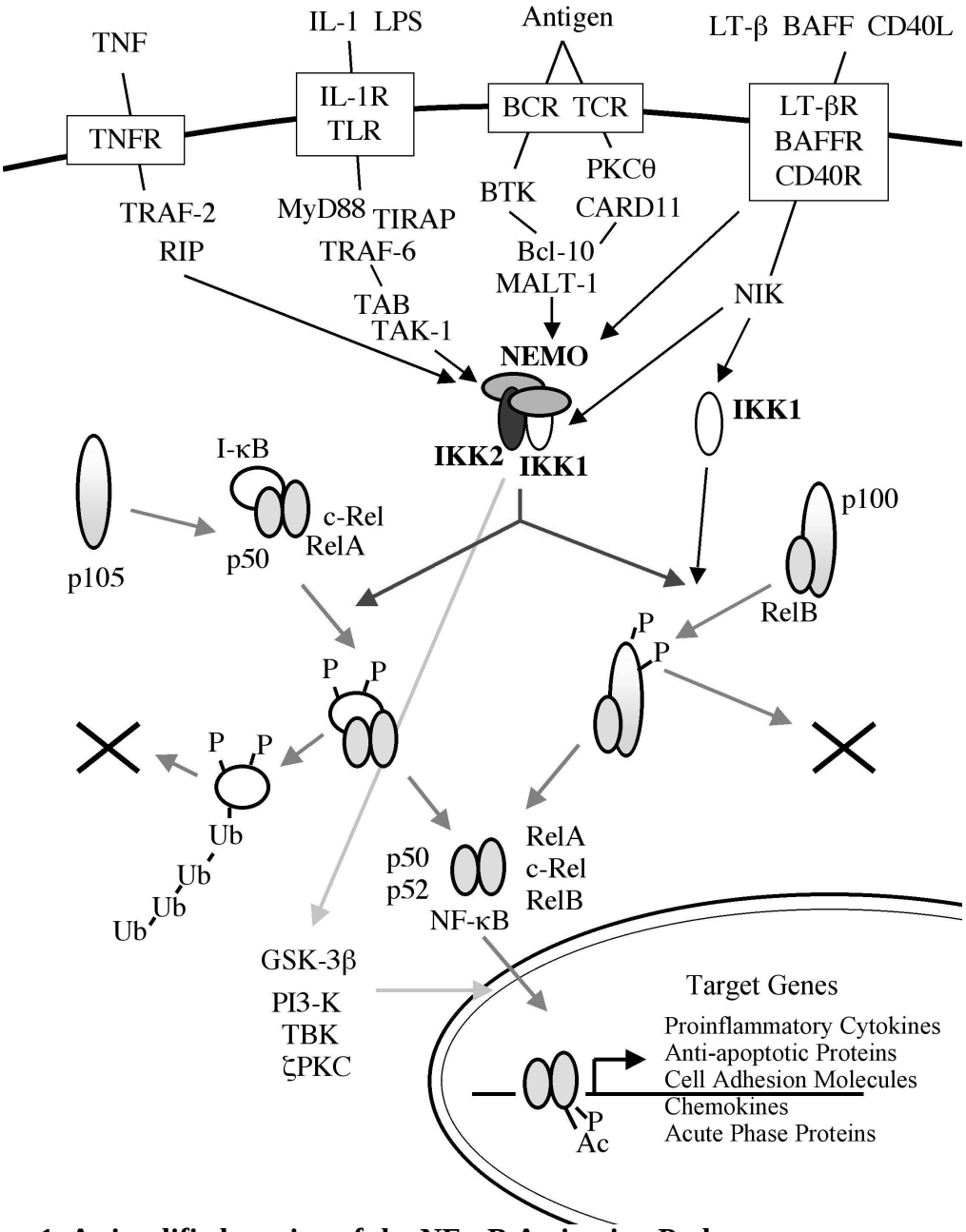

Figure 1. A simplified version of the NF-κB Activation Pathway

Proteins are depicted by name and by oval symbols. Receptors are symbolized by boxed names. Activation processes are indicated by arrows. X stands for degradation by the 26 S proteosome, P for phosphogroups and Ac for acetylated amino acid residues. This scheme was composed based on information from: Karin and Ben-Neriah, 2000; Gosh and Karin, 2002; Li and Verma 2002; Dixit and Mak, 2002.

domains are similar to those of other known serine-threonine kinases and contain an activation loop. In cells stimulated with TNF or IL-1 two serines within this activation loop become phosphorylated, causing a confirmational change that results in kinase activation. Replacement of serines 177 and 181 in the activation loop of IKK2 with alanins prevents activation of IKK, whereas their replacment with glutamic acid (which mimicks phosphoserine) results in constitutive IKK activity (Rothwarf et al., 1998). NEMO was cloned independently by genetic complementation of cell lines, which do not respond to NF-κB activating stimuli (Yamaoka et al., 1998) and as a component of the purified IKK complex (Mercurio et al., 1999; Rothwarf et al., 1998). It is a 48 kDa glutamine-rich protein without apparent catalytic activity, which contains a LZ domain**,** extended coiled-coil motifs and a putative zinc finger motif.

Recent reports on knockout mice revealed different physiological roles for IKK1 and IKK2. IKK1-deficient mice die shortly after birth showing skeletal abnormalities and a thickened hyperproliferative epidermis (Hu et al., 1999; Li et al., 1999a; Takeda et al., 1999). Lack of differentiation and increased proliferation of *ikk1*$^{-/-}$ keratinocytes occurs independently of IκB kinase function and NF-κB activation. IKK1 seems to be essential for the secretion of an as yet unidentified secreted differentiation factor, termed kDIF (Hu et al., 2001). Mice containing a kinase-inactive version of IKK1 (IKK1^{SA}) are born at normal mendalian ratios and develop normally. IKK1^{SA} female mice exhibit defective development of the mammary gland during pregnancy due to lack of expression of the NF-κB-dependent gene cyclin D1 (Cao et al., 2001). Stimulation of *ikk1*$^{-/-}$ mouse embryonic fibroblasts (MEFs) and thymocytes by either TNF or IL-1 leads to essentially normal NF-κB activation, indicating that IKK1 is dispensable for induction of IκB degradation in response to proinflammatory cytokines (Hu et al., 1999; Li et al., 1999a; Takeda et al., 1999). IKK1 is, however, critical for the generation of p52 from its precursor p100 (Senftleben et al., 2001a) in response to inducers such as BAFF (Claudio et al., 2002), LTβ (Dejardin et al., 2002) or CD40 (Coope et al., 2002). Since p100 associates preferentially - but not exclusively - with RelB (Solan et al., 2002) this pathway mainly induces p52/RelB dimers (Fig 1). In mammary epithelium IKK1 is also responsible for IκB degradation and induction of NF-κB in response to specific signals, such as RANKL (Cao et al., 2001). Recently it has been found activation of NF-κB can occur independently of NEMO; BAFF induces processing of p100 to p52 in a NEMO-deficient B cell line (Claudio et al., 2002) and

LT-beta induces DNA-binding p50 and RelB subunits in the absence of NEMO (Saitoh et al., 2002).

IKK2 knockout mice die between embryonic days 12.5-14.5 from massive liver degeneration due to TNF-induced hepatocyte apoptosis (Li et al., 1999b; Li et al., 1999c; Tanaka et al., 1999), a phenotype similar to that of p65/RelA knockout mice that die between embryonic days 14.5-15.5 (Beg et al., 1995). NF-κB activation upon stimulation with TNF or IL-1 is severely impaired in *ikk2*$^{-/-}$ MEFs, suggesting that IKK2 is the kinase responsible for NF-κB activation by inflammatory cytokines. IKK2-knockout mice are viable on a TNFR1-/- background, but the mice still succumb to opportunistic infections within two to three weeks of birth (Senftleben et al., 2001b).

IKK1 and 2 are required for optimal induction of NF-κB-induced transcription, since both kinases are involved in phosphorylation of the transactivation domain of the p65 subunit of NF-κB in response to IL-1 and TNF (Sizemore et al., 2002). In addition both kinases are required for transcription of the majority of NF-κB-dependent genes activated by these stimuli (Li et al., 2002).

NEMO is essential for NF-κB activation (Rothwarf et al., 1998; Yamaoka et al., 1998), however, its exact role in the function of the IKK complex remains obscure. Oligomerization of NEMO is essential for IKK activity (Agou et al., 2002; Li et al., 2001; Poyet et al., 2000) and numerous studies suggest that NEMO acts by connecting the IKK to upstream activators (Cooke et al., 2001; Huang et al., 2002; Jain et al., 2001). The human and mouse genes coding for NEMO are located on the X chromosome, arranged head to head with the proximal glucose-6-phosphate dehydrogenase housekeeping gene (G6PD) (Galgoczy et al., 2001; Jin and Jeang, 1999). Three alternative transcripts with different non-coding 5' exons have been described. A CpG island, which has been described as essential for the ubiquitous expression of *g6pd* (Toniolo et al., 1991), also drives expression of the *Nemo* gene. Remarkably, the genes overlap in their 5' non-coding regions. An alternative Nemo-promoter has been identified in intron 2 of *g6pd*. This promoter shows very low basal activity and may be involved in stress/time- and/or tissue-dependent expression of NEMO (Galgoczy et al., 2001).

1.3 Incontinentia Pigmenti

Recently, genetic studies revealed that mutations in the human *NEMO* gene are the cause of Incontinentia Pigmenti (IP) or Bloch-Sulzberger Syndrome (Smahi et al., 2000). IP is an X-linked dominant, male-lethal genetic disorder characterized by unusual patterns of skin pigmentation (Landy and Donnai, 1993). The skin lesions seen in IP evolve through characteristic stages, which frequently overlap or appear together. Affected females show an erythematous, vesicular rash that appears shortly after birth and is accompanied by massive eosinophilic granulocyte infiltration into the epidermis. Subsequently verrucous hyperkeratotic lesions evolve that disappear over time, leaving behind areas of hyperpigmentation in a pattern that respects the lines of Blashko (Happle, 1985; Landy and Donnai, 1993). In the final stage this hyperpigmentation fades, and pale hairless patches or streaks remain on the skin (Landy and Donnai, 1993). Another consistent feature of IP is non-random X-inactivation in peripheral blood leukocytes (PBL). IP patients show completely skewed patterns of X-inactivation in PBL, suggesting that cells expressing the mutated X-chromosome are counter-selected (Parrish et al., 1996). Other manifestations of IP include abnormalities of the teeth, eyes, hair and the central nervous system (Carney, 1976; Landy and Donnai, 1993).

1.4 The Role of the IKK Complex and NF-κB in B Cells

Activated NF-κB/Rel proteins are involved in important and diverse functions of B cells, such as proliferation, isotype switching and cytokine production (Gerondakis et al., 1998; Grossmann et al., 1999; Gugasyan et al., 2000). NF-κB is constitutively active in mature B cells indicating that this signaling pathway could be important for B cell maintenance. Indeed, early studies employing gene targeting technology showed that mice deficient for more than one of the NF-κB subunits have defects in B cell development. Adoptive transfer experiments using fetal liver cells of p50/RelA double knockout mice resulted in absence of B lymphopoiesis. However, when p50-/-RelA-/- fetal liver cells were mixed with wild-type bone marrow cells they gave rise to mature B cells in the spleen, demonstrating that this phenotype is non-cell autonomous (Horwitz et al., 1997). More detailed studies using similar adoptive transfer experiments of mixed fetal liver cells showed that p50-/- or p50-/-RelA-/- B cells

cannot develop into marginal zone (MZ) B cells (Cariappa et al., 2000). Similarly RelA-/-c-Rel-/- fetal liver cells fail to give rise to $IgM^{low}IgD^{+}$ mature B cells. RelA-/-c-Rel-/- immature (IM) B cells undergo accelerated cell death in culture and express abnormally low levels of Bcl-2. It remains unclear, however, whether the block in B cell development in RelA-/-c-Rel-/- mice is due to a cell-autonomous effect or not (Grossmann et al., 2000). In p50/p52 double knockout mice B cell development is blocked at the immature stage, at the T1 - T2 transition (Figure 12), shortly after B cells exit from the BM (Franzoso et al., 1997). Mice deficient for B cell-activating factor (BAFF), a B cell survival factor expressed on myeoid cells, have an arrest in B cell development at the same stage as p50/p52 double knockout mice. Subsequently it was shown that BAFF induces processing of p100 to p52 via one of its receptors on B cells, BAFFR, and NIK, but independently of NEMO (Claudio et al., 2002). B cell specific inhibition of NF-κB activity by transgenic expression of a trans-dominant form of IκB-α leads to a reduction of mature splenic B cells and recirculating $B220^{high}IgM^{+}$ bone marrow cells (Bendall et al., 1999). Mice deficient for p50 have normal numbers of follicular (FO) B cells (Cariappa et al., 2000). It has been shown, however, that the *in vivo* turnover of p50-/- B cells is increased compared to WT B cells (Grumont et al., 1998; Pohl et al., 2002). Whether this is due to a defect intrinsic to the B cell lineage or to a defect in other cell-types is not clear. *Ex vivo* isolated p50-deficient B cells die faster than wild-type B cells, indicating that p50 could play a role in mature B cell survival. A direct analysis of whether mature B cells, once generated, depend on NF-κB mediated survival signals in a cell-autonomous fashion *in vivo*, has not been performed so far.

Most signals that activate NF-κB converge at the IKK complex. It has been shown that B cells lacking IKK1 activity are short-lived and have a reduced capacity to proliferate. Very few IKK1-deficient B cells develop into $IgD^{+}IgM^{low}$ mature B cells in the spleen (Kaisho et al., 2001; Senftleben et al., 2001a). It is controversial whether there is an overall reduction of NF-κB binding activity in IKK1-deficient B cells (Kaisho et al., 2001) or whether the maturation defect is solely due to lack of processing of p100 to p52(Senftleben et al., 2001a). Together with data from BAFF-deficient and p50/p52-double knockout mice it seems plausible that the B cell defect in *Ikk1-/-* radiation chimeras is due to lack of BAFF-induced processing of p100 via NIK and IKK1. *Ikk2-/-* radiation chimeras lack peripheral blood B cells (Senftleben et al., 2001b), similarly

to the p50/p65 double knockout radiation chimeras (Horwitz et al., 1997), but it is not clear yet whether the inability of IKK2-deficient fetal liver cells to give rise to B cells is a B cell-autonomous phenomenon or not. In transgenic mice expressing a dominant-negative version of IKK2 specifically in B cells, B cells develop normally but show defects in proliferation and antibody responses (Ren et al., 2002b).

Thus, whereas IKK1 is important for the generation of mature B cells, the role of IKK2 is controversial and little is known about the importance of NEMO in B cell development. Whether activation of NF-κB through IKK is also essential for maintenance of mature B cells remains unresolved.

1.5 The Role of the IKK Complex and NF-κB in T Cells

To address the role of NF-κB in T cells initial studies have employed either targeted disruption of one or two of the Rel subunits or T cell lineage-specific transgenic expression of various non-degradable IκBα mutants (termed superrepressors or IκBαDN). Transgenic expression of IκBαDN (Boothby et al., 1997; Ferreira et al., 1999) or of mIκBβ (Attar et al., 1998) directed by the lck-promoter, of IκBαDN directed by the CD2-promoter (Hettmann et al., 1999), or of human IκBα under control of a β-globin promoter/CD2 enhancer contruct (Esslinger et al., 1998; Esslinger et al., 1997) led to a reduction of peripheral T cells to varying degrees, probably reflecting differences in promoter strength and specificity and of the IκB repressor used. One common feature of these mice is that CD8 cells are more diminished then CD4 cells. The remaining T cells in these different mice have defects in proliferative responses, in IL-4, IL-10 and INFγ secretion (Aune et al., 1999; Ferreira et al., 1999) and they are more susceptible to Fas - and activation-induced apoptosis *in vitro* (Aune et al., 1999; Boothby et al., 1997; Ferreira et al., 1999). Treatment of quiescent human blood lymphocytes with pharmacological NF-κB inhibitors *in vitro* induced slow T cell apoptosis associated with a gradual downregulation of Bcl-2 (Bureau et al., 2002).

Studies using knockout mice revealed the roles of individual Rel proteins in T cell activation (reviewed in (Caamano and Hunter, 2002; Denk et al., 2000)). p50-/-p52-/- double knockout mice lack mature T cells and radiation chimeras reconstituted with p50-/-RelA-/- fetal liver cells show complete absence of lymphopoiesis. In both cases, however, adoptive transfer experiments showed that these defects are not cell-

autonomous but rather track with cells outside the T lineage (Franzoso et al., 1997; Horwitz et al., 1997). Analysis of mice engrafted with c-Rel/RelA double knockout fetal liver cells showed a deficit of peripheral T cells, which could not be rescued by the enforced expression of the survival factor bcl-2 (Grossmann et al., 2000). It is not clear, however, whether the defect seen in c-Rel-/-RelA-/- fetal liver chimeras is based on a T cell-autonomous requirement for NF-κB or not. These studies demonstrate that interference with NF-κB activation in various ways leads to diminished mature T cell populations with impaired functions. They also show, however, that peripheral T cells with impaired NF-κB function can be generated and sustained *in vivo*.

Mice lacking RelA or IKK2 die early in embryogenesis displaying dramatic TNF-induced destruction of the liver (Beg et al., 1995; Li et al., 1999b; Li et al., 1999c; Tanaka et al., 1999). Similarly to p50-/-RelA-/- fetal liver cells also IKK2-deficient fetal liver cells failed to reconstitute mature T cells in irradiated hosts. Also in this case co-transfer experiments showed that the defect is not due to a cell-autonomous requirement of IKK2 in T cells. In addition, IKK2-/-TNFR-/- double knockout mice, which are viable and reach 3-4 weeks of age, show nearly normal thymocyte development leading to the suggestion that defective T cell development in chimeras reconstituted with IKK2-deficient fetal liver is caused by TNF induced killing of thymocytes (Senftleben et al., 2001a). Adoptive transfer experiments showed that peripheral T cells develop in the absence of IKK1 (Kaisho et al., 2001; Senftleben et al., 2001a). Transgenic expression of dominant-negative versions of IKK1 or IKK2 under the control of the human CD2 promoter did not interfere with the development of splenic CD4 and CD8 T cells. Even co-expression of dominant-negative IKK1 and 2 had no overall effect on T cell development (Ren et al., 2002a).

Thus lack of either IKK1 or IKK2 in T cells does not interfere with the generation of mature T cells; nor does simultaneous dominant-negative interference with IKK1 and 2 signaling. These data suggest that the IKK does not play an important role in T cell development. Mice in which NF-κB activation is inhibited by transgenic expression of non-degradable IκB proteins have reduced T cell numbers. This suggests that either NF-κB activation can occur in absence of IKK signaling in T cells or that IKK1 and 2 can compensate for the lack of the other.

1.6 Objectives

When I started this project IKK1, 2 and NEMO had just been cloned and nothing was known about their roles *in vivo*. In view of the high overall redundancy in the NF-κB signaling pathway, the inactivation of the *Nemo* gene appeared to me as uniquely suited to completely block NF-κB activation by a single gene knockout. RelA knockout mice die around embryonic day 15 due to extensive liver degeneration and it seemed possible that NEMO knockout mice would have a similar phenotype. The assessment of the role of genes in tissues of adult mice is impossible in knockout mice with early embryonic lethality. I opted to circumvent this problem by using the approach of conditional gene targeting, which allows the deletion of genes in specific cell types of the adult mouse (Rajewsky et al., 1996). Therefore I decided to generate a conditional *nemo* allele ($nemo^{FL}$) in order to analyze the role of NEMO and NF-κB in mouse development and immune cells. The complete blockade of NF-κB signaling by removal of NEMO was to be compared to the lack of IKK2 activity, through side by side comparison of the newly generated $nemo^{FL}$ mice with available IKK2 conditional mouse strains.

2 MATERIALS AND METHODS

2.1 Molecular Biology Methods

Common methods of molecular biology were performed according to standard protocols (Sambrook et al., 1989). Enzymes were obtained from the following companies: Boehringer Mannheim (Mannheim), GIBCO-BRL (Gaithersburg, USA), NEB (Beverly, USA), Stratagene (USA), Takara (Japan) and USB (Cleveland, USA). Size markers for agarose gel electrophoresis were obtained from GIBCO-BRL (1 kb marker, l-HindIII marker).

2.1.1 Competent Cells and Isolation of Plasmid DNA

Competent *Escherichia coli* DH5α cells were prepared according to the protocol of Inoue et al. (Inoue et al., 1990) and used in heat shock transformations of plasmid DNA. Rapid DNA ligation was performed with the Takara DNA Ligation Kit (Takara, Japan) according to the manufacturers instructions.

Plasmid DNA was isolated from transformed *Escherichia coli* DH5α bacteria with an alkaline lysis method (Birnboim, 1983). The procedure was according to the protocol of (Zhou et al., 1990). Plasmid DNA of a higher purity was obtained with QIAGEN columns (QIAGEN, Hilden) following the supplier's instructions.

2.1.2 Isolation of Genomic DNA from ES Cells and Mouse Organs

Cells were lysed over night at 37°C in lysis buffer (10 mM Tris-HCl, pH 8; 10 mM EDTA; 150 mM NaCl; 0.2% SDS; 400 mg/ml *Proteinase K*). Subsequently, DNA was precipitated from the solution by the addition of an equal volume of Isopropanol. The DNA was pelleted by centrifugation, washed in 70% EtOH and resuspended in TE-buffer (10 mM Tris-HCl, pH 8; 1 mM EDTA). From ES cell clones, that were grown in 96-well tissue culture dishes, DNA was extracted and prepared according to the protocol of (Pasparakis and Kollias, 1995).

Mouse tissue was incubated for 5 h to o/n at 56°C in lysis buffer (0.1 M Tris-HCl, pH 8.5; 5 mM EDTA; 0.2% SDS; 0.2 M NaCl; 600 mg/ml *Proteinase K*). Undissolved debris was

pelleted and the supernatant was mixed with an equal volume of isopropanol to precipitate the DNA. The DNA was washed in 70% EtOH, dried and resuspended in ddH_2O.

2.1.3 Agarose Gel Electrophoresis and DNA Gel Extraction

Separation of DNA fragments by size was achieved by electrophoresis in agarose gels (0.7% - 2.5%; 1 x TAE (Sambrook et al., 1989); 0.5 mg/ml ethidiumbromide). DNA fragments were recovered from agarose gel slices with either the QIAEX II or the QIAquick Gel Extraction Kit (QIAGEN, Hilden) following the manufacturer's protocols.

2.1.4 DNA Sequencing

DNA fragments were sequenced with the 'Taq DyeDeoxyTerminator Cycle Sequencing Kit' (Applied Biosystems), which is a PCR-based modification of the Sanger et al. (Sanger et al., 1977) protocol. The fluorescently labelled DNA pieces were separated and analysed with ABI373A and ABI377 systems (Applied Biosystems) with the help of S. Wilms. Sequencing of the murine *Nemo* locus was in part performed by Exelixis.

2.1.5 Quantitation of DNA

The concentration of nucleic acids was determined by measuring the absorption of the sample at 260 nm and 280 nm in a spectrophotometer (Pharmacia). An OD_{260} of 1 corresponds to approximately 50 µg/ml for double stranded DNA or 40 µg/ml for RNA and single stranded DNA. Purity of nucleic acids can be estimated by the ratio OD_{260}/OD_{280}, pure preparations of DNA and RNA show a ratio of 1.8 and 2.0, respectively. Alternatively, the DNA sample was electrophoresed in an agarose gel, and the concentration was estimated from the band intensity in comparison with a standard.

2.1.6 Polymerase Chain Reaction (PCR)

PCR (Mullis and Faloona, 1987; Saiki et al., 1985) was used to screen mice and ES cells for the presence of targeted alleles or transgenes and to amplify fragments for sequencing. Reactions were performed either in Hybaid machines (MWG-Biotech) or Trio-thermocyclers (Biometra).

Name	Sequence (5'-3')	$T_{Ann.}$ [°C]	Location	Direction
27	GCCTTGGTGCTCCCTAACTCT	62	*Nemo* intron2	sense
39	GATTCGCAGCGCATCGCCTT	62	neo^r	anti-sense
40	TCACATCACATCGTTATCCTT	62	*Nemo* intron2	anti-sense
61	ATGAACAAGCACCCCTGGAAG	62	*Nemo* exon1	sense
MP65	GTTCAGAGGTTCAGTCCATTATC	60	*Ikk2* intron 5	sense
MP45	TAGCCTGCAAGAGACAATACG	60	*Ikk2* exon 6	anti-sense
MP49	TCCTCTCCTCGTCATCCTTCG	60	*Ikk2* intron 6	anti-sense
M35	GACAAGCGTTAGTAGGCACAT	60	Flpe6	sense
M36	GAGAAGAACGGCATAGTGCGT	60	Flpe6	anti-sense
Cre1	CATCGCCATCTTCCAGCAG	62	Cre	sense
Cre2	CAATTTACTGACCGTACAC	62	Cre	anti-sense
Cre8	CCCAGAAATGCCAGATTACG	60	Cre	sense
CD19c	AACCAGTCAACACCCTTCC	60	neo^r	anti-sense

Table 1. List of primers routinely used for typing
The sequences are shown from 5' to 3'. Direction is designated "sense", if the primer orientation coincides with the transcriptional orientation of the adjacent gene, and "anti-sense" otherwise.

Genotyping of mice and ES cells was generally performed in a total volume of 30 ml according to the following reaction mix: 25 pMol of each primer, 1.6 U of *Thermus aquaticus* (*Taq*) DNA polymerase (GIBCO-BRL), 250 mM dNTPs (Pharmacia), 10 mM Tris-HCl pH 8.3, 50 mM KCl, 2.5 mM $MgCl_2$, 100 ng template DNA. Amplification started with denaturation for 3 min at 94 °C followed by 30-35 cycles of 94 °C for 30 sec, 59-62 °C for 30 sec and 72 °C for 30 sec. A final extension step was performed at 72 °C for 5 min.

Primers	Mouse Strain	Allele	Product [Bp]
27, 39, 40, 61	*Nemo*-conditional	WT	432
		FN	657
		F	577
		D	842
		DN	922
M35, M36	Flpe6	Flpe	647
MP65, MP45, MP49	*Ikk2*-conditional	WT	436
		FL	533
		D	652
Cre1,Cre2	All Cre lines	Cre	1000
Cre8, Cre19c	CD19-Cre	CD19-Cre	525

Table 2. Mouse typing by PCR

Since *Pfu* DNA polymerase (Stratagene) has a 12-fold higher fidelity than *Taq* DNA polymerase, it was used for amplification of fragments for sequencing. PCR of transgenic Cre lines was performed as published.

2.1.6 Southern Blot Analysis

5-15 µg DNA were digested o/n with 50 to 100 U of the appropriate restriction enzyme. Subsequently, the DNA fragments were resolved by agarose gel electrophoresis and transferrred onto Hybond^{TM}-N+ (Amersham) or GeneScreenPlus (Dupont) nylon membranes by an alkaline capillary transfer according to the method of (Chomczynski and Qasba, 1984). Membranes were baked at 80°C for 2 hours to fix the DNA, equilibrated in 2x SSC (Sambrook et al., 1989) and then prehybridized o/n in hybridization solution (1M NaCl, 1% SDS, 10% dextran sulfate, 50 mM Tris-HCl pH 7.5, 500 µg/ml sonicated salmonsperm DNA) at 65 °C. Afterwards, the radioactively labelled probe was added to the hybridization solution and allowed to hybridize for 10 h at 65 °C in a rotating cylinder (Hybaid).

The following probes were used:

Nemo 5' external probe (probe A): A 480 Bp fragment, excised with AccI and XmnI from DNA2 (Schmidt-Supprian et al., 2000). DNA2 contains a cloned BamHI fragment of the *Nemo* genomic locus, the AccI-XmnI 480 Bp fragment is located before exon 1 of the *Nemo* gene.

Nemo 3' external probe: A 429 Bp fragment, excised with SpHI and EcoRI from DNA1 (Schmidt-Supprian et al., 2000). DNA6 contains a cloned BamHI fragment of the *Nemo* genomic locus, the SpHI-EcoRI 429 Bp fragment is located in intron 5 of the *Nemo* gene.

Nemo internal probe (probe B): A 597 Bp fragment, excised with SpHI and EcoRI from DNA2 (Schmidt-Supprian et al., 2000). DNA2 contains a cloned BamHI fragment of the *Nemo* genomic locus, the SpHI-EcoRI 597 Bp fragment is located in intron 2 of the *Nemo* gene.

Ikk2 internal probe: A BglII-StuI fragment (Pasparakis et al., 2002a).

neo^{r} probe: A fragment of 600 Bp, excised as a PstI – BamHI fragment from pMMneoflox8 (Kraus, 2001).

25 to 60 ng of sample DNA were radioactively labeled with 2.5 mC [$^{\alpha 32}$P]dATP (Amersham, Braunschweig) using the Ladderman^{TM} Labeling Kit (Takara, Japan) that is based on the principle of random primed oligolabeling (Feinberg and Vogelstein, 1984). Unincorporated radiolabeled nucleotides were removed with MicroSpinTM S-200HR columns to reduce background during hybridization (Pharmacia). The probe was denatured for 5 min in a boiling waterbath before it was added to the hybridization solution. After hybridization stringency washes were initially performed twice in 1 x SSC/0.1 % SDS and then followed by washes in 0.5 x SSC/0.1 % SDS and 0.25 x SSC/0.1 % SDS, if necessary. All washes were at 65 °C under gentle agitation for 15 min to 1 hour. After each wash the filter was monitored with a Geiger-counter. The washes were stopped when specific signals of 20 to 100 cps were detectable. Then, the filter was sealed in a plastic bag and exposed to X-ray film (Kodak XAR-5 or BioMAX MR; Eastman Kodak) at –70 °C. Film was developed in an automatic developer (Agfa). Alternatively, the filter was exposed at

RT to a phosphoimager screen (Fuji) that was analyzed on a Bio-Imaging Analyser (Fuji Bas 1000; Fuji, Japan).

2.2 Cell Biology Methods

2.2.1 Embryonic Stem Cell Culture

The conditional allele *nemo*^{FL} was generated with Bruce-4 ES cells (Kontgen et al., 1993) Culturing and transfection of ES cells was performed according to published protocols (Pasparakis and Kollias, 1995; Torres and Kuehn, 1997). To maintain the pluripotency of the ES cells, they were cultured in the presence of LIF containing ES cell medium on a layer of embryonic feeder (EF) cells. The ES cell medium (DMEM, 15 % FCS, 1 mM sodium pyruvate, 2 mM L-glutamine, 1 x non essential amino acids, 1:1000 diluted LIF supernatant, 0.1 mM 2-β-mercaptoethanol) contained FCS from a batch that had been tested to promote ES cell growth and hinder *in vitro* differentiation. ES and EF cells were grown in tissue culture dishes (Falcon, Greiner) and kept at 37°C in a humid atmosphere with 7.5% CO2. EF cells (EF medium: DMEM, 10% FCS, 1 mM sodium pyruvate, 2 mM L-glutamine) were never passaged more than three times and mitotically inactivated by mitomycin-C treatment (10 µg/ml for 2 h), prior to seeding with ES cells. ES cell colony growth was stopped before they became confluent. Colonies were washed once with PBS and then treated shortly with trypsin (0.05 % trypsin, 0.02 % EDTA in PBS; GIBCO-BRL) at 37°C until the cells detached from the dish. Optimal conditions for trypsinization of Bruce-4 cells were achieved by supplementing the solution with 1% chicken serum. The cell suspension was then used for passaging, transfection or freezing. ES cells were frozen in ES cell medium containing 10 % DMSO at –80°C and later transferred into liquid nitrogen for long term storage. For transfection, 0.6 - 1 x 10^7 ES cells were mixed with 30 to 40 µg of DNA in 1 ml transfection buffer (20 mM HEPES, pH7; 137 mM NaCl; 5 mM KCl; 0.7 mM Na_2HPO_4; 6 mM Glucose; 0.1 mM 2-β-ME) and electroporated at RT (480 mF, 230-240V). Subsequently, the ES cells were transferred onto an embryonic feeder layer and 48 hours later placed under G418 selection (300 µg/ml, 50% active). Selection against HSV-*tk* containing random integrants started at day five after transfection by supplementing the medium with 2 mM gancyclovir (Cymeven, Syntex). At around day 10

of the transfection, double resistant colonies were picked and split into EF-containing 96-well tissue culture dishes for expansion.

Specific deletion of the *loxP* flanked exon II of the *Nemo* gene and the FRT flanked *neo*^{r} selection marker cassette from targeted ES cells was achieved in a transient transfection with 30 µg of supercoiled plasmids: either pCMV-Flpe6 (Buchholz et al., 1998) and pPGK-Puro, or pCMV-Flpe6, pPGK-Cre (K. Fellenberg, unpublised) and pPGK-Puro (pFlep6, pPGK-Cre and pPgk-Puro in a ratio of 1:1:10). The conditions of the transfection were as described above. Two days after the transfection the ES cells were split and replated at a density of 2 x 10^3 cells per 10 cm tissue culture dish. Within the next seven to ten days colonies were allowed to grow up, before they were picked, trypsinized and split into a master and a duplicate 96-well plate. Cells in the duplicate plate were placed under G418 selection (700 µg/ml, 50% active) such that G418 sensitive clones were detectable by cell death. The sensitive clones were then recovered and expanded from the master plate.

2.2.2 Preparation of Cell Suspensions from Lymphoid Organs

Ex vivo isolated cells were resuspended in medium (DMEM, 5% FCS, 2 mM L-glutamine) and kept on ice. Thymus, spleen and lymph nodes were squashed between two frosted sides of a microscope slide to obtain single cell suspensions. Bones were flushed with medium to extract bone marrow cells and the peritoneal cavity was flushed with 10 ml of medium to recover cells. Erythrocytes were lysed from spleen and bone marrow preparations by incubation in lysis buffer for 2 min on ice (140 mM NH_4Cl, 17 mM Tris-HCl pH7.65). Blood from the tail vain was collected in a tube with heparin (Liquemin, Roche) and then layered on top of 7% Ficoll 400 (Pharmacia, Sweden). After centrifugation at RT with 1350 g for 15 min., lymphocytes were recovered from the interphase of the gradient.

2.2.3 Flow Cytometry

Cells (in general: 10^6 per sample) were surface stained in 30 ml PBS, 1 % BSA, 0.01 % N_3 with combinations of fluorescein isothiocyanate (FITC), phycoerythrin (PE), Cy-Chrome™ (Cyc), PERCP and/or APC conjugated mAbs for 20 min on ice. Stainings with biotinylated mAbs were followed by a second staining with either Streptavidin-Cy-Chrome™ (Pharmingen) or Streptavidin-PERCP (Becton Dickinson). After staining the samples were washed and resuspended with PBS-BSA-N_3. Stained cells were acquired on a FACScan or FACSCalibur and data were analysed using CellQuest software (Becton Dickinson). Dead cells were labelled with propidium iodide or Topro-3 and excluded from the analysis. Monoclonal antibodies, listed in Table 3, were either prepared in our laboratory by C. Uthoff- Hachenberg and B. Hampel or purchased from Pharmingen (USA).

Specificity	**Clone**	**Reference and supplier**
IgM	R33-24.12	(Gruetzman, 1981), lab-made
IgD	1.3-5	(Roes et al., 1995), lab-made
IgMb	MB86	(Nishikawa et al., 1986), lab-made
IgG2ab	G12-47/30	(Seemann, 1981), lab-made
IgG2b	R14-50	(Müller, 1983), lab-made
IgE	95.3	(Baniyash and Eshhar, 1984), lab-made
NP	B1-8m	(Reth, 1981), lab-made
NP	B1-48	(Reth, 1981), lab-made
NP	S43-10	(Wildner, 1982), lab-made
NP	S24/63/63	(Baumhackel et al., 1982), lab-made
NP	N1G9	(Cumano and Rajewsky, 1985), lab-made
NP	B53-8	(Reth, 1981), lab-made
NP	B53-12	(Reth, 1981), lab-made
B220/ CD45R	RA3-6B2	(Coffman, 1982), lab-made/Pharmingen
CD3e	145-211	(Leo et al., 1987), Pharmingen
CD4	GK.1.5/4	(Dialynas et al., 1983), Pharmingen
CD5	53-7.3	(Ledbetter and Herzenberg, 1979), Pharmingen

CD8	53-6.7	(Ledbetter and Herzenberg, 1979), Pharmingen
CD11c	HL3	(Huleatt and Lefrancois, 1995), Pharmingen
CD11b (Mac-1)	M1/70	(Springer et al., 1979), lab-made/Pharmingen
CD19	1D3	(Krop et al., 1996), Pharmingen
CD21/CD35	7G6	(Kinoshita et al., 1988), Pharmingen
CD22	Cy34.1	(Symington et al., 1982), Pharmingen
CD23	B3B4	(Rao et al., 1987), Pharmingen
CD24/HSA	M1/69	Springer et al. 1978, Pharmingen
CD25 (IL2Rα)	7D4	(Malek et al., 1983), Pharmingen
CD43	S7	(Gulley et al., 1988), Pharmingen
CD44	KM114	(Miyake et al., 1990), Pharmingen
CD45Rb	16A	(Bottomly et al., 1989), Pharmingen
CD62L (L-Selectin)	MEL-14	(Gallatin et al., 1983), Pharmingen
CD69	H1.2F3	(Yokoyama et al., 1988), Pharmingen
CD86/B7.2	GL1	(Inaba et al., 1994), Pharmingen
CD90/Thy1.2	CFO-1	(Opitz et al., 1982), Pharmingen
CD95 (Fas)	Jo2	Pharmingen
CD103 (α_{IEL})	M290	(Kilshaw and Baker, 1988), Pharmingen
CD152 (CTLA-4)	UC10-4F10-11	(Tivol et al., 1995), Pharmingen
I-A^b	AF6-120.1	(Wall et al., 1983), Pharmingen
H-$2K^b$	AF6-88.5	(Loken and Stall, 1982), Pharmingen
H-$2K^d$	SF1-1.1	(Abastado et al., 1987), Pharmingen
Ly6-G (Gr-1)	RB6-8C5	(Fleming et al., 1993), Pharmingen
MHC class II	M5/114	(Bhattacharya et al., 1981), Pharmingen
BP-1	BP-1	(Cooper et al., 1986), Pharmingen
HSA	30F1	(Ledbetter and Herzenberg, 1979), lab-made
TCRβ	H57-597	(Kubo et al., 1989), Pharmingen

Table 3. List of antibodies used for flow cytometry and ELISA.

2.2.4 Magnetic Cell Sorting and FACS Sorting

Specific cell populations were either sorted or depleted from a heterogenous cell suspension by magnetic cell sorting (MACS; Miltenyi Biotec, Bergisch Gladbach). Cell populations were labelled with antibody-coupled microbeads (10 ml beads, 90 ml PBS-BSA-N_3 per 10^7 cells) and separated on VS, CS or Mini-MACS columns in a magnetic field (Miltenyi et al., 1990). For cell sorting B cells were purified by MACS (Miltenyi) and then stained with antibodies against various cell surface markers. B cells of individual B cell subsets were then sorted using a dual laser FACStar (Becton Dickinson). The purity of isolated populations was subsequently tested by FACS analysis: MACS-isolated B cells were typically ≥ 85% pure and sorted B cell subpopulations were ≥ 95% pure. FACS sorting was performed with the help of Christoph Goettlinger.

2.2.5 CFSE Labeling and *in vitro* T Cell Activation

T cells were purified using MACS (CD90- or CD4-beads after depletion with B220- or CD19-beads, all Miltenyi) or R&D T cell enrichment columns or FACS-sorting. For activation marker studies 1.5 to 4 x 10^6 cells were plated in a 24 well plate and analyzed after 24 h. Supernatants were kept for cytokine analysis. For proliferation T cells were resuspended in 1 ml per 10^7 cells 2.5 µM CFSE (5 mM stock in DMSO, Molecular Probes) in PBS at 37 °C for 5min (Lyons and Parish, 1994). The labeling reaction was stopped by addition of 10 ml ice-cold DMEM/10 % FCS medium. The cells were then washed once in medium. Labeled T cells were plated at 0.5 x 10^6 cells per well in round bottom 96 well plates and analyzed after various time points.

Stimulations with immobilized antibodies against CD3 (Clone 145-2C11, Pharmingen) or CD3 and CD28 (Clone 37.51, Pharmingen) were performed either by precoating plastic plates with antibody or by adding antibody-coated beads to the cell suspensions. Beads (surfactant-free sulfate white polystyrene latex, 4.9 µm diameter, intrafacial dynamics corporation) were incubated with the antibodies in PBS at 37 °C rotating for 2h, washed twice with PBS and resuspended in medium.

2.3 Biochemistry and Immunohistochemistry

3.2.1 Protein Extract Preparations

MEFs were resuspended at 10^6/15 µl cells in hypotonic solution (10 mM Hepes [pH 7.9], 10 mM KCl, 2 mM $MgCl_2$, 0.5 mM DTT, 0.1 mM EDTA, supplemented with various protein inhibitors) and incubated for 10 min at 4 °C. Then NP-40 was added to 10 % and the cells were microfuged at 13,000 rpm for 1 min. The supernatant containing the cytoplasmic fraction was recovered and the nuclear pellet was resuspended in 10^6/10 µl cells of high salt buffer (20 mM Hepes [pH 7.9], 420 mM NaCl, 1.5mM $MgCl_2$, 0.5 mM DTT, 0.2 mM EDTA
and 10 % glycerol) and incubated on ice for 30 min. Nuclear extracts were recovered after centrifugation at 10,000 rpm for 10 min at 4 °C and stored at – 80 °C.

3.2.2 Western Blotting

Cytoplasmic extracts were electrophoresed by SDS-PAGE (10 %) and transferred to immobilon-NC membranes (Millipore). The membranes were blocked with superblock (Pierce), or 3 % NF-milk/PBS or 5 % BSA/PBS and probed using various antibodies. Membranes were then incubated with goat anti-rabbit IgG-horseradish peroxidase (HRP) conjugates and developed using the ECL or ECL$^+$ kit (APB).

Specificity	**Clone, Manufacturer**
β-Actin	(AC-15, Sigma)
G6PD	(A 9521, Sigma)
IκBα	(C21, Santa Cruz)
IKK1	(IMG-136, Imgenex)
IKK2	(10AG2, Upstate Biotechnology)
IKK2	(AHP547, Serotec)
NEMO	(rabbit anti-NEMO serum, Yamaoka et al, 1998)
SHP-2	(sc-280; C-18, Santa Cruz)

Table 4. List of antibodies used for Western Blotting

3.2.3 Electromobility Shift Assay

1 µg to 5 µg of nuclear extract (for MEFs) or NP-40 whole cell lysate (for sorted T cells) were incubated for 30 min at room temperature with 2 µg poly(dI-dC) (Pharmacia) and 0.5 ng of ^{32}P-labelled κB probe derived from the H-2K^{b} promoter (Yamaoka et al., 1998) in binding buffer (10 mM TrisHCl [pH 7.5], 50 mM NaCl, 0.5 mM DTT, 0.1 mM EDTA, 0.1 mg/ml BSA and 4 % glycerol). Samples were fractionated on a 5 % non-denaturing PAGE and visualized by autoradiography. Other probes used were NF-κB (Promega), Oct-1 (Promega) and NF-1 (Rothwarf et al., 1998).

For supershift assays nuclear extracts or whole cell lysates were preincubated for 30 min at RT with antibodies against p50 (sc-114, Santa Cruz), p52 (rabbit antiserum, upstate biotech), RelA (sc-109, Santa Cruz), c-Rel (sc70, Santa Cruz) or RelB (sc-226; C-19, Santa Cruz).

3.2.4 Measurement of IL-6 and TNF Production

MEFs were plated at 4 x 10^4 cells per well onto 48 well plates in DMEM containing 10 % FCS. After 24 h cells were stimulated in triplicate samples with 1 or 10 ng/ml IL-1β, 10 ng/ml TNF or 1 µg/ml LPS for 16 h. The concentration of IL-6 and TNF in the culture supernatant was determined by ELISA (R&D Systems), according to manufacturer's instructions.

3.2.5 Measurement of TNF-Induced Cell Death

MEFs (2 x 10^4 cells per well) were plated onto 96 well plates and cultured for 24 h in DMEM containing 10 % FCS. Then the cells were stimulated in DMEM containing 5 % FCS with either 10 ng/ml TNF or 10 ng/ml TNF plus 300 ng/ml Cycloheximide (Tanaka et al., 1999). TNF induced cell death was determined by a celldeath kit (Promega) according to manufacturers instructions. Each condition was measured in triplicate samples.

3.2.6 Preparation of Thin and Ultrathin sections

Tissues fixed in 4 % paraformaldehyde were subsequently treated with 2 % osmium tetroxide in 0.1 M PBS for 2 h at 4°C, washed in 0.1 M PBS, dehydrated in a graded ethanol series and embedded in araldite. The 0.5 µm thin slices were stained with

methylene blue and investigated using a Zeiss Axiophot (Zeiss). Ultrathin 60 nm sections were examined using an electron microscope (902A, Leo) after further contrasting with uranyl acetate-lead citrate. Sections were cut by B. Hampel, C. Hoffmann, E. Janßen, and J. Siodladczek.

3.2.7 Histological Analysis and Immunohistochemistry

Paraffin sections were cut at 5-10 µm and stained with hematoxylin and eosin or giemsa-azur-eosin-methylene blue solution (Merck). Immunohistochemistry was performed on paraffin sections using antibodies against NOS-II (SA200, Biomol), Ki-67 (Dianova) and the 85 kD cleavage fragment of PARP (Promega). After treatment with 3 % normal goat serum sections were incubated with the second antibody (Dako). The histological analysis was done in collaboration with Wilhelm Bloch (Institut I für Anatomie, Joseph Stelzmann Strasse 9, D-50931 Köln, Germany).

2.4 Mouse Experiments

Mouse experimental procedures like vasectomy of males, tail bleeding as well as breeding of foster mothers and the general handling, marking of mice were performed according to Hogan (Hogan et al., 1987) and Silver (Silver, 1995).

2.4.1 Mice

C57BL/6, C57BL/6 x Balb/c, 129/Sv and CD1 mice were obtained from Bomholtgard (Denmark), Charles River, Harlan Winkelmann or Jackson Laboratories. CB20 mice were taken from breedings in our animal facility. Balancer-Cre mice (Betz et al., 1996), CD4-Cre (Lee et al., 2001), CD19-Cre mice (Rickert et al., 1995; Rickert et al., 1997), *deleter*-Cre mice (Schwenk et al., 1995) and Mx-Cre mice (Kuhn et al., 1995) were intercrossed with the newly generated $Nemo^{FL}$ strain, the $Ikk2^{FL}$ (Pasparakis et al., 2002a) and the $Ikk2\Delta K^{FL}$ (Pasparakis et al., 2002b) in conventional facilities.

2.4.2 Immunizations

Primary T dependent antigen responses were induced with alum precipitated NP-CG (4-hydroxy-3-nitrophenylacetyl chicken-γ- globulin) (Weiss and Rajewsky, 1990). The immunogen was prepared by mixing 1 volume of (1 mg/ml in PBS) with 1 volume of 10 % $KAl(SO_4)_2$. The solution was adjusted to pH 6.5 and kept 30 min on ice. Then, the precipitate was washed three times in PBS and resuspended in PBS. Mice were immunized by i.p. injections of 5 or 50 µg NP17-CG in a volume of 200 µl.

2.4.3 ELISA - Serum Analysis

Ig serum concentrations were determined by C. Uthoff-Hachenberg with enzyme-linked immunosorbent assays (ELISA, (Kendall et al., 1983)) as described in Roes and Rajewsky (Roes and Rajewsky, 1993). Microtiter plates (Costar) were coated in PBS plus reagent at 4 °C o/n, and subsequently blocked at RT for 30 min in PBS, 0.5 % BSA, 0.01 % N_3, pH 7.2. Next, serially diluted sera samples were applied to the wells and incubated at 37 °C for 1 hour. Then, secondary biotinylated antibody was added for 1 hour at 37 °C. Detection of the biotinylated reagent was achieved with SA-conjugated alkaline phosphatase (AP, Boehringer: 30 min at RT) and p-nitrophenylphosphate as substrate (Boehringer). Following each incubation step, unbound antibodies or SA-conjugated AP were removed by five washes with tapwater. The OD_{405} was measured with an ELISA-photometer (Anthos 2001, Anthos Labtech Instruments) and the relative antibody concentrations were determined by to a standard. Affinities of IgG1 and l NP-specific antibodies were determined by calculating the association constant as described by Cumano and Rajewsky (Cumano and Rajewsky, 1986), following a method developed by Herzenberg et al. (Herzenberg and Black, 1980). Relative binding of serum antibodies to NP5-BSA versus NP14-BSA was determined by ELISA in comparison to anti-NP antibody standards of known affinity.

Coating	**Biotin-Conjugate**	**Specificity**	**Standard**
R33-24.12	gam IgM (SBA)	IgM	B1-8µ
RS 3.1	R33-60	IgMa	267.7
Mb86	R33-60	IgMb	B1-8m

gam IgG1 (Sigma)	gam IgG1 (SBA)	IgG1	N1G9
ram IgG2aa (Nordic)	gam IgG2a (SBA)	IgG2aa	41.2-3
G12-47/30	G12-47/30	IgG2ab	S43-10
R14-50 gam	IgG2b (SBA)	IgG2b	D3-13F1
2E.6 gam	IgG3 (SBA)	IgG3	S24/63/63
gam IgA (Sigma)	gam IgA	(SBA)	IgA 233.1.3
95.3	ram IgE (Pharmingen)	IgE	B1-8e
187.1	R33-18-10.1	κ	S8
NP-BSA	gam IgM (SBA)	NP/IgM	B1-8μ
NP-BSA	RS3.1	NP/IgMa	267.7
NP-BSA	MB86	NP/IgMb	B1-8μ
NP-BSA	gam IgG1 (SBA)	NP/IgG1	N1G9
NP-BSA	gam IgG2a (SBA)	NP/IgG2a	S43-10
NP-BSA	gam IgG3 (SBA)	NP/IgG3	S24/63/63
NP-BSA	gam λ (SBA) / LS136		NP/λ N1G9
NP-BSA	gam κ	(SBA) NP/κ	S8

Table 5. Antibody combinations to determine serum antibody isotypes.

2.4.4 BrdU Labeling

Mice were fed with BrdU (Sigma-Alrich) in the drinking water (1 mg/ml) for one or two weeks (Forster et al., 1989; Gray, 1988). Splenocytes were stained with FITC-conjugated anti-B220 mAbs (clone RA33.A1.CL6) and fixed with 70 % methanol followed by 2 % formalin in PBS. Cell were then treated with 1M HCl/0,5 % Tween 20 for 15 min at 37 ^{o}C followed by 0, 1 % $Na_2B_4O_7$. Cells were finally stained with a biotin-conjugated anti-BrdU mAb (Alexis Biochemicals) and streptavidin-Cychrome and analyzed with a FACSCalibur (Becton Dickinson). Alternatively BrdU-Incorporation was measured using a commercially available kit following manufacturers instructions (Pharmingen).

2.4.5 Anti IL-7R Antibody Injections

Mice were injected intravenously with 1 mg of anti-IL-7R mAb (clone A7R34) (Sudo et al., 1993) every other day for four weeks before sacrifice. Cell suspensions from the various lymphoid organs were analyzed by FACS. DNA isolated from MACS-purified splenic B cells was analyzed with Southern blotting.

3. RESULTS

3.1 Generation of a Conditional *nemo* Allele

The murine gene encoding NEMO is located on the X chromosome, less than 4 kb from the *G6pd* gene (Figure 2A). Two BamHI fragments from a BAC containing the murine *Nemo* gene were subcloned and sequenced and found to contain the first 7 coding exons of *Nemo* and the entire region between the coding sequences of the *Nemo* and *G6pd* genes: DNA 2 (6.7 kb, containing *Nemo* exons I and II) and DNA 1 (7.6 kb, encompassing exons III-VII) (Figure 2). For the generation of NEMO-deficient mice a conditional *nemo* allele was produced. Deletion of exon II introduces a frameshift followed by a premature termination codon, and should thus inactivate the *Nemo* gene. In order to test this hypothesis a *Nemo* cDNA lacking exon 2 was cloned and expressed in a NEMO-deficient B cell line (Yamaoka et al., 1998). Expression of this cDNA failed to restore NF-κB activation in this cell line, showing that deletion of exon 2 indeed leads to a *nemo* null allele (data not shown).

Therefore I decided to place *Nemo* exon II between two loxP sites in the mouse genome. Accordingly a targeting vector was designed to flank exon II of *Nemo* with two loxP sites: A FRT site flanked cassette, containing a *neo*^{r} gene (PMC1neopA, Stratagene) and the *Flpe6* gene (Buchholz et al., 1998) under the control of the ACE promoter (Howard et al., 1993) was cloned and placed into the second intron of the *Nemo* gene (Figure 2). This cassette was originally designed and cloned in order to excise itself in the male germline, analogous to the gene self-excision method by Bunting et al. (Bunting et al., 1999). Unfortunately, it was later found that a two Bp deletion in the *Flpe6* coding sequence rendered the FLPE nonfunctional and the cassette had to be deleted *in vitro* by transient expression of Flpe6. A 2.0 kb XmnI-BglII fragment was used as 5' homology region, a 2.0 kb BglII-SpeI fragment was placed between the two loxP sites and a 5.5 kb SpeI-ClaI fragment was used as 3' homology region. A thymidine kinase gene was used for negative selection of clones with random integration of the targeting vector. Bruce-4 ES cells (Kontgen et al., 1993) derived from C57Bl/6 mice, were transfected, cultured and selected as previously described (Pasparakis and Kollias, 1995; Torres and Kuehn, 1997). Out of 398 G418 and gancyclovir resistant colonies 6 were identified as homologous recombinants with cointegration of the second loxP site (FN) by Southern blot analysis of BamHI digested

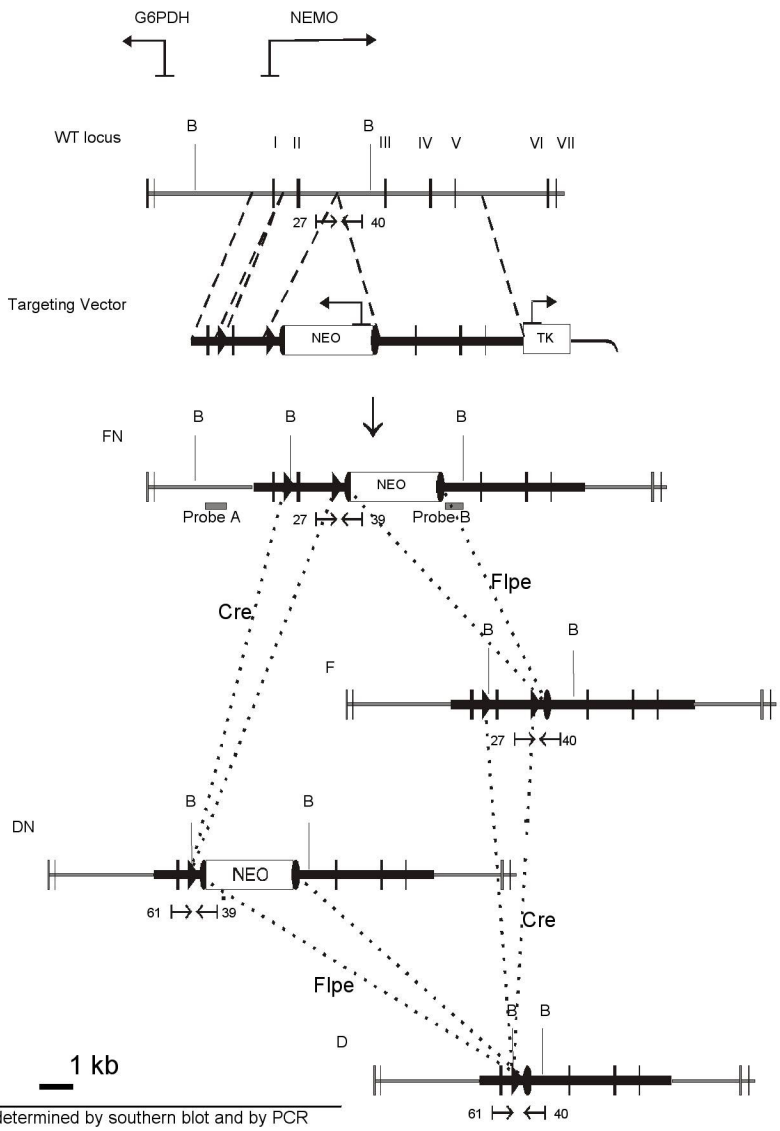

nemo genotypes determined by southern blot and by PCR

	WT	FN	F	DN	D
Probe A [kb]	6.8	2.9	2.9	2.9	2.9
Probe B [kb]	6.8	6.6	3.2	4.6	1.2
PCR [bp]	431	657	576	922	841

Figure 2. Generation of *Nemo* knockout Mice

Schematic representation of the targeting. The structure of the *Nemo* gene with the first seven coding exons (I-VII) is shown at the top. Homologous recombination into the *Nemo* locus resulted in the floxed, neo^r cassette containing genotype (FN). The remaining genotypes floxed (F), deleted containing neo^r (DN) and deleted (D) have been generated *in vitro* through Cre and/or Flp mediated recombination (see methods). The sizes of the BamHI (B) restriction fragments and PCR products indicative for each genotype are given in the table at the bottom. The closed triangles represent loxP sites, the closed ovals FRT sites. Transcriptional orientation of genes is indicated by arrows. Homologous sequences contained in the targeting vector are shown with a bold line.

DNA, using an AccI-XmnI 480 bp fragment as 5' external probe (probe A) (Figures 2 and 3A). Two *Nemo*$^{FN/Y}$ ES cell clones were then transiently cotransfected with either Flpe6 and puromycin, or Flpe6, Cre and puromycin encoding plasmids (pFlep6, pPgkcre and pPgkpuro in a ratio of 1:1:10) to generate ES cells lacking the *neo*^{r} cassette and/or NEMO coding exon II (genotypes F, DN and D, see Figures 2 and 3A). Experimental procedures were essentially as described (Pasparakis and Kollias, 1995; Torres and Kuehn, 1997), except that puromycin selection (1 μg/ml) was applied between 24-72 hours after transfection. ES cell clones containing *neo*^{r} deletion (F), exon II deletion (DN) or *neo*^{r} and exon II deletions (D) were identified by Southern blot analysis of BamHI digested DNA using probe B (600 bp SpHI-EcoRI fragment) (Figures 2 and 3A). Chimeric mice were generated by injection of *Nemo*$^{FN/Y}$, *Nemo*$^{F/Y}$ and *Nemo*$^{D/Y}$ ES cells into blastocysts from CB20 or Balb/C mice. Matings of male chimeras to C57BL/6 females yielded germline transmitted female offspring of pure C57BL/6 genetic background in all three cases. *Nemo*$^{D/WT}$ mice were generated by crossing either chimeras transmitting the *Nemo*^{FN} genotype with Cre-deleter (Schwenk et al., 1995) yielding *Nemo*$^{DN/WT}$ females or by crossing chimeras transmitting the *Nemo*$^{D/Y}$ genotype to wild-type C57BL/6 females, yielding *nemo*$^{D/WT}$ heterozygous females. Since *nemo*^{DN} and *nemo*^{D} are similarly *nemo*-knockout alleles and no difference could be detected between the two both *Nemo*$^{DN/WT}$ and *Nemo*$^{D/WT}$ are referred to as *Nemo*$^{D/WT}$. NEMO-deficient embryos were generated by crossing *Nemo*$^{D/WT}$ mice to chimeras transmitting the *Nemo*^{D} genotype. DNA was analyzed by Southern blot analysis as described above, or by PCR, using 4 primers in one reaction: 27, 39, 40 and 61 (Figures 3A and B). RT-PCR analysis of RNA and Western blot analysis of extracts from *Nemo* deleted ES cell clones revealed the presence of a shortened mRNA and absence of NEMO protein (not shown). Evidence that targeting of the *Nemo* genomic locus did not interfere with expression of the neighboring *G6pd* gene was obtained by RT-PCR (not shown) and Western analysis (Figure 3C). Chimeric mice were generated using either *Nemo*$^{FN/Y}$ or *Nemo*$^{D/Y}$ ES cell clones. Chimeras generated from *Nemo*$^{D/Y}$ ES cells developed skin lesions 5 to 9 days after birth. The lesions seemed to be restricted to the ES cell derived black colored skin areas. The most severely affected animals died at this stage, whereas some chimeras recovered with complete disappearance of the skin phenotype. Chimeras generated from *Nemo*$^{FN/Y}$ cells developed normally.

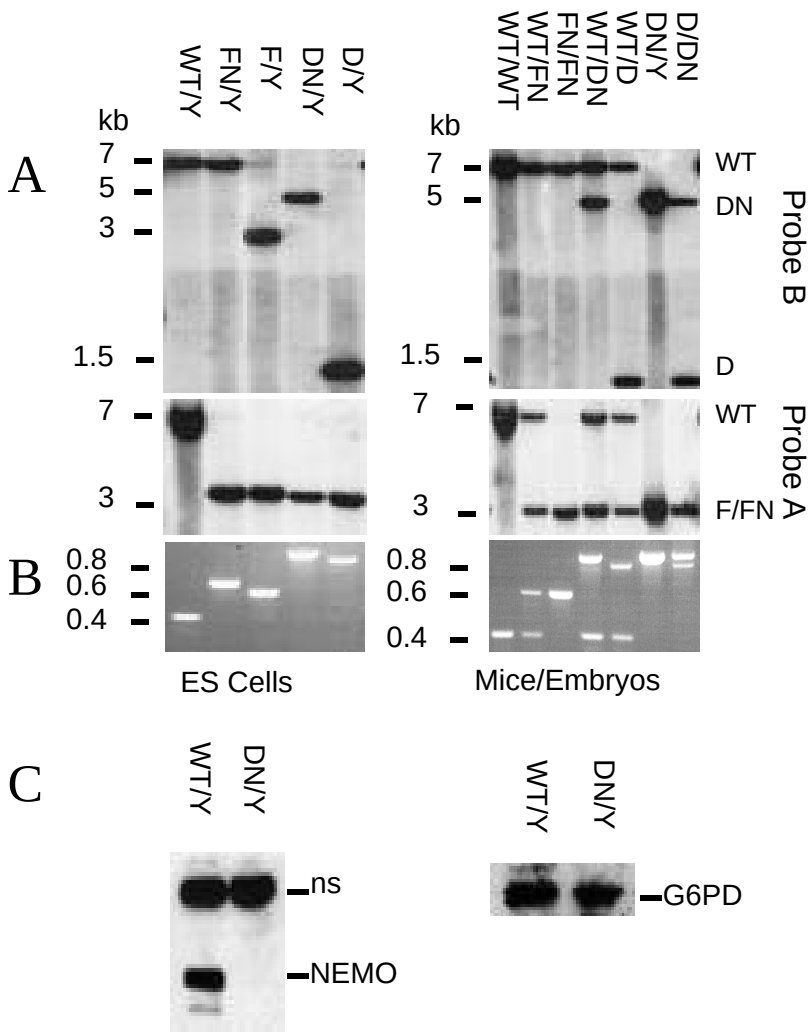

Figure 3. Generation of *Nemo* knockout Mice II

(A) Southern blot analysis of BamHI digested genomic DNA from ES cell clones, mice and embryos. Left panel: DNA from parental (WT/Y) and targeted ES cells carrying the genotypes FN/Y, F/Y, DN/Y and D/Y. Right Panel: DNA from wild type (WT/WT), heterozygous FN (WT/FN), homozygous FN (FN/FN) and heterozygous deleted (WT/DN and WT/D) mice, and from hemizygous DN (DN/Y) and homozygous (D/DN) deleted embryos.

(B) Genotyping of genomic DNA from the above described ES cells, mice and embryos by PCR using primers 27, 39, 40 and 61.

(C) Western blot analysis of NEMO and G6PD protein expression in cytoplasmic extracts of wild type (WT/Y), and *Nemo* knockout (DN/Y) MEFs. ns, non-specific.

3.2 Analysis of *Nemo*-knockout Mice

3.2.1 Liver Degeneration in NEMO-deficient Embryos

NEMO-deficient embryos were generated by crossing heterozygous knockout (*Nemo*$^{DN/WT}$) females with male chimeras generated from *Nemo*-deleted (*Nemo*$^{D/Y}$) ES cells. Examination of E12.5 NEMO-deficient embryos by TUNEL-assay revealed degeneration of the liver due to massive apoptosis of hepatocytes. Heterozygous *Nemo* knockout embryos also showed increased hepatocyte apoptosis when compared to wild type embryos (data obtained in collaboration with Dr. Bloch, not shown).

3.2.2 NEMO is Essential for NF-κB Activation

Western blot analysis showed complete absence of NEMO protein in MEFs isolated from E12.5 NEMO-deficient embryos (Figure 3C). To assess the role of NEMO in the induction of NF-κB we measured NF-κB activation by various means. In order to directly compare the inhibitory effect of NEMO-deficiency to that of IKK2-deficiency on the activation of NF-κB by proinflammatory stimuli, we included *ikk2* knockout MEFs (Pasparakis et al., 2002a) into the analysis. Stimulation of the cells by TNF, IL-1 or LPS failed to induce any detectable NF-κB DNA binding activity in NEMO-deficient MEFs (Figure 4A), although the p65 and p50 NF-κB subunits are expressed at normal levels in these cells (not shown). In IKK2-deficient MEFs TNF and IL-1, but not LPS, induced NF-κB DNA binding activity, although the levels of induction were strongly reduced compared to wild type MEFs. Analysis of IκBα protein levels in cytoplasmic extracts yielded corresponding results (Figure 4A).

Inhibition of NF-κB activity has been shown to sensitize cells to TNF induced apoptosis (reviewed in (Barkett and Gilmore, 1999)). As shown in Figure 4B, NEMO-deficient MEFs are extremely sensitive to TNF cytotoxicity even in the absence of cycloheximide. Addition of the protein-synthesis inhibitor cycloheximide renders cells more sensitive to apoptosis, since it blocks de novo synthesis of new anti-apoptotic proteins. Under the same conditions, *Ikk2*$^{D/D}$ cells show twofold increased viability compared to NEMO-deficient cells. To examine the role of NEMO in the expression of NF-κB-dependent genes we measured the production of IL-6 and TNF in these cells. NEMO-deficient cells failed to produce detectable amounts of IL-6 upon stimulation with IL-1, TNF or LPS while *Ikk2*$^{D/D}$ MEFs produced significantly reduced IL-6

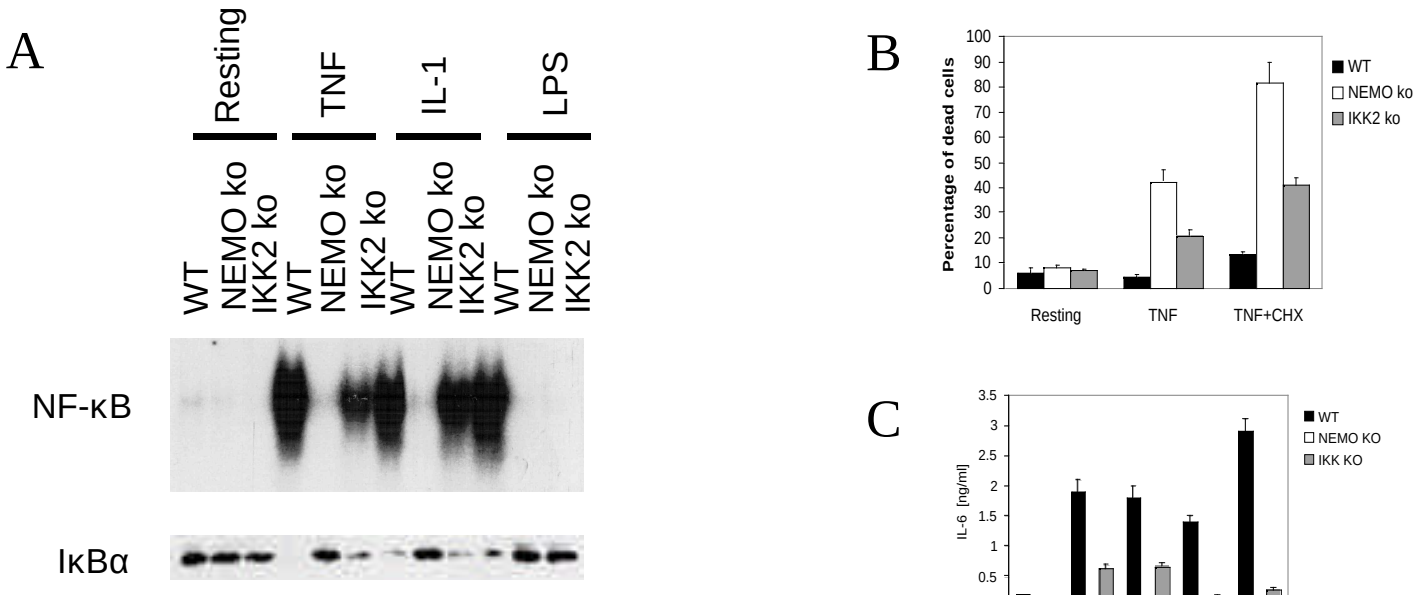

Figure 4. Comparison of NF-κB activation in wild type, NEMO-deficient and IKK2-deficient MEFs.

(A) Nuclear translocation of NF-κB was demonstrated by electromobility shift assay and degradation of IκBα was analyzed by Western blot. MEFs were incubated with murine recombinant TNF (10 ng/ml) or IL-1β (10 ng/ml) for 15 min and with LPS (1 μg/ml) for 45 min.

(B) Sensitivity to TNF induced cytotoxicity. MEFs were left untreated (resting) or stimulated with 10 ng/ml TNF in the absence or presence of 300 ng/ml cycloheximide (CHX) for 20 h. The amount of cell death was determined by measurement of LDH activity using a commercially available kit (Promega). Mean and standard deviation of triplicate samples are shown as the percentage of dead cells relative to the total cell number for each condition.

(C) Production of cytokines induced by proinflammatory stimuli. MEFs were treated for 16 h with various stimuli in the indicated concentrations. Levels of IL-6 and TNF in cell culture supernatants were determined by ELISA. Results are shown as the mean and standard deviation of triplicate samples.

compared to wild type cells (Figure 4C). Both NEMO- and IKK2-deficient MEFs did not release detectable amounts of TNF in response to LPS (Figure 4C). These results show that NEMO is essential for the induction of NF-κB by proinflammatory signals, while in the absence of IKK2 residual NF-κB activation still occurs, probably mediated by IKK1.

3.2.3 NEMO-deficient Mice Model Incontinentia Pigmenti

Heterozygous *Nemo*-knockout Female Mice Develop Skin Lesions

Heterozygous *Nemo* knockout mice (*Nemo*$^{D/WT}$) developed a striking skin defect that became visible 3 to 4 days after birth, when mice start to develop skin pigment. At that time point the skin showed areas of reduced or absent pigmentation in a pattern similar to that seen in chimeric mice (Figure 5A). The extent to which the skin is affected varies between different mice, probably reflecting the random pattern of X-inactivation. 6 to 7 days after birth the skin of the *Nemo*$^{D/WT}$ mice becomes hard and inflexible, displaying areas of defective hair growth and extreme scaling. From the appearance of the skin lesions on, *Nemo*$^{D/WT}$ mice are increasingly growth-retarded and look runted (Figure 5B). Most of the animals die 6 to 10 days after birth. From 33 *Nemo*$^{D/WT}$ females born from these initial matings, 29 (88%) died within this time interval: 5 at day 6, 12 at day 7, 6 at day 8, 4 at day 9 and 1 at day 10. The 4 (12 %) surviving mice gradually recovered and the scaling skin areas disappeared progressively, leaving behind some patches lacking hair growth (Figure 5C). After completion of the histological analyses these matings were stopped to prevent unnecessary suffering of the mice.

Histopathology of the Skin in Heterozygous *Nemo*-knockout Mice

In normal skin, keratinocytes proliferate in the basal layer of the epidermis and move outwards to the suprabasal layers where they progressively accumulate keratin and finally die as fully differentiated keratinocytes when they reach the cornified layer (Fuchs, 1993). Microscopic examination of skin sections from 4 and 8 days old *Nemo*$^{D/WT}$ mice revealed an altered skin structure with a dramatic increase in the thickness of both the suprabasal and the cornified layer of the epidermis (Figures 6Ad and Ae), compared to the skin of littermate controls (Figures 6Aa and Ab). At 6 weeks of age most of the skin of surviving *Nemo*$^{D/WT}$ mice shows normal morphology (Figure

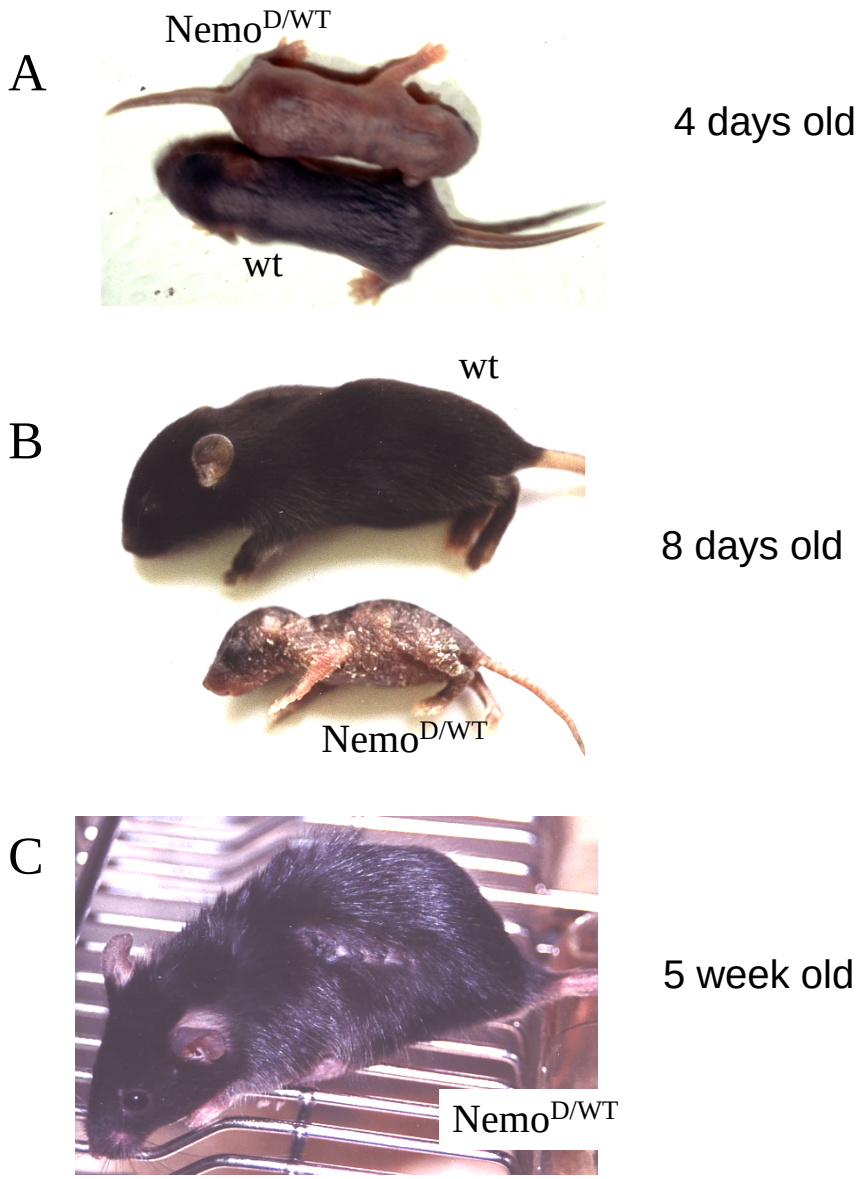

Figure 5. Heterozygous *nemo*$^{D/WT}$ female mice develop a disease of the skin similar to human IP

(A) 4 days old *nemo*$^{D/WT}$ female and wild type male littermate.

(B) 8 days old *nemo*$^{D/WT}$ female and wild type male littermate. This picture shows an extreme case of the runting and wasting seen in ***nemo***$^{D/WT}$ females.

(C) 5 week old surviving *nemo*$^{D/WT}$ female mouse. A stripe of the skin showing hyperpigmentation and absence of hair growth is observed.

6Ac) and only small patches are affected, displaying similar, albeit less severe, histological alterations as the skin of 4 and 8 day old mice (Figure 6Af). In wild type skin dead keratinocytes composing the cornified layer lack nuclei or cellular organelles (Figures 6Aa and Ab). In contrast, recognizable cell bodies with nuclei are observed in the cornified layer of the epidermis from *Nemo*$^{D/WT}$ mice (Figure 6Ad and Ae), indicating that in these animals keratinocytes that are not fully differentiated reach the cornified layer.

In sections from affected skin areas in *Nemo*$^{D/WT}$ mice, abnormal gaps form between keratinocytes of the basal and suprabasal layers (Figures 6Ad-f). To further investigate this phenomenon electron microscopy was used. As can be seen in Figure 6 Ag, the cells in the basal layer of normal epidermis are tightly packed. In contrast, in affected skin areas of *Nemo*$^{D/WT}$ mice basal layer keratinocytes appear to be in loose contact with each other, forming filopodia that extend into the dilated intercellular spaces (Figures 6Ah-i). In addition, alterations in tonofilaments and in desmosomal contacts were observed in keratinocytes in the epidermis of *Nemo*$^{D/WT}$ mice (not shown). Dyskeratotic cells showing abnormal tonofilament structure and absence of desmosomes were also observed in the skin of human IP patients (Schamburg-Lever and Lever, 1973).

Granulocyte Infiltration in the Epidermis and Melanin Deposits in the Dermis are Common Features in *nemo*$^{D/WT}$ Mice and Human IP Patients.

A prominent feature of IP at stage I is the presence of massive inflammatory infiltrates in the epidermis (Landy and Donnai, 1993). Histological examination of sections from the skin of 4 days old *Nemo*$^{D/WT}$ mice reveals the presence of numerous inflammatory foci with pronounced infiltration of granulocytes into the epidermis (Figure 6Ba). Only a few areas showing granulocyte infiltration can be detected in the epidermis of 8 days old *Nemo*$^{D/WT}$ mice (not shown), indicating that at that age the initial inflammatory stage is declining.

One of the best described features of IP is the presence of hyperpigmentation (Landy and Donnai, 1993). Several studies showed that hyperpigmentation is caused by the presence of increased number of phagocytes containing melanosome complexes in the dermis (Schamburg-Lever and Lever, 1973; Zillikens et al., 1991). Histological examination of skin from a stage III IP patient shows the presence of phagocytes

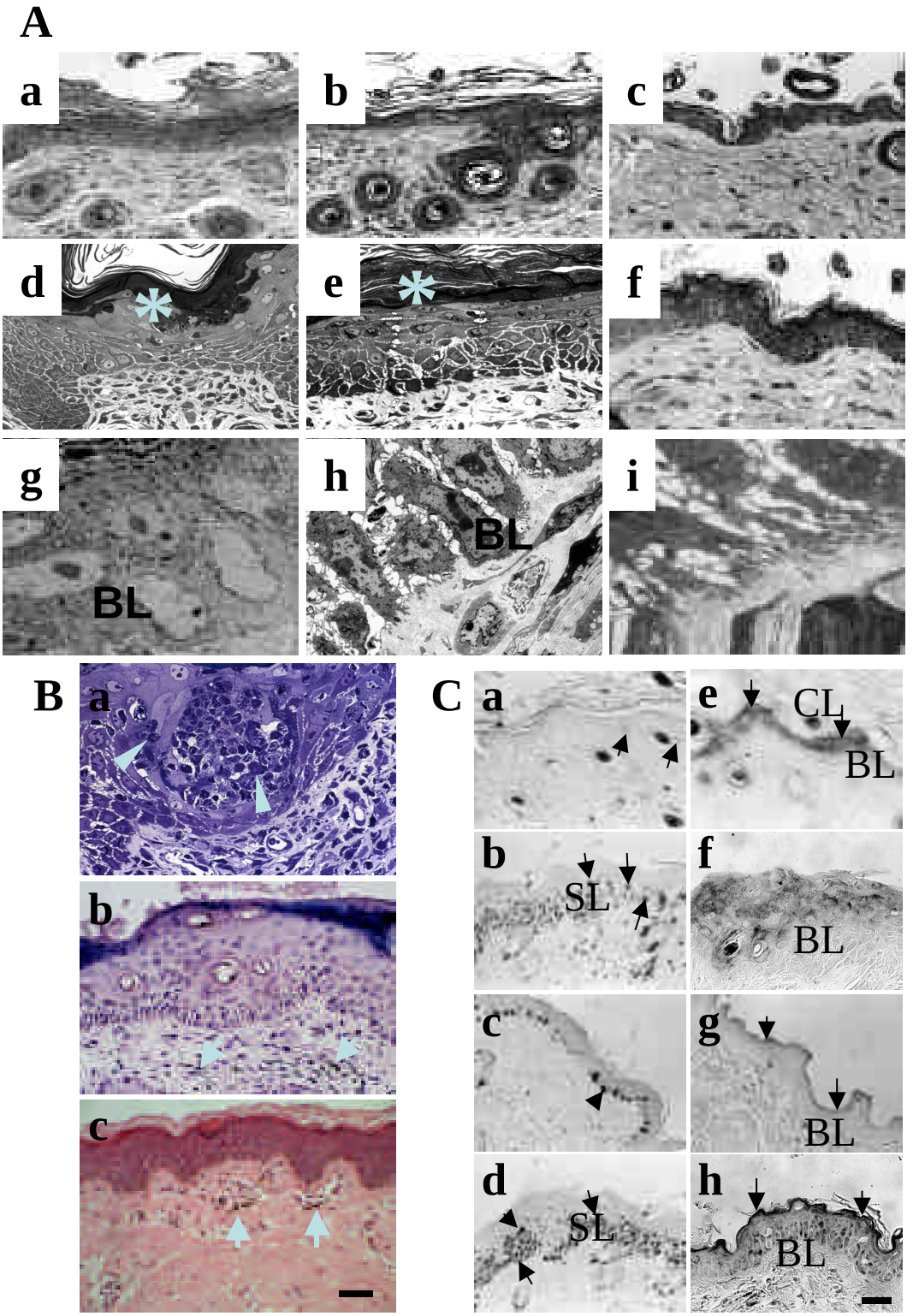
A
a
b
c
d
e
f
g
h
i
BL
BL
B
a
b
c
C
a
e
CL
BL
b
SL
f
BL
c
g
BL
d
SL
h
BL

Figure 6. Histopathology of the epidermis in *Nemo*$^{D/WT}$ mice.

(A) Skin structure in *Nemo*$^{D/WT}$ (c-f, h, i) and wild type mice (a, b, g) was examined by light microscopy on 0.5 µm sections stained with methylene blue (a-f) or by electron microscopy on 60 nm slices (g-i). Increased thickness of the epidermis and widening of intercellular spaces between keratinocytes are apparent in the skin from 4 days (d) and 8 days (e) old *Nemo*$^{D/WT}$ mice compared to controls (a and b respectively). In addition, the cornified layer (indicated by an asterisk) is thickened and shows abnormal structure with recognizable cell fragments (d, e). Sections from unaffected skin areas of a 6 week old *Nemo*$^{D/WT}$ mouse show normal structure (c), while in affected areas the epidermis is thickened (f). Basal layer keratinocytes in the skin from 8 days old *Nemo*$^{D/WT}$ mice are in loose contact with each other with filopodia (arrows) extending into the intercellular spaces (h, i), in contrast to the tight adherence observed between basal keratinocytes in skin sections from control mice (g). BL, basal layer. Bars = 35µm (A-F); 3.5µm (g and h); 2µm (i).

(B) Granulocyte infiltration and hyperpigmentation in the skin of *Nemo*$^{D/WT}$ mice.

(a) Methylene blue stained skin sections from 4 days old *Nemo*$^{D/WT}$ mice show clusters of infiltrating cells, mainly granulocytes (arrowheads) into the epidermis.

(b) Depositions of melanin granulas (arrows) in the dermis are observed in skin sections from 6 week old mice (Giemsa staining).

(c) Similar melanin depositions are seen in sections from hyperpigmented skin areas from stage III IP patients (hematoxylin-eosin-safran staining). Slides from IP patients were obtained from Christine Bodermer and Sylvie Fraitag.

Bars = 35µm (a); 50µm (b and c)

(C) Increased proliferation and apoptosis in the epidermis of *Nemo*$^{D/WT}$ mice.

(a-d) Detection of proliferating cells in skin sections stained with an antibody to Ki-67. In the epidermis of 8 days old control mice (a) and in unaffected areas from 6 week old *Nemo*$^{D/WT}$ mice (c) only a few cells in the basal layer proliferate (arrows). In contrast, nearly all of the basal and many suprabasal keratinocytes proliferate in the epidermis from affected skin areas in 8 days old (b) and 6 week old (d) *Nemo*$^{D/WT}$ mice. Arrows indicate Ki-67 positive cells.

(e-f) Immunohistochemical detection of apoptotic cells by staining with antibodies to the 85 kD fragment of PARP. In sections from 8 days old wild type mice (e) and from normal skin areas of 6 week old *Nemo*$^{D/WT}$ mice (g), apoptotic cells are detected only at the border between the suprabasal and the cornified layers (arrowheads). In contrast, increased apoptosis is detected in suprabasal keratinocytes in affected skin areas from 8 days old and 6 week old *Nemo*$^{D/WT}$ mice (f, h). In the epidermis of affected skin areas from 6 week old Nemo$^{D/WT}$ mice apoptotic cells are also detected in the basal layer (h). BL, basal layer; SL, suprabasal layer; CL, cornified layer. Bars = 40 µm (a-d); 30 µm (e-h).

Histology was performed in collaboration with Dr. Wilhelm Bloch.

containing melanin in the dermis (Figure 6Bc). A similar picture is observed in sections from affected skin patches from a 6 week old *Nemo*$^{D/WT}$ mouse (Figure 6Bb).

Increased Proliferation and Apoptosis in the Epidermis of Heterozygous *Nemo*-knockout Mice.

Epidermal homeostasis is based on a steady state between proliferation of cells in the basal layer and apoptosis of terminally differentiated keratinocytes at the border between the suprabasal and cornified layers (Fuchs, 1993). To determine whether the epidermal hyperplasia observed in the skin of *Nemo*$^{D/WT}$ mice is caused by increased proliferation of keratinocytes, we stained skin sections from *Nemo*$^{D/WT}$ and wild type mice with an antibody to Ki-67, an antigen expressed in proliferating cells. In contrast to wild type skin where only some cells of the basal layer are Ki-67 positive (Figure 6Ca), nearly all of the basal and many suprabasal keratinocytes are labeled for Ki-67 in the skin of 8 days old *Nemo*$^{D/WT}$ mice (Figure 6Cb). A similar picture is observed in affected skin patches at the age of 6 weeks (Figure 6Cd), while in skin areas of these mice showing normal morphology, only some cells of the basal layer expose Ki-67 (Figure 6Cc).

Staining with antibodies to the 85 kDa fragment of poly-(A)DP-ribose polymerase (PARP) reveals the presence of apoptotic cells selectively at the border between the suprabasal and cornified layers of the epidermis in wild type mice (Figure 6Ce) and in unaffected areas from a 6 week old *Nemo*$^{D/WT}$ mouse (Figure 6Bg). In contrast, apoptotic cells are detected also in the suprabasal layers in affected areas of 8 days old *Nemo*$^{D/WT}$ mouse skin (Figure 6Cf). At 6 weeks of age, this pattern of increased apoptosis is extended to both basal and suprabasal keratinocyte layers, but is detected only in small affected patches showing abnormal structure and increased proliferation (Figure 6Ch). It seems therefore that a combined increase of proliferation and apoptosis of keratinocytes contributes to the skin phenotype observed in *Nemo*$^{D/WT}$ mice.

3.2.4 Lack of NEMO-deficient Lymphocytes in Chimeras Generated with *Nemo*-knockout ES Cells

One of the consistent features of IP is the complete skewing of X inactivation in blood leukocytes (Parrish et al., 1996). We used chimeric mice generated from ES cells

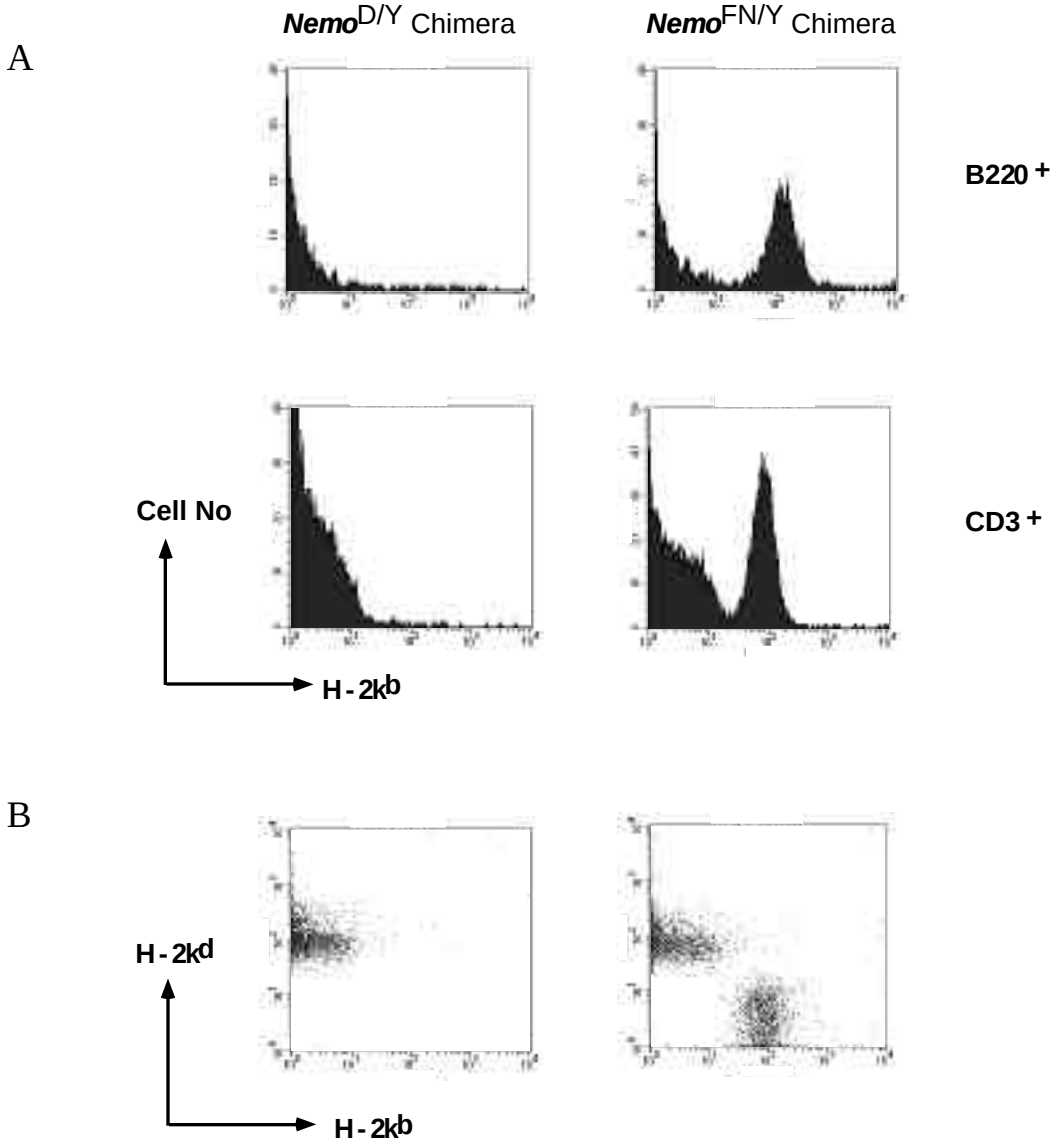

Figure 7. Absence of ES cell derived lymphocytes in chimeras generated with NEMO-deficient ES cells.

Flow cytometric analysis of PBL from chimeras generated from floxed (*nemo*$^{FN/Y}$) or NEMO-deficient (*nemo*$^{D/Y}$) ES cells. Cells were stained with anti-CD45R/B220, anti-CD3ε, anti-H2-k^{d} and anti-H2-k^{b} monoclonal antibodies. Host derived lymphocytes are H2-k^{d} positive and ES cell derived lymphocytes are H2-k^{b} positive. **(A)** Histograms showing H2-k^{b} expression levels of B220^{+} (B cells) and CD3^{+} (T cells) gated lymphocyte populations. **(B)** Dot plot showing H2-k^{b} and H2-k^{d} staining of total PBL. Results are representative of 5 chimeras per genotype.

carrying either a deleted (*nemo*$^{D/Y}$) or a floxed (*nemo*$^{FN/Y}$) *nemo* allele, to test whether a similar skewing occurs against lymphocytes derived from the NEMO-deficient ES cells. X inactivation in the mouse embryo starts after 4.5 days post coitum (d.p.c.) (Tan et al., 1993), while ES cells are injected into blastocysts at 3.5 d.p.c. Thus chimerism can be considered as a simulation of lyonization in females. This is further supported by the observation that male chimeras obtained from *Nemo*$^{D/Y}$ ES cells displayed a skin phenotype similar to that seen in *Nemo*$^{D/WT}$ female mice.

The targeted ES cells are derived from C57BL/6 mice and were injected into CB20 or Balb/c blastocysts. Thus host and ES cell derived lymphocytes can be distinguished by haplotype-specific staining for Class I MHC molecules, since C57BL/6 mice express the H-2^{b} and CB20 and Balb/c mice the H-2^{d} haplotype. Flow cytometric analysis of PBL from chimeras generated from ES cells containing a floxed *nemo* allele (*nemo*$^{FN/Y}$), reveals the presence of both ES cell and host derived B and T lymphocytes (Figure 7A and B). ES cell derived B and T cells were not detected in chimeras generated from *Nemo* knockout (*Nemo*$^{D/Y}$) ES cells, although normal numbers of B and T cells derived from the host blastocyst were present (Figure 7A and B), indicating that NEMO-deficient lymphocytes either do not develop or are counter-selected in these chimeras.

3.3 Analysis of a Kinase-dead Mutant of IKK2

In the absence of IKK2 IKK complexes consist of NEMO associated with IKK1 homodimers and exhibit inducible kinase activity (Li et al., 2000; Rothwarf and Karin, 1999). To eliminate IKK2 kinase activity without disrupting IKK stoichiometry another conditional *ikk2* allele, allowing replacement of IKK2 by a kinase-dead molecule (IKK2ΔK) upon Cre-expression, was generated by Manolis Pasparakis (Pasparakis et al., 2002b). This allele (*ikk2*Δ*K*^{FL}) was produced by placing only exon 7 of the *Ikk2* gene between lox P sites. After deletion of exon 7, exons 6 and 8 splice in frame and the resulting mRNA should produce a truncated IKK2 protein lacking amino acids 160-189, which include the two serines of the activation loop ($Ser_{177, 181}$) that are essential for the activation of the kinase (Mercurio et al., 1997) (Figure 8).

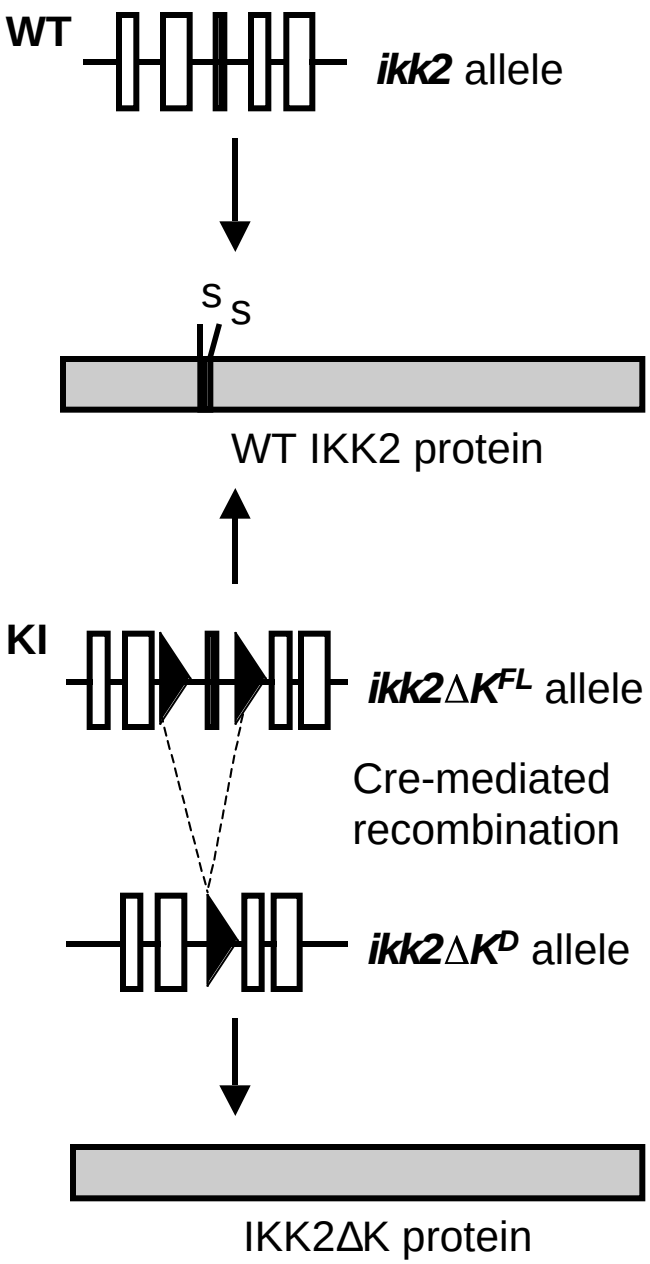

Figure 8. The conditional *ikk2*Δ*K* allele. Schematic representation of the wild-type (WT) *ikk2* allele, which producesWT IKK2 protein and the *ikk2*Δ*K* allele, which after deletion of loxP-flanked exon 7 generates a kinase-dead version of IKK2 (IKK2ΔK). Open and filled boxes represent exons, triangles represent loxP sites and the two serines of the IKK2 activation loop are indicated using the amino acid single letter code.

I conducted the biochemical analysis of MEFs generated from *Ikk2*Δ*K*$^{D/WT}$ and *Ikk2*Δ*K*$^{D/D}$ embryos and compared them to *Ikk2*$^{D/WT}$, *Ikk2*$^{D/D}$ and WT MEFs. The *ikk2*Δ*K*^{D} allele produces a protein that is recognized by antibodies raised against IKK2, which has a slightly lower molecular weight (Figure 9A). The level of the IKK2ΔK protein in *Ikk2*Δ*K*$^{D/D}$ MEFs is lower than that of IKK2 in WT MEFs (Figure 9A). This could be due to either decreased expression or increased degradation/instability of IKK2ΔK. IKK2ΔK is integrated into the IKK complex, as shown by immunopricipitation with antibodies raised against NEMO. Subsequent Western blotting showed that NEMO interacts with IKK2ΔK and IKK1 in *Ikk2*Δ*K*$^{D/D}$ MEFs (Figure 9B). Kinase-dead IKK2 can act as a dominant negative protein (Delhase et al., 1999). In *Ikk2*Δ*K*$^{D/WT}$ MEFs, heterozygous expression of IKK2ΔK did not reduce NF-κB activation in response to LPS or TNF compared to heterozygous IKK2 knockout or WT MEFs. This could be due to the low level of IKK2ΔK protein. In *Ikk2*Δ*K*$^{D/D}$ MEFs LPS induced activation of NF-κB all but abolished, as in IKK2 knockout MEFs (Figures 9C and 4A). In response to 20 min TNF treatment a residual activation of similar magnitude could be observed in both IKK2 mutant MEFs (Figure 9C). Subsequently a detailed time-course analysis of the NF-κB response to IL-1 or TNF treatment was undertaken, comparing WT, NEMO deficient, IKK2 deficient and *Ikk2*Δ*K*$^{D/D}$ MEFs (Figures 10A and B). No significant difference in NF-κB DNA binding monitored by EMSA or IκB-α degradation could be detected between *Ikk2*-knockout and *Ikk2*Δ*K*$^{D/D}$ MEFs. Subsequently, the activation of NF-κB-dependent genes in WT, *Nemo*-knockout, *Ikk2*-knockout and *Ikk2*Δ*K*$^{D/D}$ MEFs was tested by measuring two different parameters that are known to depend on NF-κB acivity: TNF-mediated cytotoxicity (Barkett and Gilmore, 1999) (Figure 11A) and production of IL-6 in response to proinflammatory stimuli (Figure 11B). WT MEFs are resistant whereas NEMO-deficient MEFs are extremely sensitive to TNF-induced apoptosis (Makris et al., 2000; Rudolph et al., 2000; Schmidt-Supprian et al., 2000), since they fail to express NF-κB-dependent anti-apoptotic proteins. In this setting, *Ikk2*Δ*K*$^{D/D}$ MEFs are more sensitive to TNF-induced apoptosis than *Ikk2*$^{D/D}$ MEFs (Figure 11A). Similarly the production of IL-6 in response to IL-1, LPS or TNF is reduced in *Ikk2*Δ*K*$^{D/D}$ MEFs compared to IKK2 knockout MEFs, but it is not completely abolished as in NEMO-

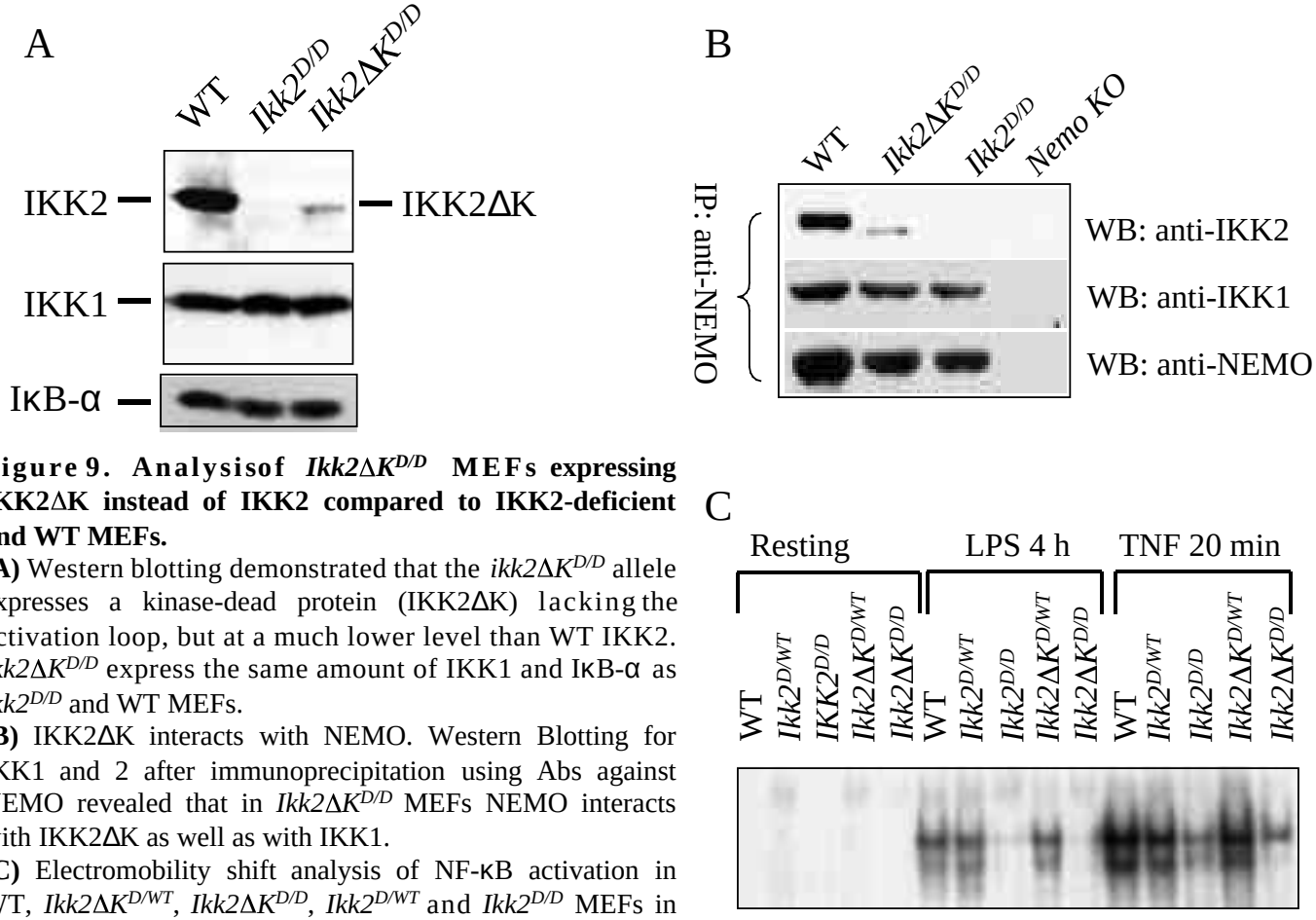

Figure 9. Analysisof *Ikk2ΔK$^{D/D}$* MEFs expressing IKK2ΔK instead of IKK2 compared to IKK2-deficient and WT MEFs.

(A) Western blotting demonstrated that the *ikk2ΔK$^{D/D}$* allele expresses a kinase-dead protein (IKK2ΔK) lacking the activation loop, but at a much lower level than WT IKK2. *Ikk2ΔK$^{D/D}$* express the same amount of IKK1 and IκB-α as *Ikk2$^{D/D}$* and WT MEFs.

(B) IKK2ΔK interacts with NEMO. Western Blotting for IKK1 and 2 after immunoprecipitation using Abs against NEMO revealed that in *Ikk2ΔK$^{D/D}$* MEFs NEMO interacts with IKK2ΔK as well as with IKK1.

(C) Electromobility shift analysis of NF-κB activation in WT, *Ikk2ΔK$^{D/WT}$*, *Ikk2ΔK$^{D/D}$*, *Ikk2$^{D/WT}$* and *Ikk2$^{D/D}$* MEFs in response to LPS and TNF.

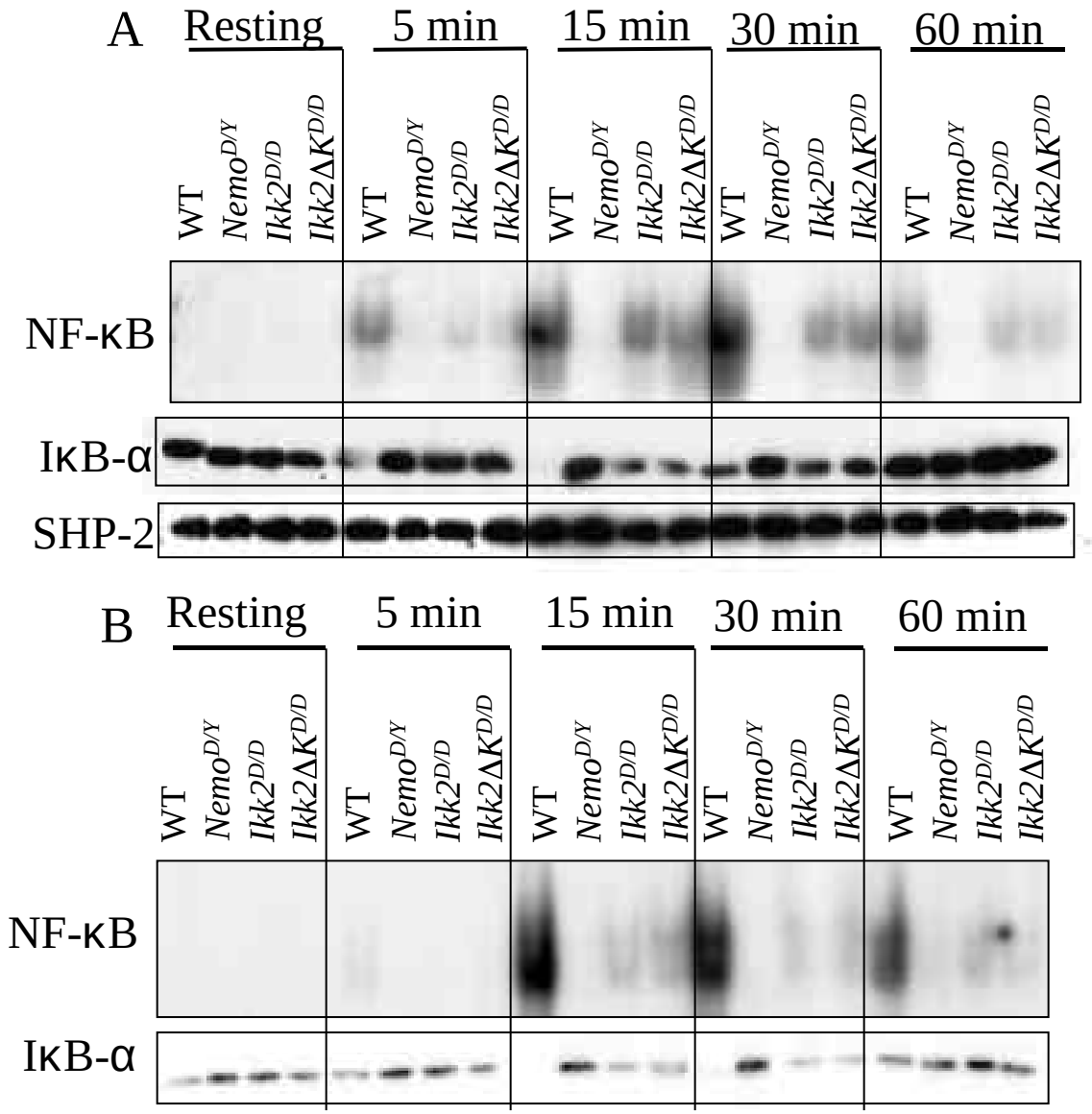

Figure 10. Time course analysis in NF-κB activation in wild type, NEMO-deficient, IKK2-deficient and IKK2ΔK-expressing MEFs.

(A) MEFs were stimulated with IL-1β (10 ng/ml) for the indicated time-periods before preparation of nuclear and cytosolic extracts. Nuclear translocation of NF-κB was demonstratedby electromobilityshift assay. IL-1β induced degradation of IκBα was analyzed by Western blot. The blot was reprobed with Abs to SHP-2 as a loading control.

(B) MEFs were stimulated with TNF (10 ng/ml) for the indicated time-periods. Nuclear translocation of NF-κB was demonstrated by electromobility shift assay and degradation of IκBα was analyzed by Western blot

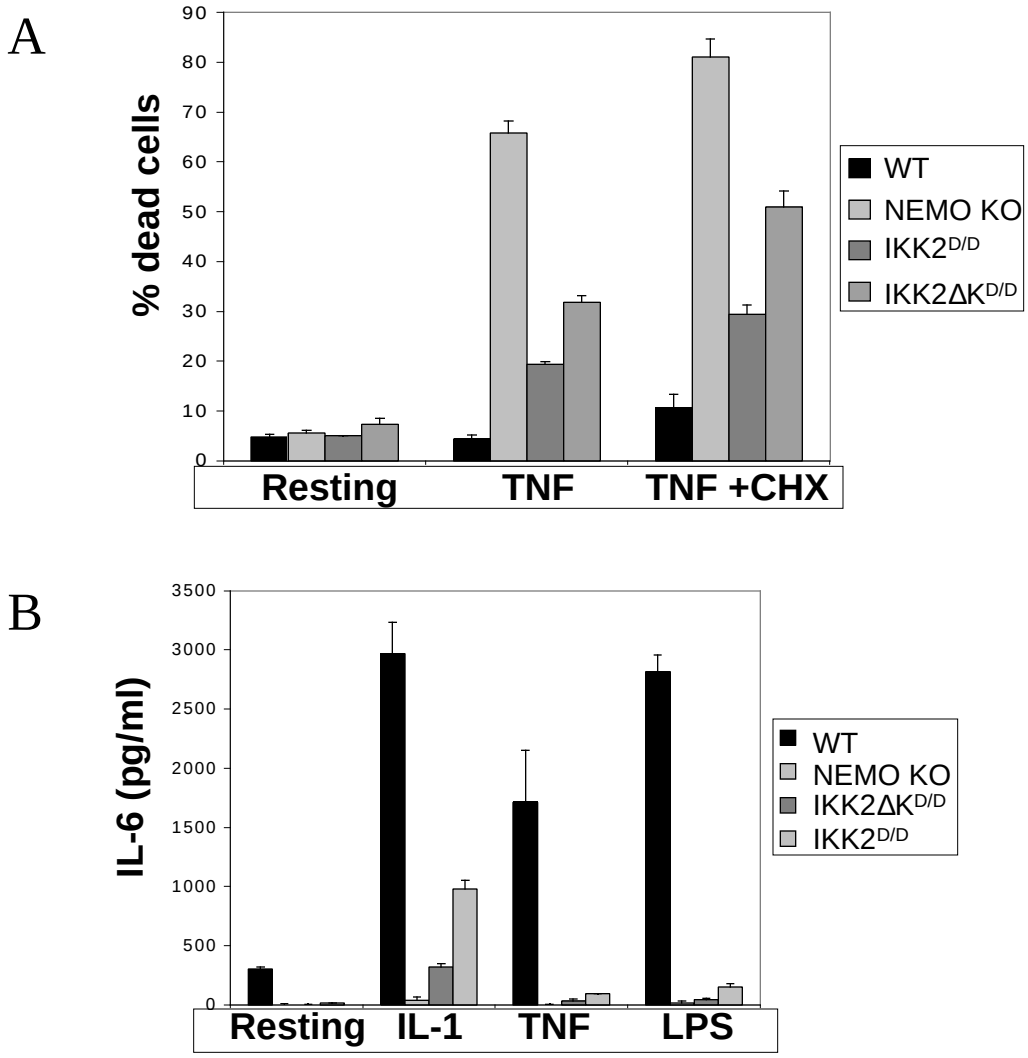

Figure 11. Comparison of TNF-induced Cell death and IL-6 production in wild type, NEMO-deficient, IKK2-deficient and IKK2-kinase dead MEFs.

(A) Sensitivity to TNF induced cytotoxicity. MEFs were left untreated (resting) or stimulatedwith 10 ng/ml TNF in the absence or presence of 300 ng/ml cycloheximide (CHX) for 20 h. The amount of cell death was determined by measurement of LDH activity using a commercially available kit (Promega). Mean and standard deviation of triplicate samples are shown as the percentage of dead cells relative to the total cell number for each condition.

(B) Production of cytokines induced by proinflammatory stimuli. MEFs were treated for 16 h with various stimuli in the indicated concentrations. Levels of IL-6 in cell culture supernatants were determined by ELISA. Results are shown as the mean and standard deviation of triplicate samples.

deficient MEFs (Figure 11B). These results indicate that NF-κB activation is more impaired in *Ikk2*Δ*K*$^{D/D}$ MEFs than in IKK2 knockout MEFs, although inhibition is not as complete as in NEMO deficient MEFs.

3.4 The IKK Complex is Essential for B Cell Maintenance

To delete the loxP flanked *nemo* and *ikk2* alleles in B lymphocytes we used a transgenic mouse strain expressing Cre recombinase under the control of the endogenous CD19 locus (Rickert et al., 1997). This CD19-Cre mouse has been shown to delete loxP flanked alleles specifically in the B cell lineage. The deletion efficiency was shown to be 75-80% in bone marrow and over 95% in splenic B cells (Cazac and Roes, 2000; Inui et al., 2002; Rickert et al., 1997) (Figure 12). The fact that deletion efficiency is higher in splenic than in bone marrow B cells indicates that Cre-mediated deletion is an ongoing process during B cell development and maturation, leading to the essentially complete deletion of loxP flanked alleles in mature B cells.

3.4.1 Flow Cytometric Analysis of the B Cell Compartment in *CD19-Cre/Ikk2*$^{FL/D}$, -*Ikk2*Δ*K*$^{FL/D}$ and -*Nemo*$^{FL/Y}$ Mice

Initial FACS analysis of B cell populations in *Ikk2*$^{FL/FL}$, *Ikk2*$^{FL/D}$, *Ikk2*Δ*K*$^{FL/FL}$, *Ikk2*Δ*K*$^{FL/D}$ and *Nemo*$^{FL/Y}$ mice did not show any differences compared to controls. In order to facilitate Cre-mediated deletion, I used mice in which only one loxP flanked allele remains to be deleted (*CD19-Cre/Ikk2*$^{FL/D}$, -*Ikk2*Δ*K*$^{FL/D}$ and -*Nemo*$^{FL/Y}$) for my experiments. FACS analysis of B cell populations in these mouse strains revealed very similar pictures. In the bone marrow early B cell development was essentially normal and the only difference found compared to control mice was a 2-4 fold reduction of mature recirculating B cells (Figure 13A and B). In the spleen the percentage of B cells was strongly reduced, leading to an inverted B/T cell ratio (Figures 14A and B). The reduction seems to occur mainly in the IgM^{low}IgD^{+} mature B cell population. Splenic B cells were then subdivided into immature (IM -CD21^{low}HSA^{high}), follicular (FO - CD21^{int}HSA^{low}) and marginal zone (MZ - CD21^{high}HSA^{int}) B cells according to CD21 and HSA expression (Allman et al., 1993; Bigos et al., 1999) (Figure 12). This analysis

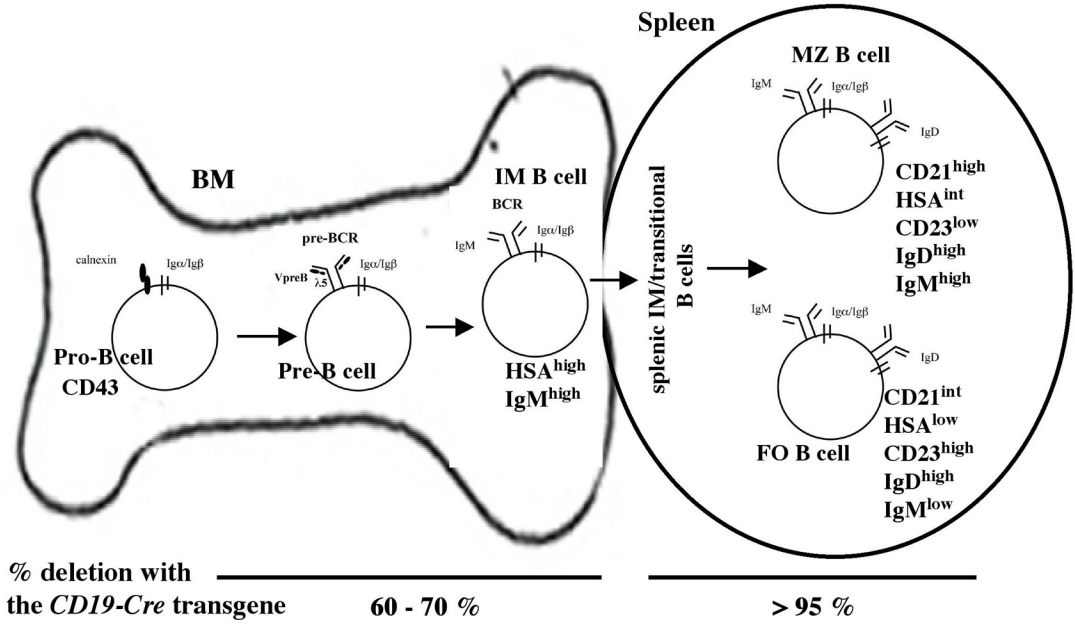

Fig 12. Sketch of B cell development and deletion efficiency of the *CD19-Cre* mouse line.
Cell surface marker used for separation of individual B cell subsets are indicated on cells as they appear. Deletion of loxP-flanked alleles by *CD19-Cre* is essentially complete in splenic B cells. Immature (IM) B cells in the spleen are transitional B cells that can be subdivided into three subsets (all $HSA^{high}CD21^{-\ to\ int}$) (Allman et al., 2001):
T1 ($AA4^{+}IgM^{high}$), T2 ($AA4^{+}IgM^{high}CD23^{+}$) and T3($AA4^{+}IgM^{low}CD23^{+}$). In this thesis T1 - T3 are collectively referred to as splenic IM B cells ($HSA^{high}CD21^{-\ to\ int}$ B cells). IM = immature, FO = Follicular, MZ = Marginal Zone.

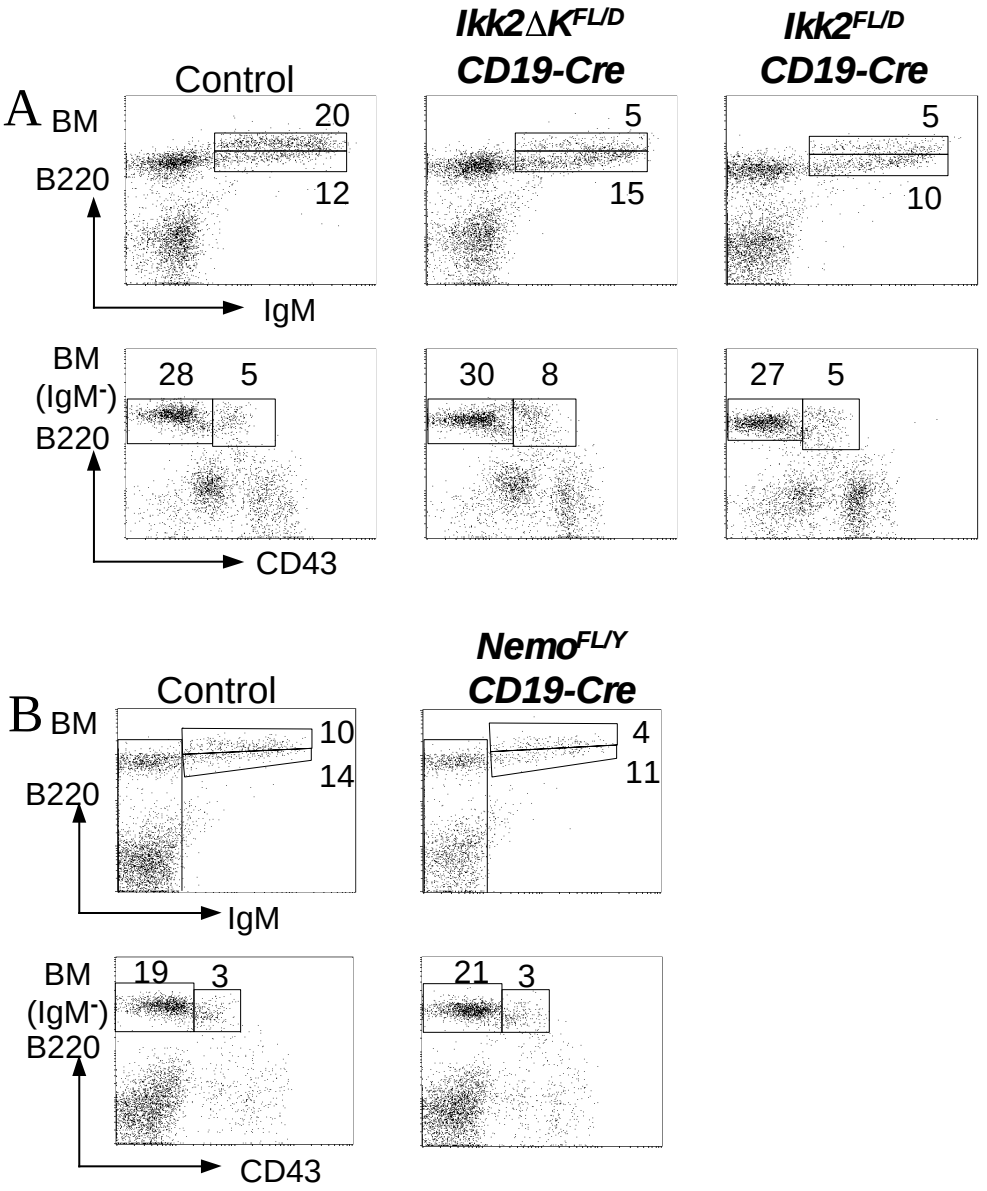

Figure 13. FACS analysis of bone marrow B cell populations.
(A) *CD19-Cre/Ikk2*$^{FL/D}$, *Ikk2*Δ*K*$^{FL/D}$ and controlsand **(B)** *CD19-Cre/Nemo*$^{FL/Y}$ and control mice. Genotypes are as indicated. Cell surface markers are shown as coordinates and gated cell populations are indicated in brackets. The numbers next to boxed lymphocyte populations refer to the percentages of live cells in the lymphocyte gate.

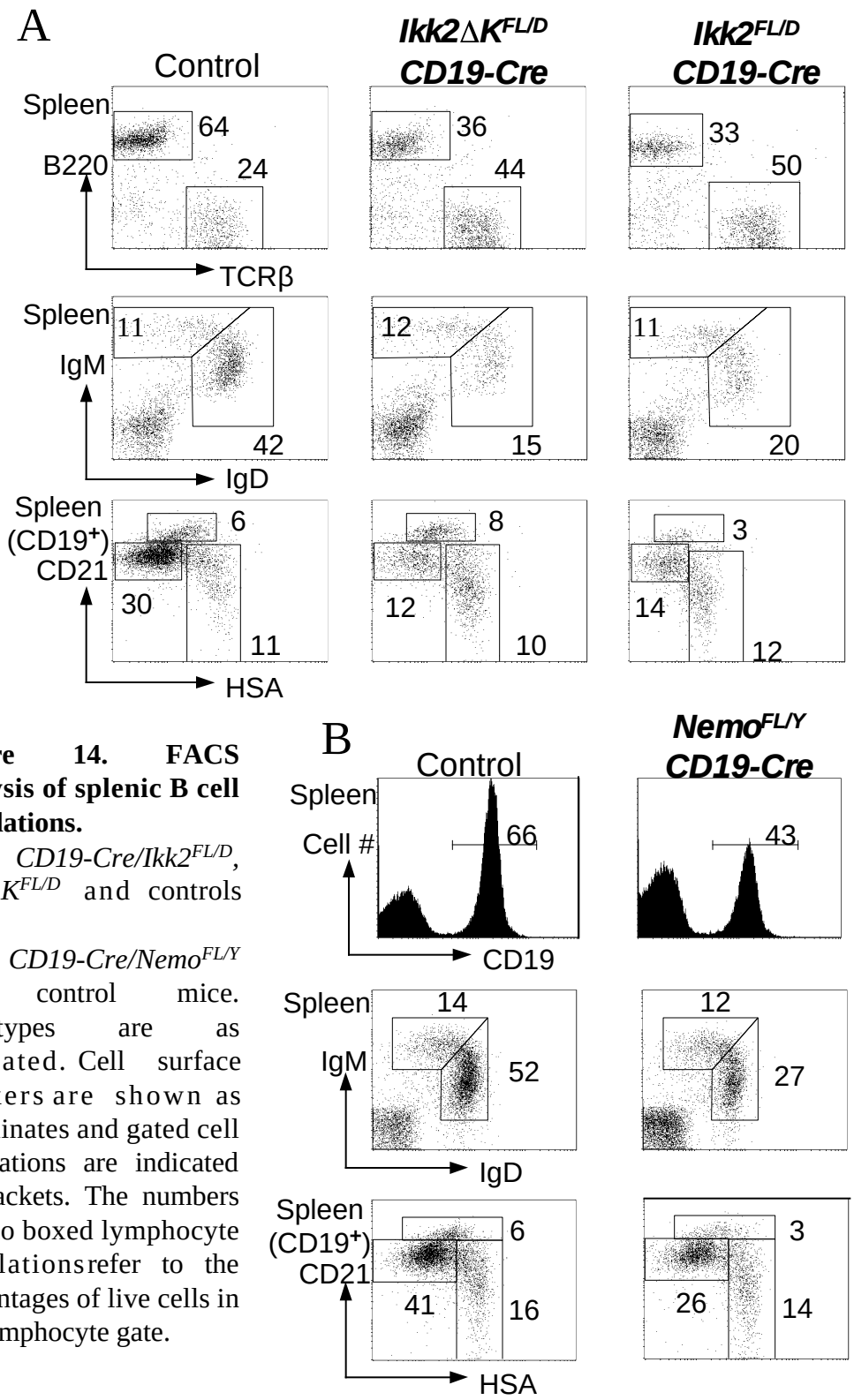

Figure 14. FACS analysis of splenic B cell populations.
(A) *CD19-Cre/Ikk2$^{FL/D}$*, *Ikk2ΔK$^{FL/D}$* and controls and
(B) *CD19-Cre/Nemo$^{FL/Y}$* and control mice. Genotypes are as indicated. Cell surface markers are shown as coordinates and gated cell populations are indicated in brackets. The numbers next to boxed lymphocyte populationsrefer to the percentages of live cells in the lymphocyte gate.

revealed that, compared to controls, the FO B cells are the most diminished B cell population in the spleens of *CD19-Cre/Ikk2*$^{FL/D}$, *-Ikk2*Δ*K*$^{FL/D}$ and *Nemo*$^{FL/Y}$ mice (Figure 14A and B**).** Lymph node B cells and both B1 and B2 cells in the peritoneal cavity of these mice were also strongly reduced compared to control mice (data not shown).

3.4.2 Reduction of Absolute B Cell Numbers in Mice with B cell Specific Ablation of NEMO or IKK2

FACS analysis showed a strong reduction of mature B cells in mice with B-cell specific ablation of NEMO or IKK2. Calculation of the absolute cell numbers of individual B cell populations in the spleens of *CD19-Cre/Ikk2*$^{FL/D}$, *-Ikk2*Δ*K*$^{FL/D}$ and *-Nemo*$^{FL/Y}$ mice revealed a 3-4 fold decrease in the total number of splenic B cells in all mutant mouse strains compared to controls (Figure 15A and Table 6). FO and MZ B cells were most severely affected (Figure 15C and D and Table 6). Analysis of IM B cells revealed a different picture in the three different mouse-strains. This population was not significantly affected in *CD19-Cre/Ikk2*$^{FL/D}$ mice, while a clear reduction was observed in *CD19-Cre/Nemo*$^{FL/Y}$ mice and *CD19-Cre/Ikk2*Δ*K*$^{FL/D}$ mice showed an intermediate picture (Figure 15B and Table 6).

Cell-Type	Controls	*CD19-Cre Ikk2*$^{FL/FL\ or\ FL/D}$	*CD19-Cre Ikk*Δ*K2*$^{FL/FL\ or\ FL/D}$	*CD19-Cre Nemo*$^{FL/Y\ or\ FL/FL}$
Total	**42.0 ±** 11.2	**12.8 ±** 1.1	**9.9 ±** 4.3	**11.9 ±** 1.7
IM	**6.1 ±** 1.6	**5.0 ±** 1.0	**2.9 ±** 1.0	**1.8 ±** 0.5
FO	**27.3 ±** 9.1	**5.5 ±** 0.5	**3.7 ±** 2.0	**8.5 ±** 1.5
MZ	**3.9 ±** 1.4	**0.9 ±** 0.2	**2.4 ±** 1.1	**1.1 ±** 0.3

Table 6. Size of B cell subsets in CD19-Cre/IKK-conditional mice compared to control mice

The average of absolute numbers of live B cells is shown in millions plus/minus standard deviation (*CD19-Cre/Ikk2*$^{FL/D\ or\ FL/FL}$: n = 3**;** *CD19-Cre/Ikk*Δ*K2*$^{FL/FL\ or\ FL/D}$: n = 5; *CD19-Cre/Nemo*$^{FL/Y\ or\ FL/FL}$: n = 4; Controls: n = 12).

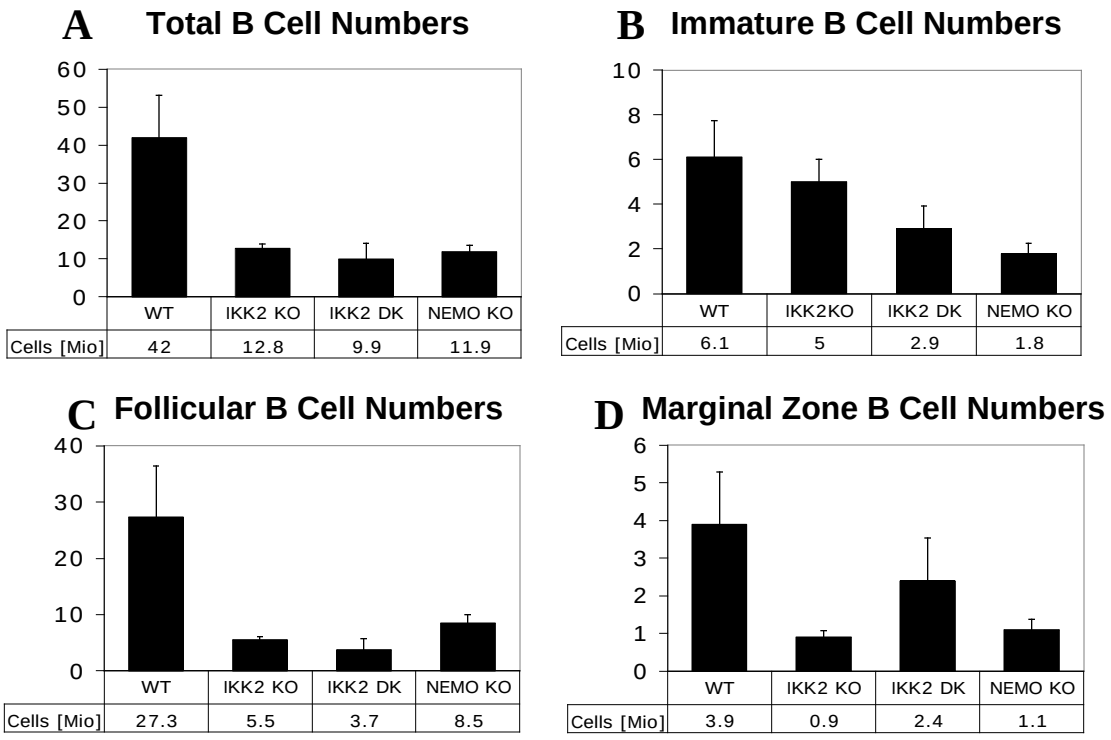

Figure 15. Reduction of B cell numbers in *CD19Cre/IKK*-conditional mice. Absolute numbers of B cell subpopulations in the spleens of *CD19-Cre/Ikk2*$^{FL/D}$, *CD19-Cre/Ikk2*Δ*K*$^{FL/D}$ and *CD19-Cre/Nemo*$^{FL/Y}$ compared to control mice are shown. **(A)** Total B cell numbers **(B)** Immature B cells **(C)** Follicular B cells **(D)** Marginal Zone B cells. Bar charts showing the absolute cell numbers for the indicated B cell population in the spleen for each of the following mouse strains: CT (controls), IKK2 KO (*CD19-Cre/Ikk2*$^{FL/D}$), IKK2 DK (*CD19-Cre/Ikk2*Δ*K*$^{FL/D}$) and NEMO KO (*CD19-Cre/Nemo*$^{FL/Y}$). For each group three to eight mice were analyzed. Error bars indicate standard deviation. The absolute cell numbers for each population were calculated by multiplying the percentage of each B cell subset of all live splenocytes obtained from the FACS analysis with the total number of live cells recovered from the perspective spleen.

3.4.3 Preferential Loss of Splenic B Cells of the Deleted Genotype in *CD19-Cre/Ikk2$^{FL/D}$*, *-Ikk2ΔK$^{FL/D}$* and *-Nemo$^{FL/Y}$* Mice

The strong decrease of peripheral B cell numbers in mice with B cell specific ablation of NEMO or IKK2 activity suggests that inhibition of IKK signaling interferes with the development or persistence of B lymphocytes. However, all different subpopulations of B cells are present in *CD19-Cre/Ikk2$^{FL/D}$*, *-Ikk2ΔK$^{FL/D}$* and *-Nemo$^{FL/Y}$* mice, although in reduced numbers. One possible explanation for this could be that the remaining cells persist because they have escaped deletion of the loxP flanked alleles.

To investigate this hypothesis I performed Southern blot analysis of DNA isolated from FACS-purified BM and splenic B cells populations from these three strains of mice. This analysis revealed that between 64-76% of bone marrow IgM$^-$ B cells had deleted the loxP-flanked alleles (Figure 16A-C). This result is in agreement with the previously reported deletion efficiency of the CD19-Cre transgene in the bone marrow (Rickert et al., 1997) and with deletion seen in *CD19-Cre/Ikk2$^{FL/WT}$* mice, in which deletion of the loxP-flanked allele has no effect due to IKK2-expression from the remaining WT allele (Figure 16D). Between 64 - 69% of the IgM$^+$ bone marrow B cells isolated from *CD19-Cre/Ikk2$^{FL/D}$*, *-Ikk2ΔK$^{FL/D}$* and *-Nemo$^{FL/Y}$* mice have deleted the loxP-flanked allele, compared to an 87% deletion of the loxP-flanked allele in *CD19-Cre/Ikk2$^{FL/WT}$* mice. This indicates that IKK-deleted IgM$^+$ bone marrow B cells are counterselected, in accordance with the reduced number of recirculating B cells in the bone marrow of these mice. While deletion was very efficient in splenic IM *CD19-Cre/Ikk2$^{FL/D}$* and *-Ikk2ΔK$^{FL/D}$* B cells (>90%), only 44-66% of FO B cells were found to have deleted the loxP flanked alleles (Figure 16 A and B). In *CD19-Cre/Ikk2$^{FL/WT}$* mice deletion was 87% and 95% for IM and FO B cells, respectively (Figure 16D). The finding that within the follicular B cell compartment there are less cells of the deleted genotype than in the immature compartment suggests that B cells lacking IKK2 activity are counter-selected as they move on to become more mature FO B cells (Figure 16A and B). In *CD19-Cre/Nemo$^{FL/Y}$* mice deletion in IM splenic B cells was less efficient than in the IKK2 loxP flanked alleles (≈70% compared to >90%) and was not further reduced in FO B cells (Figure 16C). This indicates that the cells that delete the *nemo^{FL}* allele are already counter-selected at the immature B cell stage. A more dramatic effect is seen in MZ B cells. In all three mouse strains very few cells with deleted alleles (≤12%) were found within the marginal zone B cell population, whereas in *CD19-Cre/Ikk2$^{FL/WT}$* mice

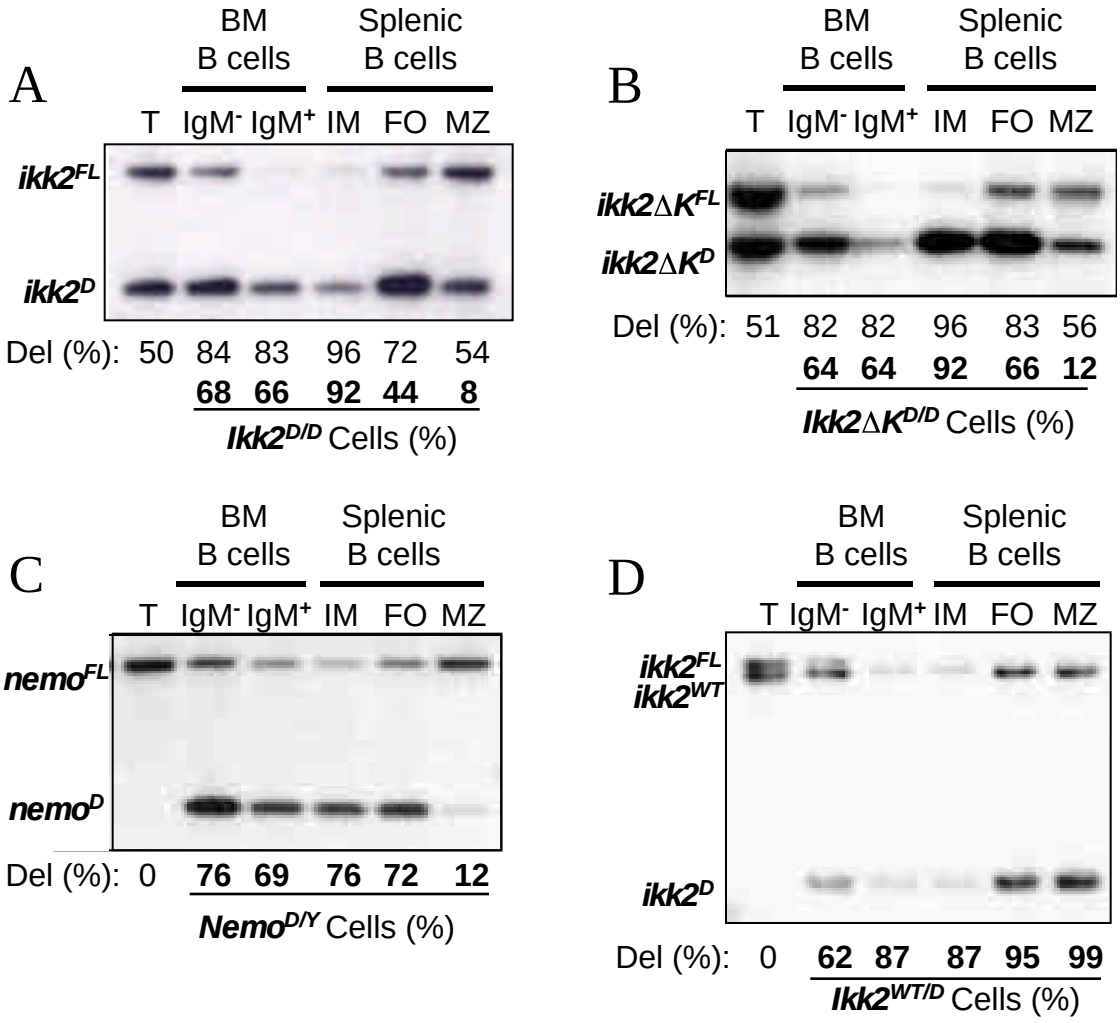

Figure 16. Counterselection against $Ikk^{D/D}$-, $Ikk2\Delta K^{D/D}$ and $Nemo^{D/Y}$ B cells in the spleen. Southern blot analyses of sorted splenic B cell populations of mice of the indicated genotypes are shown. **(A)** *CD19-Cre/*$Ikk2^{FL/D}$ mice, **(B)** *CD19-Cre/*$Ikk2\Delta K^{FL/D}$ mice, **(C)** *CD19-Cre/*$Nemo^{FL/Y}$ mice, **(D)** *CD19-Cre/*$Ikk2\Delta K^{FL/WT}$ mice. T (Tail), IgM- ($CD19^{+}B220^{+}IgM^{-}$ = pro- and pre-B cells), IgM^{+} ($CD19^{+}B220^{+}IgM^{+}$ B cells), IM ($CD19^{+}CD21^{low}HSA^{high}$ = Immature B cells), FO($CD19^{+}CD21^{int}HSA^{-}$ = Follicular B cells), MZ ($CD19^{+}CD21^{high}HSA^{int}$ = Marginal Zone B cells). The percentage of deleted alleles and cells of the deleted genotype is given below the blots. Each blot is a representative example of at least 4 mice analyzed. Del(%) = Percent of deleted alleles.

deletion was virtually complete, suggesting that IKK activity is essential for the development or maintenance of these cells (Figure 16 A-D).

Based on the above data I envisage the following scenario: Ongoing deletion continuously leads to the generation of B cells that have deleted the respective gene, but still retain enough protein to stay alive. With time and through turnover of endogenous mRNAs and proteins these cells lose their ability to signal via the IKK complex and die. Continuous influx of newly generated B cells from the BM and continuous Cre-mediated deletion of the loxP flanked alleles leads to the deletion pattern observed in B cells of *CD19-Cre/Ikk2*$^{FL/D}$, *-Ikk2*Δ*K*$^{FL/D}$ and *-Nemo*$^{FL/Y}$ mice. This scenario predicts a higher turnover rate of mutant compared to control B cells.

3.4.4 *CD19-Cre/Ikk2*Δ*K*$^{FL/D}$ and *CD19-Cre/Nemo*$^{FL/Y}$ B Cells Have Higher *in vivo* Turnover Rates than Wild-type Control B Cells

To test this hypothesis I determined the percentage of BrdU-labeled B cells of the various B cell subpopulations in BM and spleens of *CD19-Cre/Nemo*$^{FL/Y}$ and control mice that had been fed with BrdU for one week (Figure 17). In the BM B220+/IgD- slightly more *CD19-Cre/Nemo*$^{FL/Y}$ B cells incorporated BrdU then control B cells (Figure 17A). After one week of BrdU-administration in the drinking water the proportion of BrdU-labeled splenic B cells is around 10 % (Forster and Rajewsky, 1990). These most likely represent newly formed B cells that arrived recently from the bone marrow, since peripheral B cells have a long life-span and do not proliferate a lot (Forster and Rajewsky, 1990; Hao and Rajewsky, 2001). An increase in percentage of BrdU-positive B cells in the spleen therefore would indicate a higher rate of B cell renewal in the spleen. Approximately twice as many *CD19-Cre/Nemo*$^{FL/Y}$ BM recirculating, IM, FO and MZ B cells in the spleen incorporated BrdU compared to control B cells Figure 17 B). This result shows that B cell turnover in the spleen of *CD19-Cre/Nemo*$^{FL/Y}$ mice is significantly faster than in wild-type animals. The percentage of BrdU-positive B cells within each subpopulation reflects the cellular turnover. The increased B cell turnover in *CD19-Cre/Nemo*$^{FL/Y}$ mice suggests that IKK mutant splenic B cells have a shorter half-life then control B cells.

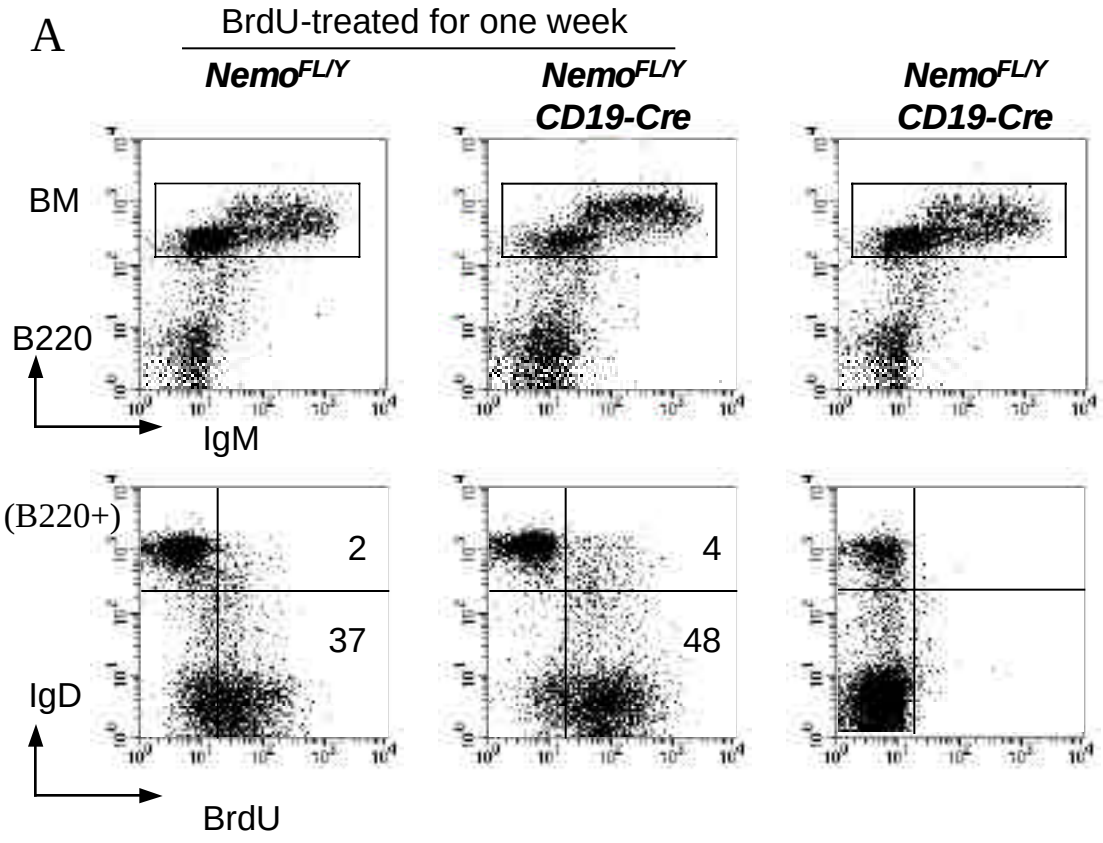

Figure 17. IncreasedB cell turnoverin *CD19-Cre/Nemo$^{FL/Y}$* mice compared to control mice.

Analysis of BrdU incorporation by bone marrow **(A)** and splenic **(B)** B cells of mice of the indicated genotypes after one week of BrdU administration in the drinking water. Cell surface markers are shown as coordinates and gated cell populations are indicated in brackets, all populations are gated on live lymphocytes. Numbers indicate percentages of BrdU-positive B cells of gated populations. B220+ (bone marrow B cells), IM ($CD19^{+}CD21^{low}HSA^{high}$ = Immature B cells), FO($CD19^{+}CD21^{int}HSA^{-}$ = Follicular B cells), MZ ($CD19^{+}CD21^{high}HSA^{int}$ = Marginal Zone B cells).

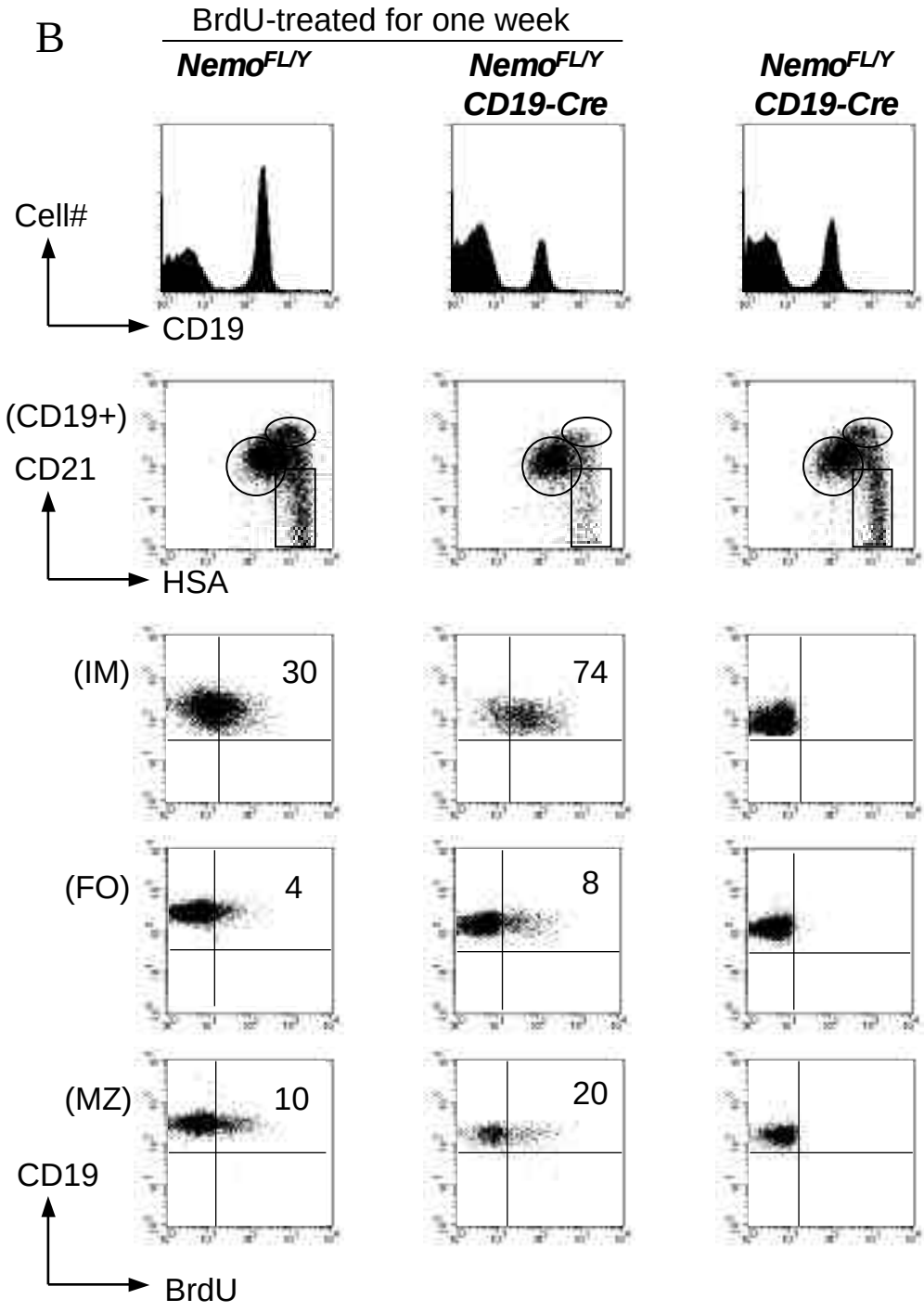
B
BrdU-treated for one week
Nemo^FL/Y
Nemo^FL/Y CD19-Cre
Nemo^FL/Y CD19-Cre
Cell#
CD19
(CD19+)
CD21
HSA
(IM)
30
74
(FO)
4
8
(MZ)
10
20
CD19
BrdU

3.4.5 Blockade of *de novo* B Cell Generation in *CD19-Cre/Ikk2*Δ*K*$^{FL/D}$ Mice leads to Disappearance of IKK2-deficient B Cells from the Spleen.

During B cell development peripheral B cells are continuously generated from the bone marrow. I decided to evaluate whether *CD19-Cre/Ikk2*Δ*K*$^{FL/D}$ B lineage lymphocytes that underwent Cre-mediated deletion can persist in the spleen by blocking influx of IM B cells from the bone marrow. This was achieved by injection of antagonistic monoclonal antibodies against the interleukin-7 receptor (IL-7R). This treatment blocks B cell development at the pro-B cell stage and thus abolishes the influx of IM B cells from the bone marrow into the periphery (Sudo et al., 1993).

After four weeks of anti-IL-7R antibody administration FACS analysis demonstrated that B cell development in the bone marrow and the influx of newly generated B cells into the spleen is indeed inhibited in antibody-treated mice (Figure 18A). Southern blot analysis of DNA isolated from purified splenic B cells of these mice revealed the absence of *Ikk2*Δ*K*$^{D/D}$ B cells (Figure 18C), whereas in untreated *CD19-Cre/Ikk2*Δ*K*$^{FL/D}$ mice 50 to 80 % of the CD19-positive splenic B cells have exon-deleted both loxP-flanked *ikk2*Δ*K* alleles (Figure 18B). This finding validates the view that the B cells with two exon-deleted *ikk2*Δ*K* alleles that are found in the spleens of *CD19-Cre/Ikk2*Δ*K*$^{FL/D}$ mice are cells that have only recently undergone Cre-mediated recombination and still retain IKK2 protein. As soon as the influx from the bone marrow is blocked, no new B cells having freshly acquired the deleted genotype enter the spleen from the bone marrow. Within a period of 4 weeks all B cells lacking IKK2 activity disappear from the spleen and only cells that have escaped Cre-mediated deletion of the loxP flanked alleles persist. These results demonstrate that IKK-mediated NF-κB activity is essential for the survival of mature B cells.

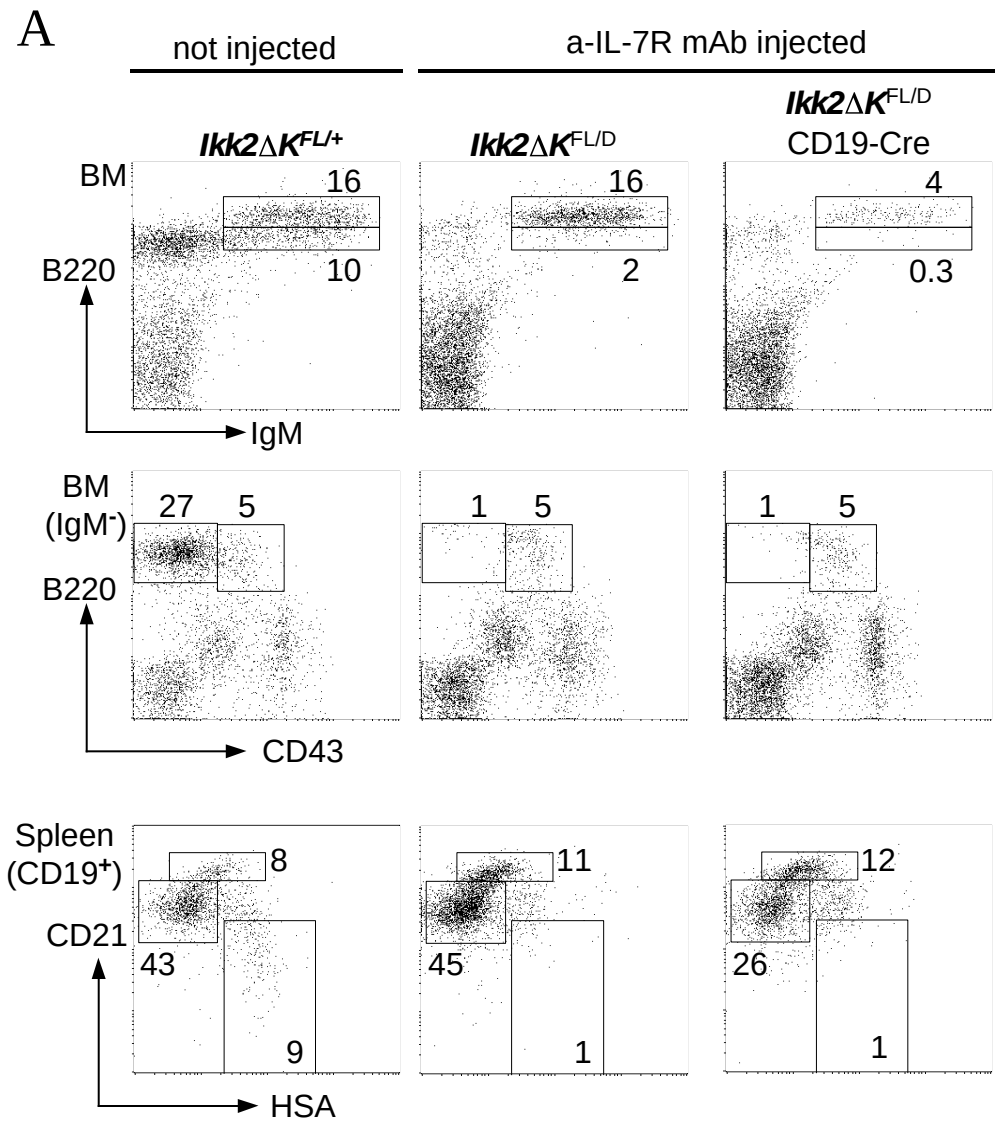

Figure 18. Block of B cell influx from the bone marrow leads to disappearance of B cells of the deleted genotype in the spleen.
(A) Verification of the block in B cell development after injection of anti IL-7R Antibodies by FACS analysis. Non-injected control mice are compared to mice that had received injections of anti IL-7R antibodies for four weeks. The genotypes are as indicated above and cell surface markers are shown as coordinates and gated cell populations are indicated in brackets. The numbers next to boxed lymphocyte populations refer to the percentages of live cells in the lymphocyte gate.

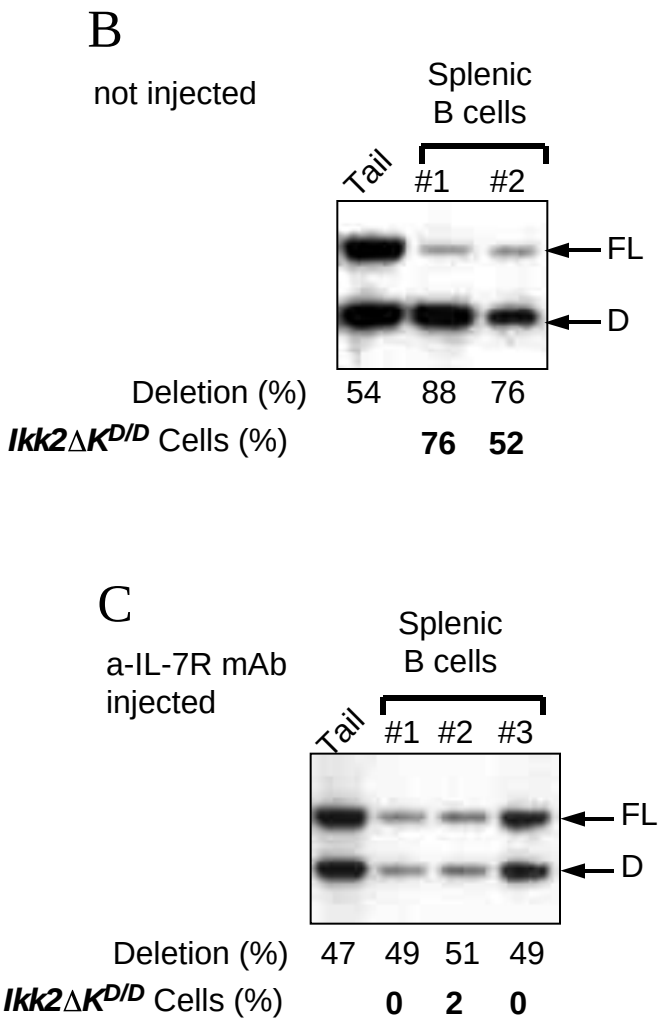

(B) Southern blot analysis of Cre mediated deletion in total splenic B cells from two different (#1,#2) *CD19-Cre/Ikk2*Δ$K^{FL/D}$ mice. The results are representative of six different mice.
(C) Southern blot analysis of Cre mediated deletion in total splenic B cells from three different (#1-3) *CD19-Cre/Ikk2*Δ$K^{FL/D}$ mice that received anti IL-7R Antibody injections for four weeks.

3.5 The Role of the IKK Complex in Mature T Cell Development

3.5.1 Naive T Cell Survival Does Not Depend on IKK2, but Lack of NEMO is Incompatible With T Cell Generation and/or Persistence

To investigate the role of IKK signaling in T lymphocytes, I sought to inhibit IKK activity specifically in T lineage cells by crossing *Ikk2*$^{FL/FL}$ and *Nemo*$^{FL/Y}$ mice with transgenic mice expressing Cre under the control of the CD4-promoter.

Cell-Type	*CD4-Cre* *Ikk2*$^{FL/FL\ or\ FL/D}$	*CD4-Cre* *Nemo*$^{FL/Y\ or\ FL/FL}$	Controls
CD8-SP	**2.29 ±** 0.28	**1.28 ±** 0.16	**2.11 ±** 0.42
CD4-SP	**7.67 ±** 0.65	**6.32 ±** 0.53	**7.59 ±** 0.90
DP	**85.36 ±** 1.98	**86.41 ±** 2.31	**85.61 ±** 2.13
DN	**2.69 ±** 0.56	**3.88 ±** 2.30	**3.43 ±** 1.33
CD4-SP/HSA$^{high+int}$	**84.08 ±** 1.79	**91.34 ±** 4.16	**82.63 ±** 2.21
/HSA^{low}	**16.54 ±** 2.14	**8.74 ±** 4.24	**17.41 ±** 2.30
CD8-SP/HSA^{high}	**17.06 ±** 3.89	**38.60 ±** 7.76	**19.54 ±** 5.40
/HSA^{int}	**52.01 ±** 5.77	**54.48 ±** 13.03	**50.84 ±** 5.16
/HSA^{low}	**30.80 ±** 4.20	**4.83 ±** 2.27	**30.11 ±** 2.31
TCR^{high}/CD8-SP	**15.32 ±** 1.62	**6.27 ±** 1.09	**13.39 ±** 2.18
/CD4-SP	**62.86 ±** 3.90	**65.79 ±** 4.59	**65.42 ±** 3.93
/DP	**20.59 ±** 5.12	**24.62 ±** 4.88	**20.07 ±** 4.85

Table 7. Percentages of thymocyte subpopulations in CD4-Cre/IKK-conditional and control mice.
Cell-types, genotypes and the number of mice analyzed per group are indicated. Average percentages of total thymocytes are shown in bold numbers plus/minus standard deviations (*CD4-Cre/Ikk2*$^{FL/D\ or\ FL/FL}$: n = 10**;** *CD4-Cre/Nemo*$^{FL/Y\ or\ FL/FL}$: n = 7; Controls: n = 17). Total thymocyte numbers do not vary significantly between the individual groups.

CD4-Cre mice are reported to delete loxP-flanked alleles in the T lineage with very high efficiency (Lee et al., 2001; Wolfer et al., 2001) (Figure 19). FACS analysis of T cell populations in *CD4-Cre/Ikk2*$^{FL/D}$ mice revealed that thymocyte development is unperturbed (Figure 20 and Table 7).

In the periphery, however, the number of T cells is reduced, the deficit being more pronounced in CD8 cells (Figures 20, 25A and B). Similar analyses in *CD4-*

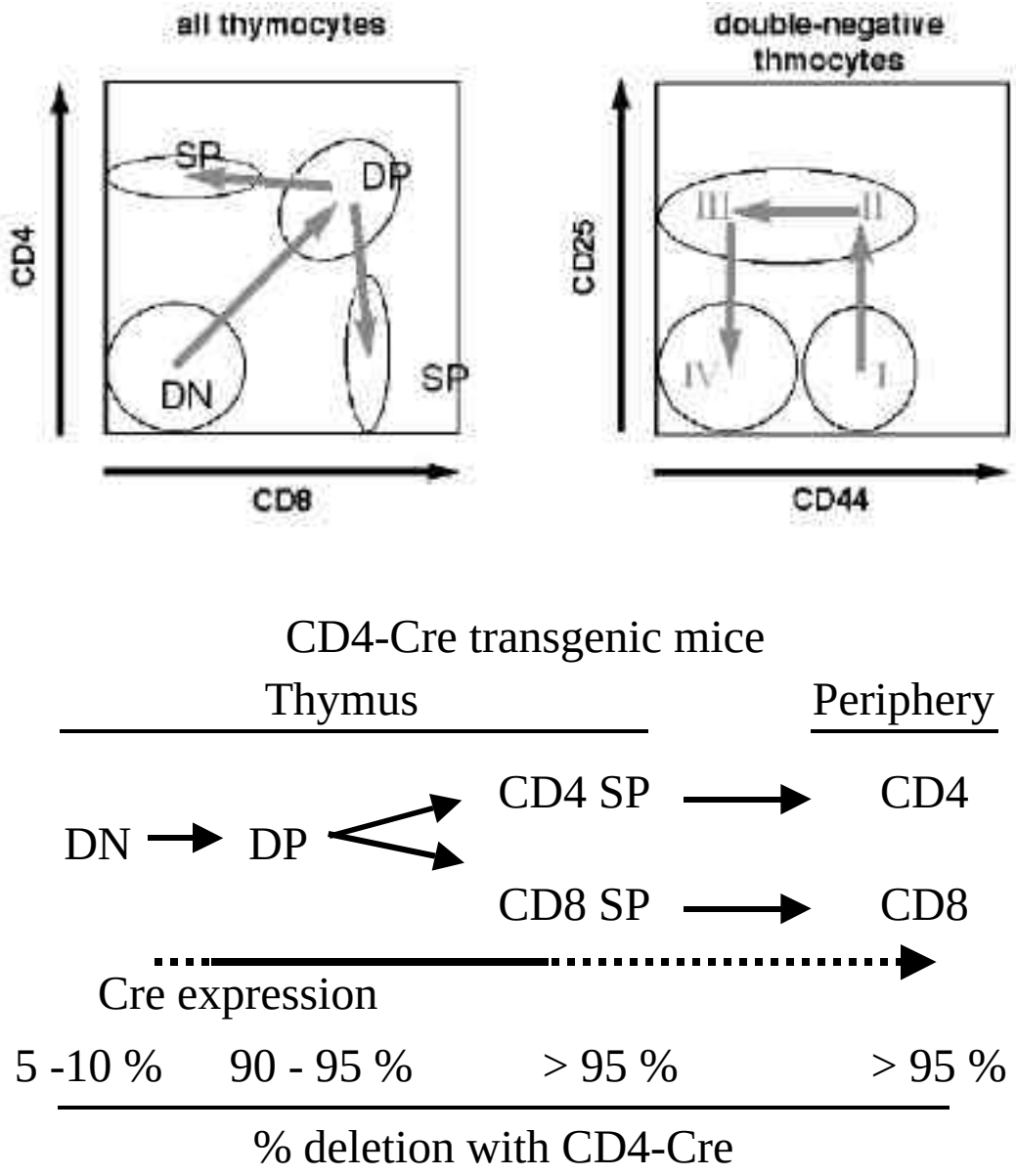

Figure 19. Sketch of T cell development in the thymus and deletion efficiency of the *CD4-Cre* mouse line

In the thymus T cell development can be visualized by the expression of the coreceptors CD4 and CD8. Thymocytes pass from the double-negative (DN) through the double-positive (DP) to the respective single-positive (SP) stages. Then they exit as CD4 and CD8 T cells into the periphery. Deletion of *loxP*-flanked alleles by the *CD4-Cre* transgeneis essentially complete from the DP-stage on.

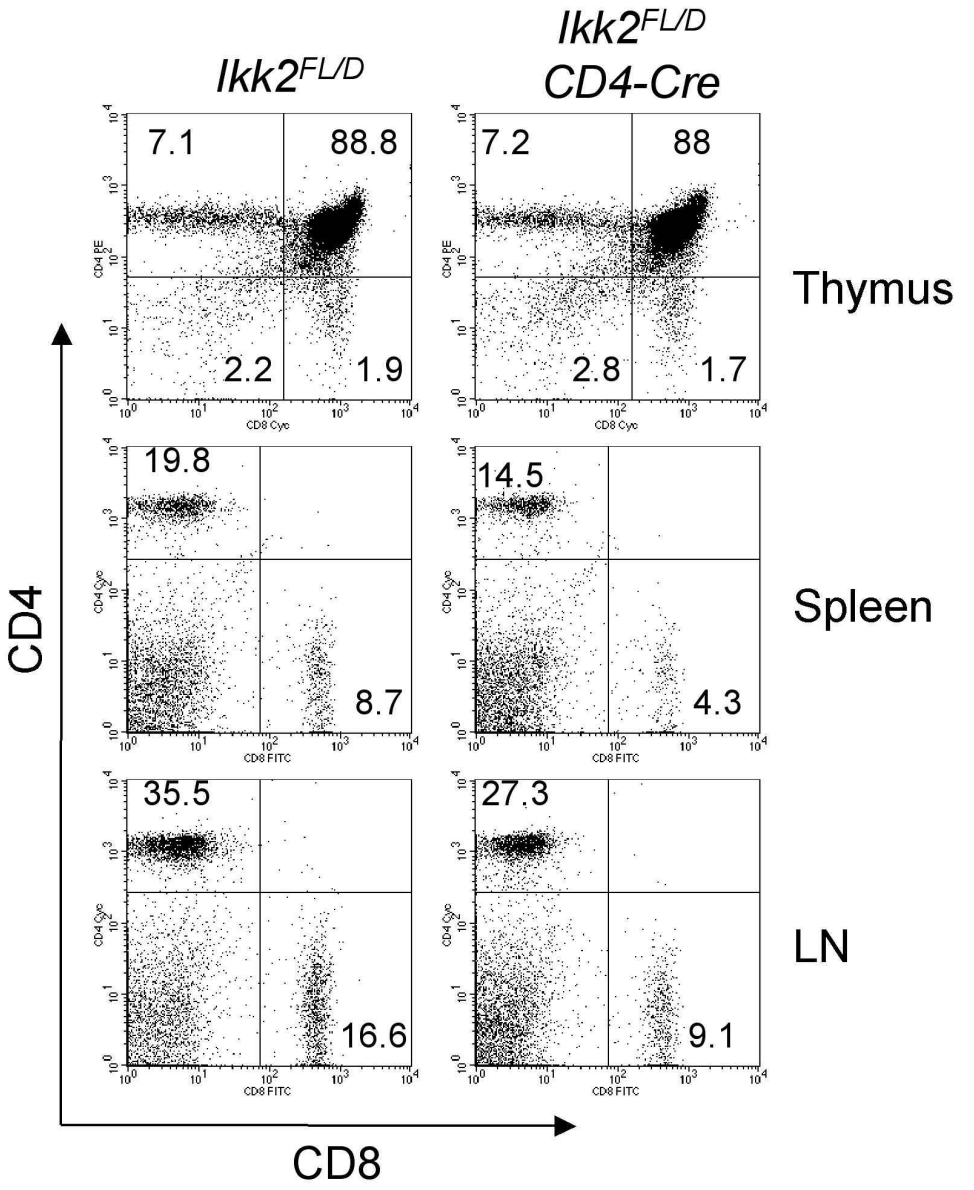

Figure 20. FACS analysis of T cell populations in *CD4-Cre/Ikk2$^{FL/D}$* mice compared to control mice.

Genotypes are as indicated. Cell surface markers are shown as coordinates. The numbers in the quadrants refer to the percentages of this T cell population of live cells in the lymphocyte gate.

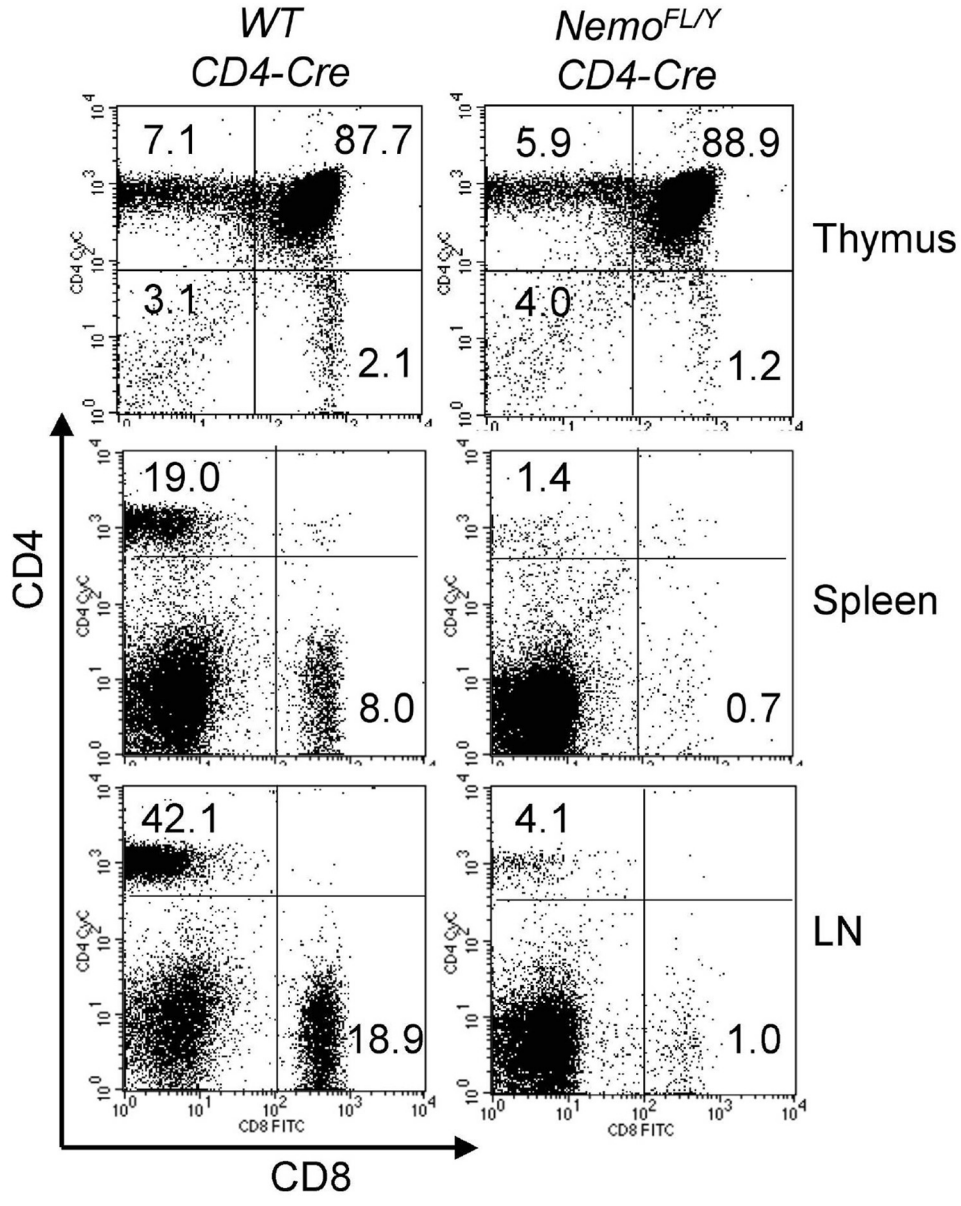

Figure 21. FACS analysis of T cell populations in *CD4-Cre/Nemo*$^{FL/Y}$ mice compared to control mice.

Genotypes are as indicated. Cell surface markers are shown as coordinates. The numbers in the quadrants refer to the percentages of this T cell population of live cells in the lymphocyte gate.

Cre/Nemo$^{FL/Y}$ mice showed a different picture. In the thymus of these mice the population of CD8 single positive cells is a little more than half the size of that of control mice while CD4 single positive cells are only mildly reduced (Figure 21 and Table I). Spleen and LN of *CD4-Cre/Nemo*$^{FL/Y}$ mice are nearly devoid of mature T cells (Figure 21). Deletion of floxed alleles by Cre transgenes is not always complete, especially when cells that have deleted their loxP-flanked alleles are counter-selected (Pasparakis et al., 2002b; Rajewsky et al., 1996). Therefore I assessed the genotype of the T cell populations found in the two CD4-Cre/IKK-conditional mouse strains. Deletion of only one out of two loxP-flanked alleles can cause problems for the assessment of deletion efficiency by Southern blot. In *CD4-Cre/Ikk2*$^{FL/FL}$ mice, for example, it is impossible to determine from a Southern blot to what extent the bands representing the loxP-flanked and the deleted alleles stem from *Ikk2*$^{FL/D}$ T cells and to what extent they stem from *Ikk2*$^{FL/FL}$ and *Ikk2*$^{FL/D}$ T cells. In order to avoid complications caused by this "incomplete" deletion, I used mice in which only one loxP flanked allele remains to be deleted (*CD4-Cre/Ikk2*$^{FL/D}$ and *-Nemo*$^{FL/Y}$*)* for monitoring deletion by Southern blot.

Southern blot analysis of DNA prepared from sorted T cell populations from *CD4-Cre/Ikk2*$^{FL/D}$ mice shows that in double positive and in single positive thymocytes, and in CD4 and CD8 T cells in the spleen and lymph nodes deletion of the loxP flanked allele is essentially complete (Figure 22A). The faint band representing loxP-flanked alleles that can be observed for CD8 SP thymocytes is most likely due to immature CD8 SP cells. These cells are immature, large, outer-cortical cells that lack the TCR complex but express CD8 (Shortman et al., 1988). Maturation of single-positive thymocytes is normal in *CD4-Cre/Ikk2*$^{FL/D}$ mice; CD8- and CD4-SP thymocytes have the same expression profile of HSA (CD24) (Figure 24A and Table). Loss of HSA-expression can be correlated to increased maturation of single-positive thymocytes. Similarly the CD4 versus CD8 ratio is normal in TCR^{high} thymocytes of *CD4-Cre/Ikk2*$^{FL/D}$ mice (Figure 24B and Table). To demonstrate that inactivation of the *Ikk2* gene in T cells of these mice leads to T cells lacking IKK2, I analyzed extracts from thymocytes and peripheral CD4 T cells by western blotting. This analysis showed that *Ikk2*$^{D/D}$ thymocytes still contain IKK2 protein (Figure 22B), probably owing to the long half-life of IKK2 (approximately 13 h in monocytic cell-lines) (Fischer et al., 1999). This means that even though thymocytes isolated from *CD4-Cre/Ikk2*$^{FL/D}$ are genetically *Ikk2*$^{D/D}$, they are not IKK2-deficient since they still contain IKK2 protein.

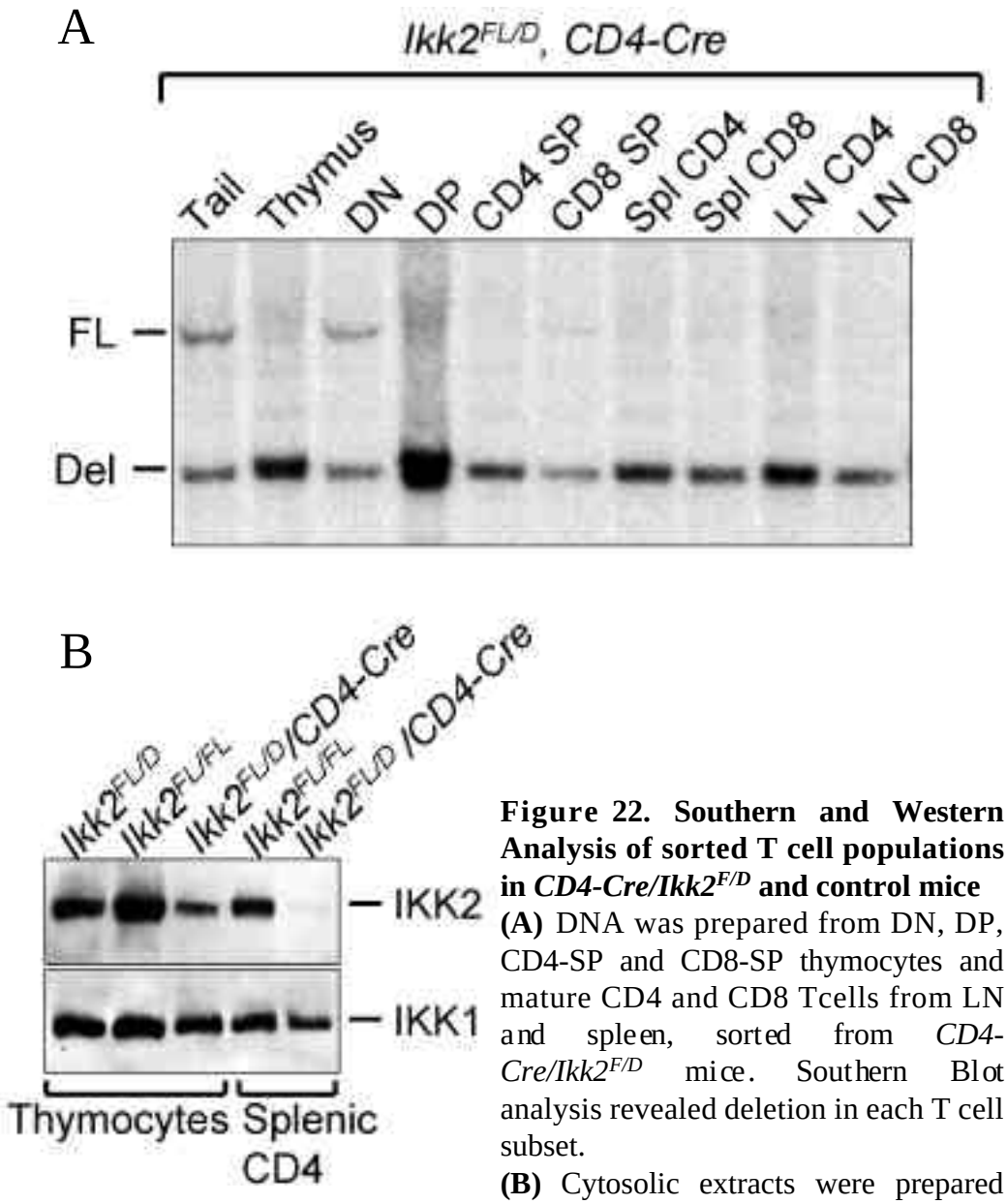

Figure 22. Southern and Western Analysis of sorted T cell populations in *CD4-Cre/Ikk2$^{F/D}$* and control mice

(A) DNA was prepared from DN, DP, CD4-SP and CD8-SP thymocytes and mature CD4 and CD8 Tcells from LN and spleen, sorted from *CD4-Cre/Ikk2$^{F/D}$* mice. Southern Blot analysis revealed deletion in each T cell subset.

(B) Cytosolic extracts were prepared from thymocytes and splenic CD4 T cells sorted from *CD4-Cre/Ikk2$^{F/D}$* and *Ikk2$^{F/FL}$* and *Ikk2$^{F/D}$* control mice. IKK2 levels in these cells are revealed by Western blotting. IKK1 levels serve as loading control.

Peripheral T cells in these mice are, on the other hand, truly IKK2-deficient, since no IKK2 protein could be detected in splenic *Ikk2*$^{D/D}$ CD4 T cells (Figure 22B).

Deletion of the loxP-flanked alleles is complete in DP and CD4-SP thymocytes of *CD4-Cre/Nemo*$^{FL/Y}$ mice,which carry only one *nemo*^{FL} allele, similar to *CD4-Cre/Ikk2*$^{FL/D}$ mice (Figure 23A). Western Blot analysis showed strong reduction of NEMO levels in DP and nearly complete absence of NEMO in CD4-SP thymocytes isolated from *CD4-Cre/Nemo*$^{FL/Y}$ compared to control mice (Figure 23 B and C). Southern blot analysis of the remaining peripheral T cells of *CD4-Cre/Nemo*$^{FL/Y}$ mice revealed that in the periphery of *CD4-Cre/Nemo*$^{FL/Y}$ mice virtually all deleted cells have disappeared. Only a weak band representing cells of the deleted genotype can be detected in DNA prepared from CD4 T cells (Figure 23A). This shows that the few T cells that are left in *CD4-Cre/Nemo*$^{FL/Y}$ mice are T cells in which deletion of the loxP-flanked alleles did not occur. These T cells accumulate in the periphery, whereas T cells of the deleted genotype cannot persist.

This view is supported by further FACS analysis: in the CD8-SP compartment of *CD4-Cre/Nemo*$^{FL/Y}$ mice the number of HSA^{++} immature CD8-SP thymocytes is equal, but there is a decrease in HSA^{int} cells and there are only very few HSA^{low} mature cells (Figure 24A and Table 7). This is paralleled by a reduction in TCR^{high} CD8-SP thymocytes (Table 7). It seems that after deletion of the loxP-flanked alleles the endogenous IKK2 or NEMO mRNA and protein are gradually lost through turn-over while the cells mature. Thymocytes and T cells that lack NEMO cannot survive and are lost. Also the HSA^{low} CD4-SP compartment is reduced (Table 7), albeit to a lesser extent. The remaining peripheral T cells in *CD4-Cre/Nemo*$^{FL/Y}$ mice express high levels of CD44, which is characteristic for T cells that undergo homeostatic expansion in a lymphopenic environment and become memory-type T cells (data not shown)(Goldrath, 2002; Goldrath et al., 2000; Surh and Sprent, 2000).

To ascertain that the effects seen in the CD4-Cre/IKK-conditional mice are due to T cell intrinsic defects I analyzed dendritic cell populations in *CD4-Cre/Ikk2*$^{FL/D}$ and -*Nemo*$^{FL/Y}$ mice compared to control mice. These mice contain normal numbers of CD11c^{+}CD4^{+} and CD11c^{+}CD8^{+} dendritic cells. Southern blot analysis of DNA from MACS-purified dendritic cells showed that the CD4-Cre transgene does not induce deletion of *ikk2*^{FL} or *nemo*^{FL} alleles in dendritic cells. I also did not detect deletion at the DNA level from FACS-purified B cells from *CD4-Cre/Ikk2*$^{FL/D}$ mice (data not shown).

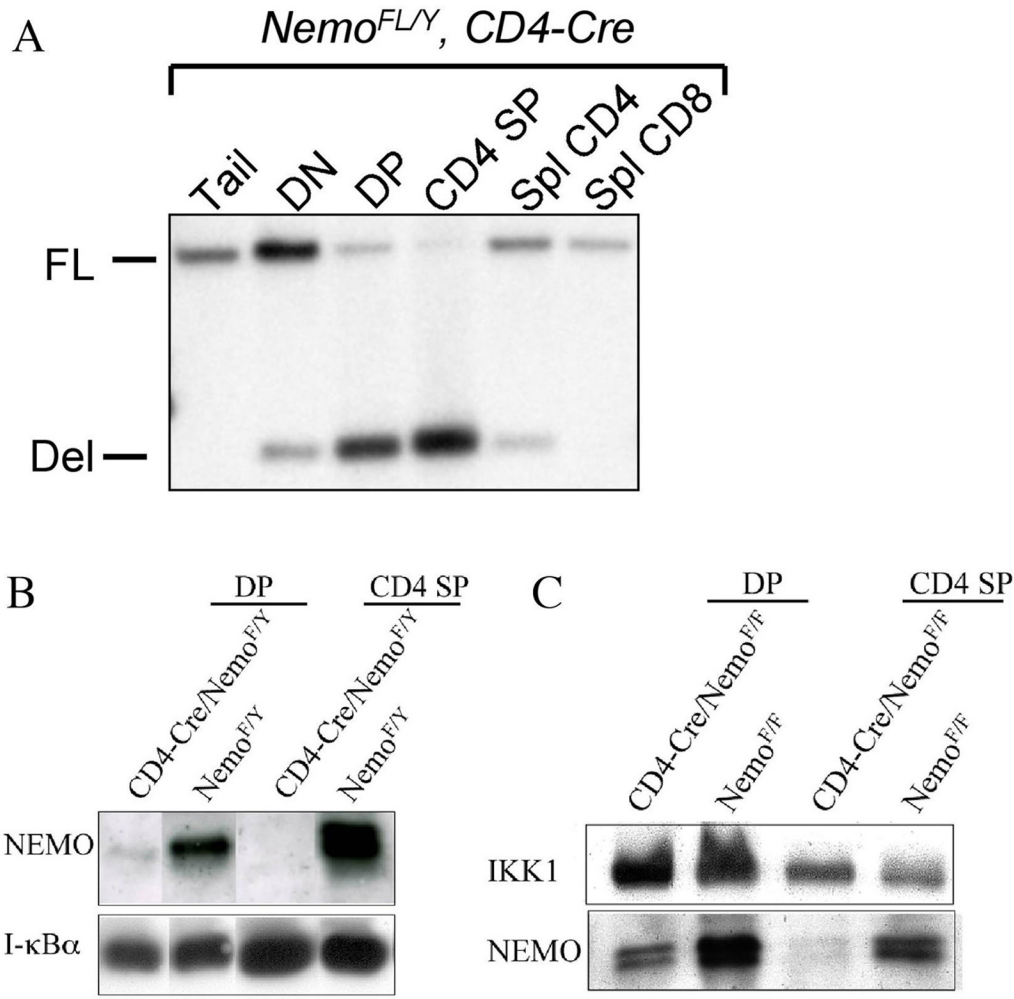

Figure 23. Southern and Western Analysis of sorted T cell populations in *CD4-Cre/Nemo$^{F/Y}$* and control mice

(A) DNA was prepared from DN, DP and CD4 SP thymocytes and mature CD4 and CD8 Tcells from the spleen, sorted from *CD4-Cre/Nemo$^{F/Y}$* mice. Southern Blot analysis revealed the deletion in each T cell subset. One representative experiment out of three is shown.

(B) Cytosolic extracts were prepared from DP and CD4 SP thymocytes sorted from *CD4-Cre/Nemo$^{F/Y}$* and *Nemo$^{F/Y}$* control mice. NEMO levels in these cells are revealed by Western blotting. IκB-α levels serve as loading control.

(C) Cytosolic extracts were prepared from DP and CD4 SP thymocytes sorted from *CD4-Cre/Nemo$^{F/F}$* and *Nemo$^{F/F}$* control mice. NEMO levels in these cells are revealed by Western blotting, IKK1 levels demonstrate equal loading.

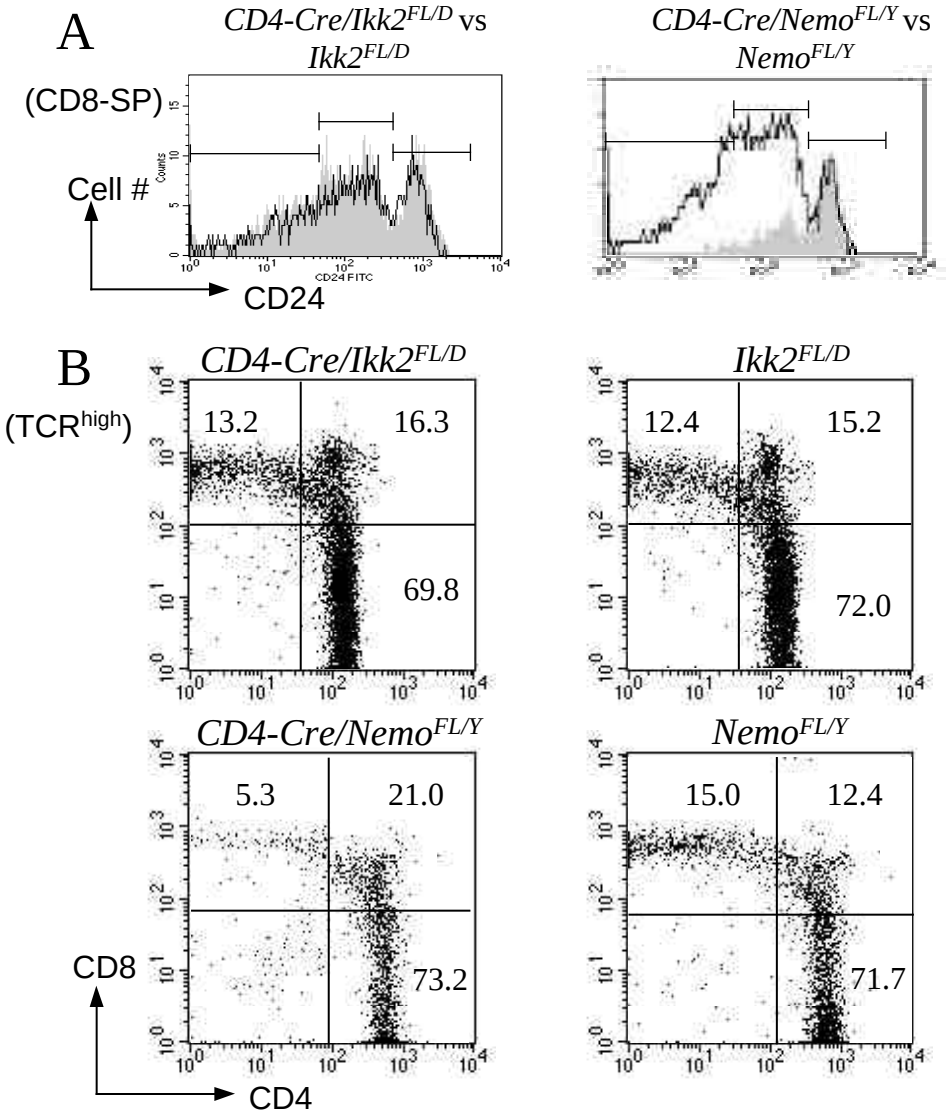

Figure 24. FACS analysis of single-positive thymocyte development in *CD4-Cre/Nemo$^{FL/Y}$* and *CD4-Cre/Ikk2$^{FL/D}$ mice* compared to control mice.
(A) Histogram of CD24 expression on CD8-SP thymocytes. White histograms show control cells and grey histograms *CD4-Cre/Ikk2$^{FL/D}$* or *CD4-Cre/Nemo$^{FL/Y}$*, respectively.
(B) Dotblots showing CD4 versus CD8 expression in TCR^{high} thymocytes. Genotypes are as indicated and gated cell populations are indicated in brackets. Cell surface markers are shown as coordinates. Numbers refer to the percentage of the respective T cell population of live cells in the lymphocyte gate or of the gated cell population indicated in brackets.

3.5.2 *CD4-Cre/Ikk2$^{FL/D}$* Mice Have Reduced CD25 and CD44 CD4 T Cell Compartments.

In the spleen and LN of *CD4-Cre/Ikk2$^{FL/D}$* mice the CD4 T cell compartment is reduced by approximately 20% and the CD8 T cell compartment by over 50% compared to control mice (Figures 25A and B and Table 8).

Organ	Cell-Type	*CD4-Cre* *Ikk2$^{FL/D\ or\ FL/FL}$*	*Ikk2$^{FL/D\ or\ FL/FL}$*
Spleen	CD4	**13.93 ±** 3.57	**17.75 ±** 3.93
	CD8	**5.54 ±** 1.94	**12.58 ±** 3.83
	B cells	**73.80 ±** 5.86	**58.17 ±** 10.12
LN	CD4	**7.54 ±** 3.57	**10.53 ±** 3.02
	CD8	**2.87 ±** 1.02	**7.70 ±** 2.25
	B cells	**15.06 ±** 6.88	**10.80 ±** 5.67

Table 8. Absolute B and T cell numbers in spleen and lymph nodes
Averages of absolute numbers of live B and T cells are shown in bold in millions plus/minus standard deviation (*CD4-Cre/Ikk2$^{FL/D\ or\ FL/FL}$*: n = 11**;** *Ikk2$^{FL/D\ or\ FL/FL}$*: n = 11).

In normal mice around 10 % of the CD4 T cells co-express the interleukin-2 receptor (IL-2R; CD25) α-chain (Asano et al., 1996). These $CD4^+CD25^+$ T cells are suggested to be generated in the thymus and it has been shown, by various *in vitro* and *in vivo* experiments, that they downregulate immune responses and inhibit development of autoimmune diseases (for recent reviews see (Curotto de Lafaille and Lafaille, 2002; Read and Powrie, 2001; Shevach, 2001; Shevach, 2002); they are therefore termed suppressor or regulatory T cells. T cell populations with immuno-suppressive properties have also been found within the $CD4/CD25^-$ T cell pool. Other CD4 T cell fractions that were shown to contain T cells with regulatory function are the $CD45Rb^{low}$ (Powrie et al., 1993) and $\alpha_E\beta_7$ (CD103)-positive (Lehmann et al., 2002) populations. In thymus, spleen and LN of *CD4-Cre/Ikk2$^{FL/D}$* mice very few $CD4^+CD25^+$ T cells can be found (Figure 25C and E and Table 9). This does not reflect the inability of *Ikk2$^{D/D}$* T cells to express CD25, since these cells upregulate CD25 *in vitro* in response to various

stimuli, such as antibodies against CD3, CD3 and CD28, PMA/Iono or ConA over a period of five days as efficiently as WT T cells (data not shown).

Organ	*CD4-Cre* *Ikk2*$^{FL/D\ or\ FL/FL}$	*Ikk2*$^{FL/D\ or\ FL/FL}$
Thymus	**1.17 ±** 0.26	**4.09 ±** 0.54
Spleen	**3.70 ±** 1.06	**13.10 ±** 3.20
LN	**3.38 ±** 2.00	**11.75 ±** 2.12

Table 9. Percentage of CD4$^+$CD25$^+$ T cells of total CD4 T cells in thymus, spleen and lymph nodes
Average numbers are shown in millions plus/minus standard deviation (*CD4-Cre/Ikk2*$^{FL/D\ or\ FL/FL}$: n = 10**;** *Ikk2*$^{FL/D\ or\ FL/FL}$: n = 10).

This lack of CD4$^+$CD25$^+$ T cells is paralleled by a similar deficiency in CD45Rb^{low} cells in *CD4-Cre/Ikk2*$^{FL/D}$ mice (data not shown), suggesting that these mice have a severe deficiency in regulatory T cell populations defined by these markers. No significant difference in $\alpha_E\beta_7$-expressing T cell numbers was found between *CD4-Cre/Ikk2*$^{FL/D}$ and control mice (data not shown). WT CD4$^+$CD25$^+$ T cells in spleen and LNs are smaller, as assessed by forward scatter, than those in the thymus, possibly reflecting a maturation process; in contrast peripheral CD4$^+$CD25$^+$ T cells isolated from *CD4-Cre/Ikk2*$^{FL/D}$ mice are of the same size as in the thymus, if not larger (Figure 25D). This indicates that the CD4$^+$CD25$^+$ T cells remaining in *CD4-Cre/Ikk2*$^{FL/D}$ mice are different from those in control mice. CD4$^+$CD25$^+$ T cells have been reported to express the cytotoxic T lymphocyte-associated antigen 4 (CTLA-4; CD152) constitutively (Read et al., 2000; Takahashi et al., 2000). CD4$^+$CD25$^+$ T cells in *CD4-Cre/Ikk2*$^{FL/D}$ mice express CTLA-4 to the same level as those in control mice and they also display a normal pattern of CD45Rb-expression (data not shown), suggesting that they could be regulatory T cells. Analysis of CD44 expression on peripheral CD4 and CD8 T cells showed that *CD4-Cre/Ikk2*$^{FL/D}$ mice have a clear deficiency in CD4$^+$CD44$^+$ memory-type T cell numbers and, to a lesser extent, in CD8$^+$CD44$^+$ cell numbers (Figure 25F and G). Indeed the reduction of CD4 T cells in *CD4-Cre/Ikk2*$^{FL/D}$ mice can largely be accounted for by the absence of subsets that were shown to contain T cells with regulatory (CD4$^+$CD25$^+$) and memory (CD4$^+$CD44$^+$) functions

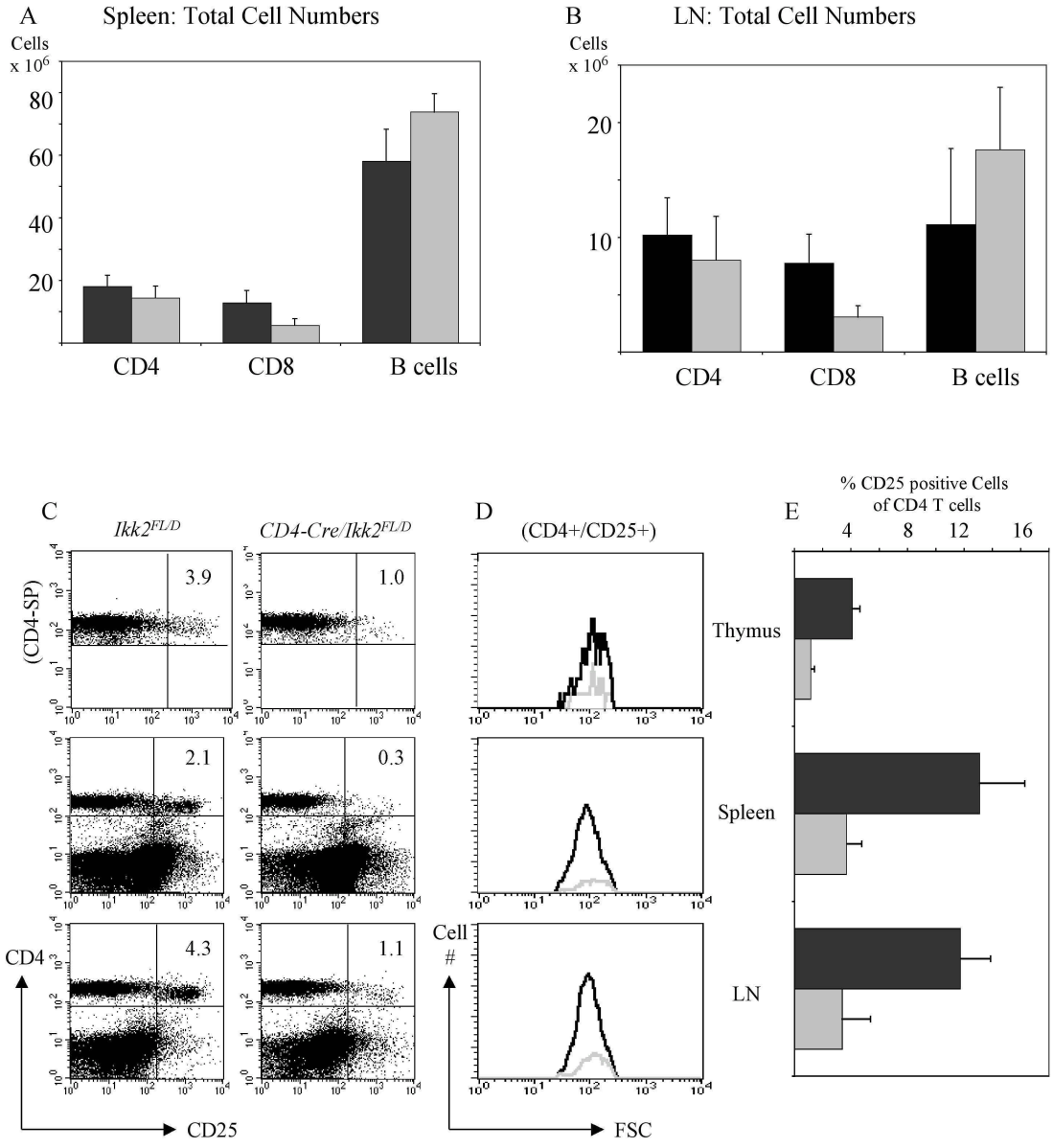
A
Spleen: Total Cell Numbers
Cells
x 10^6
80
60
40
20
CD4
CD8
B cells
B
LN: Total Cell Numbers
Cells
x 10^6
20
10
CD4
CD8
B cells
C
Ikk2FL/D
CD4-Cre/Ikk2FL/D
(CD4-SP)
3.9
1.0
2.1
0.3
4.3
1.1
CD4
CD25
D
(CD4+/CD25+)
Thymus
Spleen
LN
Cell #
FSC
E
% CD25 positive Cells
of CD4 T cells
4
8
12
16

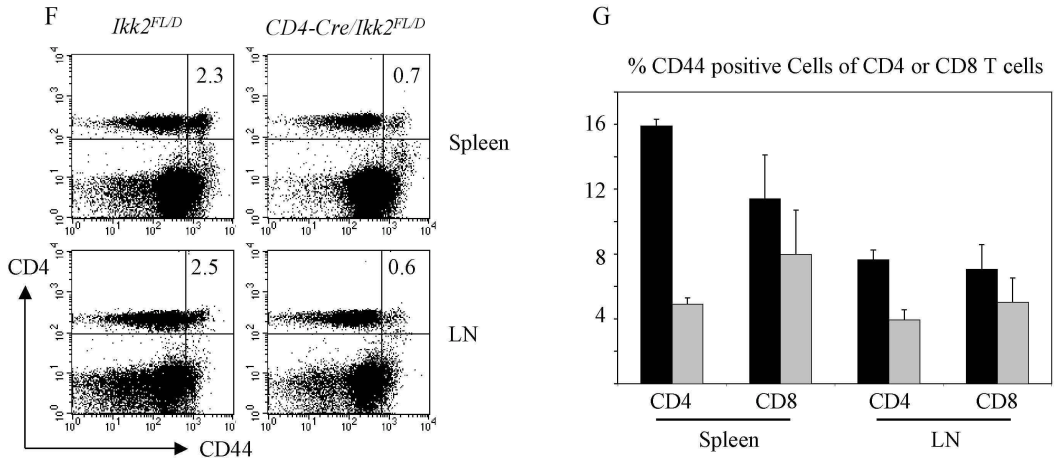

Figure 25. Analysis of T cell populations in *CD4-Cre/Ikk2$^{FL/D}$* mice compared to control mice.

(A, B) Bar charts of absolute CD4, CD8 T cell and B cell numbers in Spleen (A) and LN (B). Black bars represent control (*Ikk2$^{FL/D}$* or *Ikk2$^{FL/FL}$*; n = 10) and grey bars represent *CD4-Cre/Ikk2$^{FL/D\ or\ FL/FL}$* mice (n = 10).

(C) FACS analysis of CD25 expression on CD4 T cells in thymus, spleen and LNs.

(D) Size of CD4/CD25 T cells indicated by forward scatter. Black histograms represent control (*Ikk2$^{FL/D}$* or *Ikk2$^{FL/FL}$*) and grey histograms represent *CD4-Cre/Ikk2$^{FL/D\ or\ FL/FL}$* mice.

(E) Proportion of CD25-positive of total CD4 T cells. Black bars represent control (*Ikk2$^{FL/D}$* or *Ikk2$^{FL/FL}$*; n = 10-12) and grey bars represent*CD4-Cre/Ikk2$^{FL/D\ or\ FL/FL}$* mice (n = 10-12).

(F) FACS analysis of CD44 expression on CD4 T cells in spleen and LNs.

(G) Proportion of CD44-positive of total CD4 T cells. Black bars represent control (*Ikk2$^{FL/D}$* or *Ikk2$^{FL/FL}$*; n = 9) and grey bars represent *CD4-Cre/Ikk2$^{FL/D\ or\ FL/FL}$* (n = 9) mice.

Genotypes are as indicated. Cell surface markers are shown as coordinates and gated cell populations are indicated in brackets. The numbers in the quadrants refer to the percentage of the respective T cell population of live cells in the lymphocyte gate or of the gated cell population indicated in brackets. Error bars indicate standard deviations.

Organ	Cell-Type	*CD4-Cre* *Ikk2*$^{FL/D\ or\ FL/FL}$	*Ikk2*$^{FL/D\ or\ FL/FL}$
Spleen	CD4/CD44	**4.90 ±** 0.39	**15.92 ±** 1.22
	CD8/CD44	**8.00 ±** 2.71	**11.42 ±** 1.45
LN	CD4/CD44	**3.94 ±** 0.62	**7.64 ±** 1.40
	CD8/CD44	**5.02 ±** 1.51	**7.06 ±** 1.16

Table 10. Percentage of CD44^{+} T cells of total CD4 or CD8 T cells in spleen and lymph nodes
Average percentages are shown in bold plus/minus standard deviation (*CD4-Cre/Ikk2*$^{FL/D\ or\ FL/FL}$: n = 9**;** *Ikk2*$^{FL/D\ or\ FL/FL}$: n = 9).

3.5.3 IKK2-deficient T Cells Can Activate NF-κB, Proliferate *in vitro* and Elicit T-dependent Immune Responses

In order to test to what extent IKK2-deficient T cells can activate NF-κB, I purified peripheral T cells from *CD4-Cre/Ikk2*$^{FL/D}$ mice by FACS and activated them *in vitro* with TNF, or with antibodies directed against CD3 and/or CD28. Surprisingly, *Ikk2*$^{D/D}$ T cells could significantly activate NF-κB in response to these stimuli, only slightly less than control T cells (Figures 26A and B). Also the NF-κB subunit composition in TNF- and anti-CD3/CD28-stimulated *Ikk2*$^{D/D}$ T cells was similar to that in control T cells (Figure 26C and data not shown). I performed Western blotting to prove that the *Ikk2*$^{D/D}$ T cells used in the activation experiments are IKK2-deficient (Figure 26D).

I also found that under certain conditions *Ikk2*$^{D/D}$ CD4 and CD8 T cells can proliferate *in vitro* as efficiently as control T cells in response to a panel of stimuli (Figures 27A - C). Similarly, there was no difference between WT and *Ikk2*$^{D/D}$ CD4 and CD8 T cells in level of activation marker expression, such as CD69, CD62L, CD44 or CD25, after anti-CD3, anti-CD3/CD28, PMA/Ionomycin or Concanavalin A treatment for 24 h, or 5 days (data not shown). To test the proliferative abilities of IKK2-deficient T cells in a more physiological context I injected CFSE-labeled T cells into syngeneic C57/BL/6 RAG-/- hosts. Naïve and memory T cells proliferate spontaneously in a lymphopenic environment. During this homeostasis-driven proliferation naïve T cells gain phenotypic and functional characteristics of memory T cells (Goldrath, 2002). After 5,

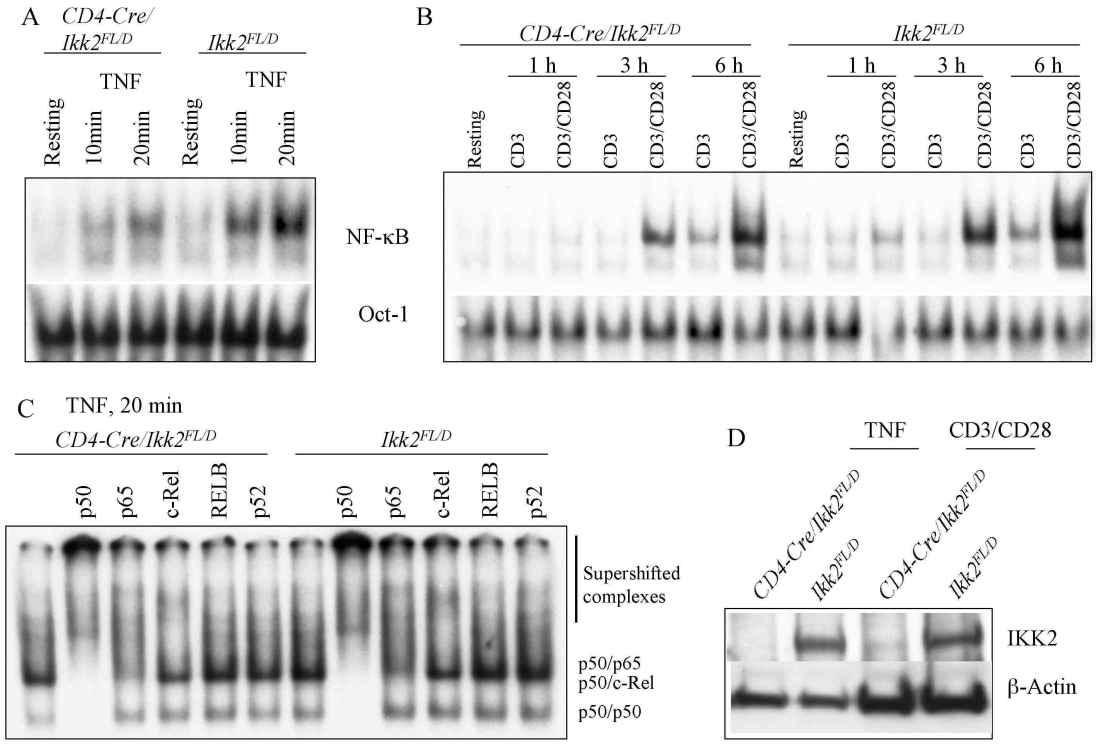

Figure 26. NF-κB activation in IKK2-deficient T cells

(A, B) NF-κB EMSA of whole cell lysates of sorted T cells from mice of indicated genotypes stimulated with TNF (**A**; 20 ng/ml) or anti-CD3 or anti-CD3/CD28 antibodies (**B**; four antibody coated beads per cell) for the indicated time-periods. Equal amount of nuclear protein was demonstrated by Oct-1 mobility shift.

(C) NF-κB Supershift-analysis of extracts of TNF (20 ng/ml - 20 min) stimulated T cells

(D) Western Blot analysis on pooled whole cell lysates of T cells stimulated with TNF (A) or anti-CD3/CD28 antibodies (B) from *CD4-Cre/Ikk2$^{FL/D}$* and *Ikk2$^{FL/D}$* mice. Equal amounts of whole cell lysate of each time point were pooled per stimulation for each genotype.

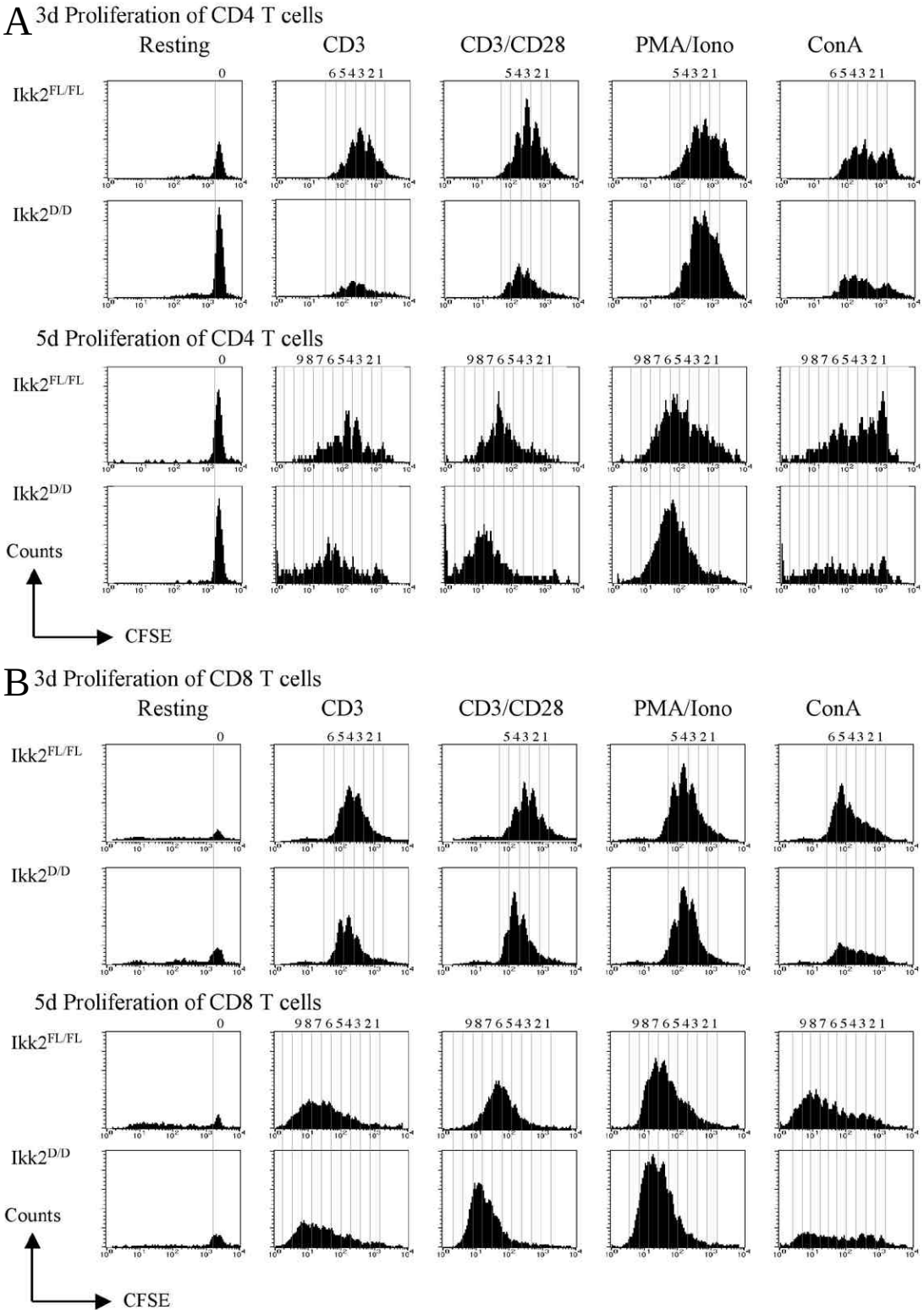
A
3d Proliferation of CD4 T cells
Resting
CD3
CD3/CD28
PMA/Iono
ConA
0
654321
54321
54321
654321
Ikk2FL/FL
Ikk2D/D
5d Proliferation of CD4 T cells
0
987654321
987654321
987654321
987654321
Ikk2FL/FL
Ikk2D/D
Counts
CFSE
B
3d Proliferation of CD8 T cells
Resting
CD3
CD3/CD28
PMA/Iono
ConA
0
654321
54321
54321
654321
Ikk2FL/FL
Ikk2D/D
5d Proliferation of CD8 T cells
0
987654321
987654321
987654321
987654321
Ikk2FL/FL
Ikk2D/D
Counts
CFSE

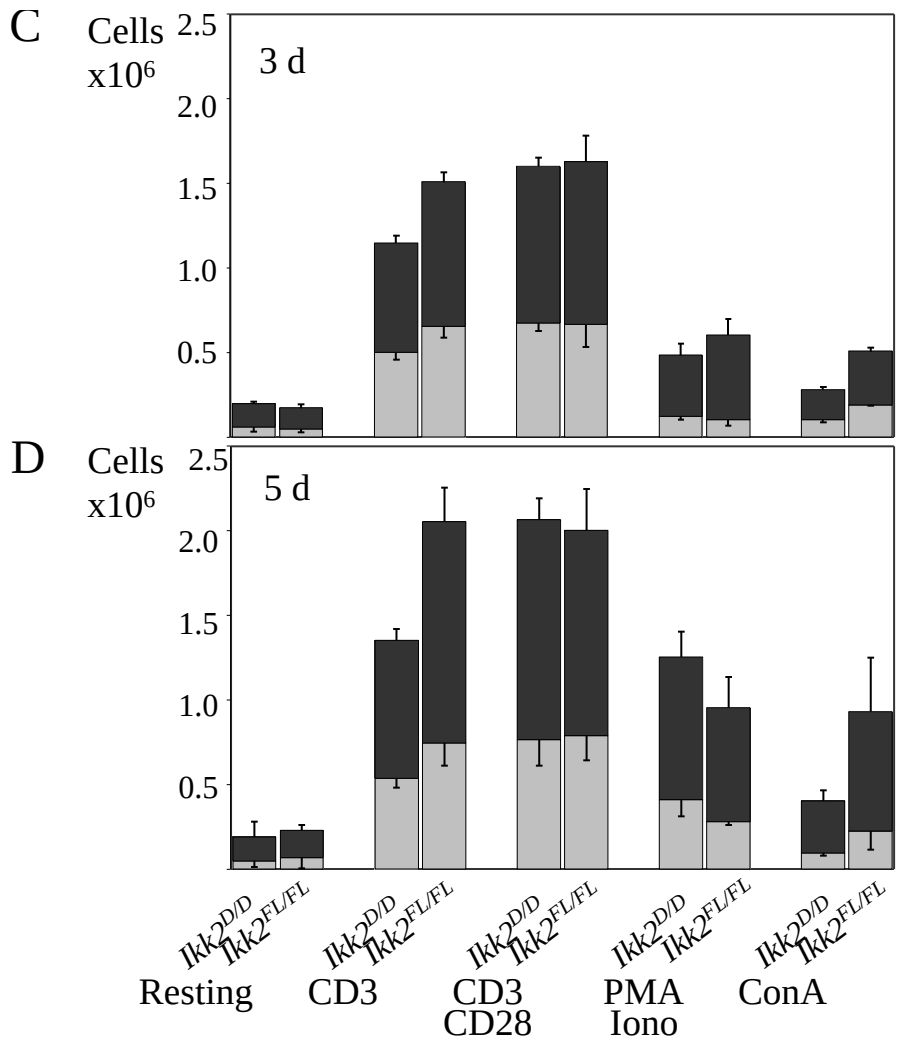

Figure 27 . ***Ikk$^{D/D}$*** **T cells can proliferate** ***in vitro*** **as well as WT T cells**
T cells were isolated from LN and spleen of *CD4-Cre/Ikk2$^{FL/D\ or\ FL/FL}$* and control mice, labelled with CFSE and activated *in vitro* to proliferate using CD3 or CD3/CD28 coated beads (one bead per cell), PMA (2 nM)/Iono (1μM) or ConA (1μg/ml). After 3 and 5 days cells were harvested, analysed by FACS **(A, B)** and counted **(C, D**). This experiment was repeated twice with similar results. **(A, B)** Analysis of cell divisions in activated *Ikk$^{D/D}$* and control T cell cultures. Histograms represent populations gated on live CD4 **(A)** or CD8 **(B)** cells as a function of CFSE intensity and cell number. T cell genotype and stimulus are as indicated next to and above the histograms. The number of cell divisions is indicated by lines and by numbers above each histogram. The results shown are representative of triplicate wells. **(C, D)** Absolute cell numbers in *Ikk$^{D/D}$* and control T cell proliferation cultures. Cell counting was performed using Trypan blue exclusion. Total cell numbers are indicated by bars (grey part = live cells; black part = dead cells). T cell genotype and stimulus are as indicated below the bar charts. Error bars represent standard deviations of triplicate samples.

6 or 10 days the mice were sacrificed, spleens and LNs were removed and proliferation was assessed by FACS-analysis (Figure 28). After five days, most of the control CD8 T cells had divided 3 to 5 times, whereas most *Ikk2*$^{D/D}$ T cells seemed to have undergone only 2 to 3 divisions (Figure 28A). A similar picture was observed after 6 days, but after 10 days IKK2-deficient and control T cells showed a similar cell-division profile (Figure 28A). CD4 T cells expand slower in a lymphopenic environment (Goldrath, 2002). After 6 and 10 days I could clearly observe control CD4 T cells that had undergone one cell division. In contrast *Ikk2*$^{D/D}$ CD4 T cells did not divide to any significant extent at any time (Figure 28B). Moreover, only very few *Ikk2*$^{D/D}$ CD8 and CD4 T cells could be recovered at all time points from spleen and LNs, in contrast to control T cells (Figure 28A and B), indicating that IKK2-deficient T cells cannot expand efficiently in lymphopenic hosts, probably due to a survival defect. However, this analysis has to be repeated with more mice to ensure the finding.

To test the function of IKK2-deficient T cells *in vivo* I immunized *CD4-Cre/Ikk2*$^{FL/D}$ and control mice with the T-dependent (TD) antigen NP-CG. B cells depend on T cell help to elicit a humoral immune response to TD antigens. Determination of Ig isotypes by ELISA showed that basal levels of immunoglobulin titers were normal in *CD4-Cre/Ikk2*$^{FL/D}$ mice, except for a slight reduction in serum concentration of IgE (Figure 29A). IKK2-deficient T cells were able to provide B cell help in the course of an immune response, since *CD4-Cre/Ikk2*$^{FL/D}$ mice mounted an efficient NP-specific immune-response. This response was delayed, however, since the serum concentration of NP-specific IgG1, λ and κ in *CD4-Cre/Ikk2*$^{FL/D}$ mice was lower than in control mice at day 7 (Figures 29B, D and E). At day 14 to 28 after immunization NP-specific IgG serum concentrations were comparable between *CD4-Cre/Ikk2*$^{FL/D}$ and control mice (Figures 29B – 7E and data not shown).

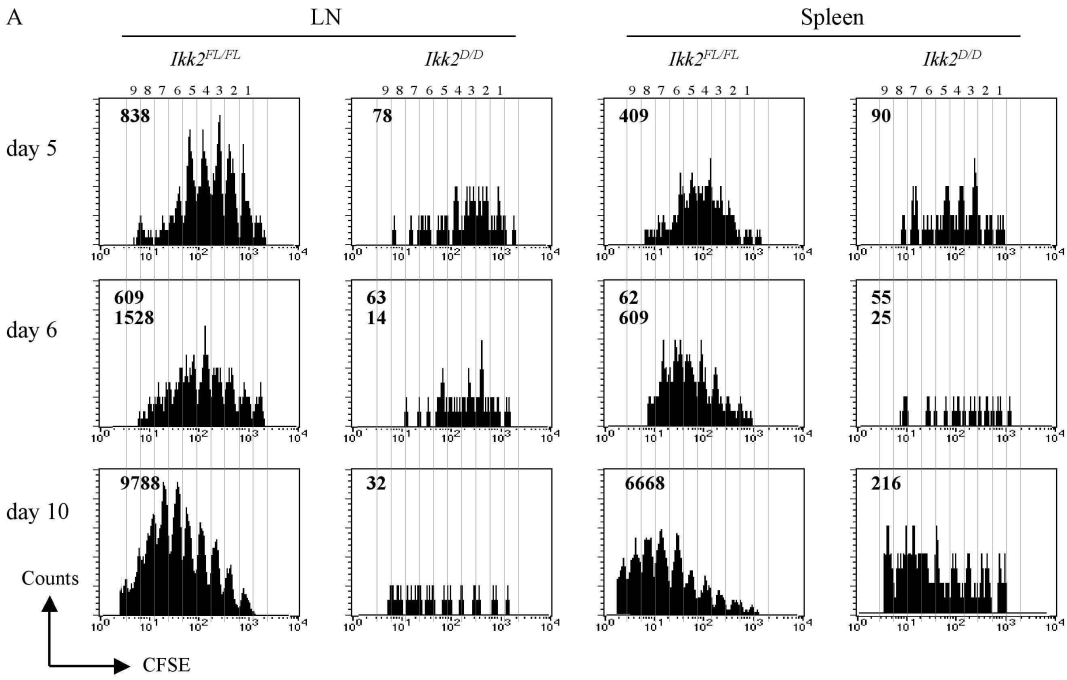

Figure 28. Homotypic proliferation in lymphopenic hosts *in vivo* of $Ikk^{D/D}$ compared to WT T cells

T cells were isolated from LN and spleen of a *CD4-Cre/*$Ikk2^{FL/D}$ mouse and a control mouse, labelled with CFSE and injected intravenously into RAG-/- hosts. After 3, 5 or 10 days RAG-/- hosts were killed and T cells from LN and spleens cells were prepared and analysed by FACS

(A) Histograms represent populations gated on live CD8 T cells as a function of CFSE intensity and cell number. T cell genotype and location are as indicated above the histograms. The number of cell divisions is indicated by lines and by numbers above each histogram. Bold numbers in the top left corner of each histogram indicate the total number of retrieved CD8 T cells from individual RAG-/- hosts.

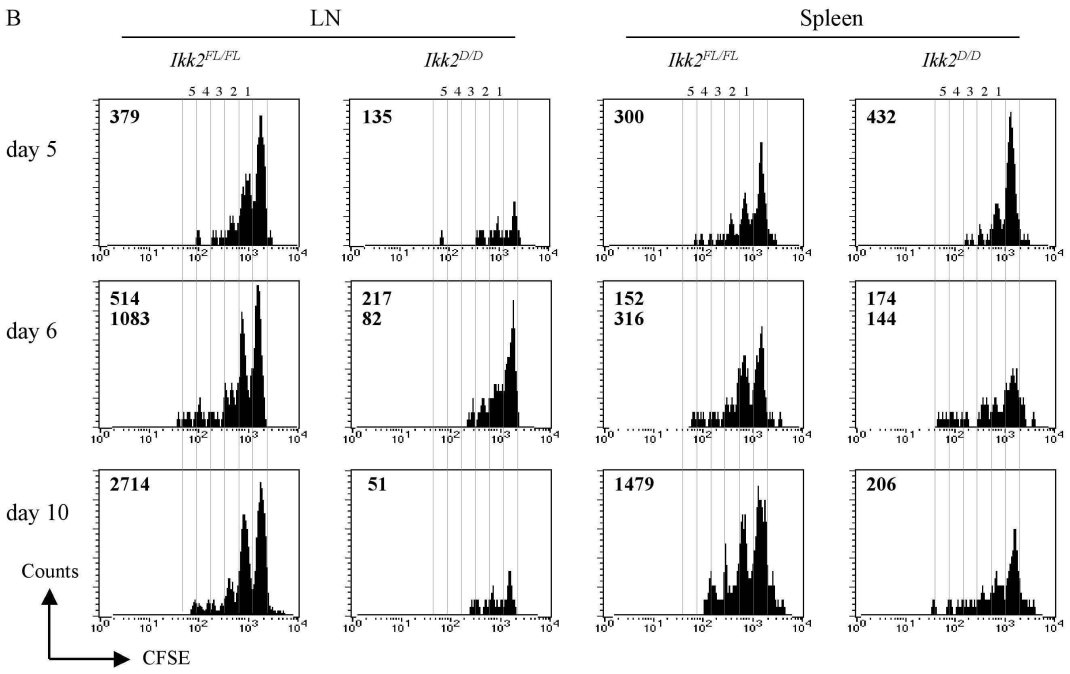

(B) Histograms represent populations gated on live CD4 T cells as a function of CFSE intensity and cell number. T cell genotype and location are as indicated above the histograms. The number of cell divisions is indicated by lines and by numbers above each histogram. Bold numbers in the top left corner of each histogram indicate the total number of retrieved CD4 T cells from individual RAG-/- hosts.

Figure 29. Serum immunoglobulin and T cell dependent (TD) humoral immune responses in *CD4-Cre/Ikk2^{FL}* compared to *Ikk2^{FL}* control mice.

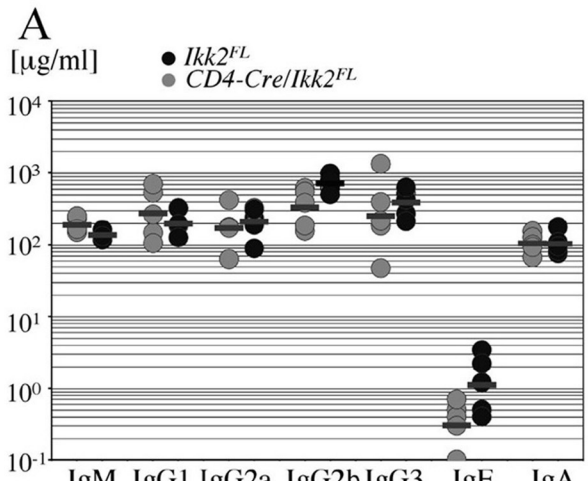

Filled circles represent control (*Ikk2$^{FL/D\ or\ FL/FL}$; n = 5*) , while open circles represent experimental (*CD4-Cre/Ikk2$^{FL/D\ or\ FL/FL}$*; n = 5) mice. Bars indicate the geometric mean.

(A) Serum immunoglobulin levels of unimmunized mice.

(B-D) Antibody-response to a TD antigen. NP-specific IgG1 **(A)**, IgM **(B)**, λ **(C)** and κ **(D)** serum levels in primary response with 50 µg NP-CG are shown at day 7, 14 and 21 after immunization.

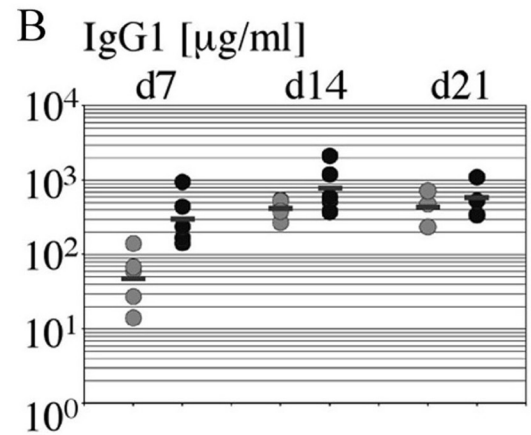

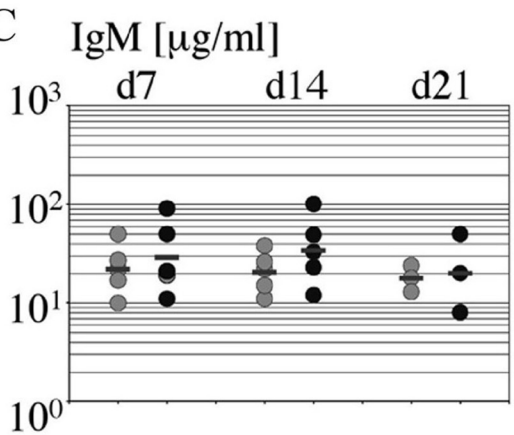

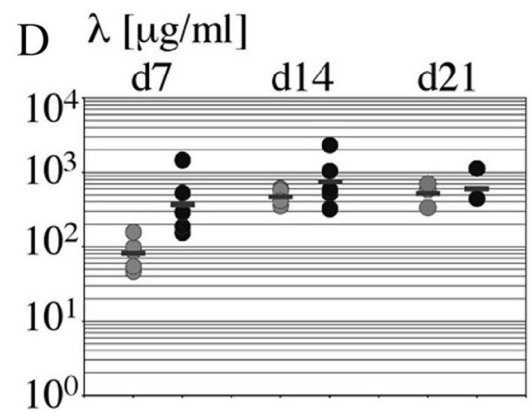

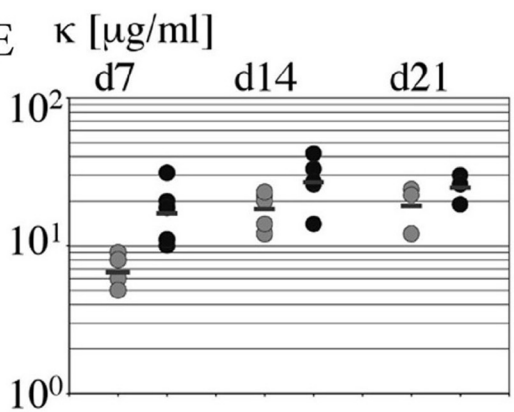

4. DISCUSSION

4.1. NEMO in NF-κB Activation and Embryonic Development

NEMO deficiency resulted in a lethal phenotype and a complete block of NF-κB activation by proinflammatory stimuli. The latter contrasted, in a side-by-side comparison, with IKK2 deficiency, which leads to reduced, but still detectable NF-κB activation under the same conditions, probably because the absence of IKK2 can be partially compensated by IKK1. It has been shown that LPS predominantly stimulates IKK2 activity (Fischer et al., 1999); in agreement with this result I find that IKK2 deficiency completely blocked NF-κB activation in response to LPS. Liver degeneration is the cause of embryonic lethality in mice lacking the RelA/p65 NF-κB subunit or IKK2 (Beg et al., 1995; Li et al., 1999b; Li et al., 1999c; Tanaka et al., 1999). A similar phenotype is also observed in NEMO-deficient embryos, but in this case liver apoptosis seems to occur earlier than in *relA*$^{-/-}$ or *ikk2*$^{-/-}$ embryos, underscoring the essential role of NEMO in the NF-κB activation process. These results were confirmed by the independent work of two other research groups (Makris et al., 2000; Rudolph et al., 2000).

4.2. NEMO-deficient Mice as an Animal Model for the Human Disease Incontinentia Pigmenti

The localization of *Nemo* on the X chromosome predicts that random X inactivation will generate a chimerism of NEMO-deficient and NEMO-containing cells in all tissues of *Nemo*$^{D/WT}$ females. Given the central role of the NF-κB signaling pathway in the regulation of various cellular responses (Gerondakis et al., 1998; Kanegae et al., 1998; O'Neill and Kaltschmidt, 1997), the presence of NEMO-deficient cells in the body could cause defects in multiple tissues. Indeed, recent work has shown that mutations in the human *NEMO* gene cause Incontinentia Pigmenti (IP) (Smahi et al., 2000).

I show here that heterozygous *Nemo* knockout mice develop a skin phenotype that closely resembles the cutaneous manifestations observed in IP patients. The skin abnormalities in these animals seem to occur in stages that correlate to the different

stages described for IP. A few days after birth numerous inflammatory foci are found in the epidermis of *Nemo*$^{D/WT}$ mice, showing massive infiltration of granulocytes into the epidermis, resembling the inflammatory phase I of IP (Landy and Donnai, 1993). At eight days, granulocyte infiltrates into the epidermis are reduced, suggesting that at this age features reminiscent of an initial inflammatory episode are declining, as in stage II of IP (Landy and Donnai, 1993). Histological examination of the skin from *Nemo*$^{D/WT}$ mice revealed epidermal hyperplasia with thickening of both the suprabasal and the cornified layer. Electron microscopy showed that in the epidermis of *Nemo*$^{D/WT}$ mice basal layer keratinocytes are in loose contact forming dilated intercellular spaces. This defect may be associated with alterations in tonofilaments and loss of desmosomal structures that were also observed. Presence of dyskeratotic keratinocytes displaying abnormal tonofilaments, loss of desmosomal contacts, and dilated intercellular spaces are reported in stage II IP patients (Schamburg-Lever and Lever, 1973). Hyperpigmentation caused by the presence of increased numbers of melanosome containing phagocytes in the dermis is the hallmark of IP, occurring at stage III (Schamburg-Lever and Lever, 1973; Zillikens et al., 1991). A similar phenomenon was also observed in the *Nemo*$^{D/WT}$ mouse model, at 6 weeks of age. Furthermore, I and others found that NEMO deficiency results in embryonic lethality in hemizygous males both in mice and in humans (Rudolph et al., 2000; Smahi et al., 2000). It will be interesting to see whether aborted male IP embryos also show liver degeneration due to hepatocyte apoptosis.

A further similarity between IP patients and *Nemo*$^{D/WT}$ mice relates to the hematopoietic system. The blood leukocytes of IP patients exhibit a completely skewed pattern of X-inactivation, suggesting that cells expressing the mutated chromosome are selectively eliminated (Scheuerle, 1998). Strikingly, chimeras generated from *Nemo* knockout ES cells did not possess any ES cell-derived lymphocytes. Thus, lymphocytes lacking NEMO expression either do not develop or are counter-selected.

How can the dominant feature of the disease developing in IP patients and *Nemo*$^{D/WT}$ mice, namely the skin disorder, be explained? Several reports have suggested that NF-κB activation is essential for the normal development of the epidermis. A dramatic skin phenotype is reported in IKK1 knockout mice which die shortly after birth showing a thickened hyperproliferative epidermis lacking keratinocyte differentiation (Hu et al., 1999b; Li et al., 1999a; Takeda et al., 1999). However, this was later demonstrated to

be independent of I-κB kinase activity and of NF-κB (Cao et al., 2001; Hu et al., 2001). In a different experimental setting, keratinocyte-specific inhibition of NF-κB by expression of a dominant-negative IκBα transgene under the control of the keratin 14 promoter was applied to study the role of NF-κB in stratified epithelium (Seitz et al., 1998). These transgenic mice developed epidermal hyperplasia within 4 days after birth, lacked evidence of normal hair formation, exhibited growth retardation and died within 5 to 7 days after birth. Based on these results, the authors proposed that functional loss of NF-κB leads to keratinocyte hyperproliferation. The same group also showed that NF-κB inhibition results in increased apoptosis of keratinocytes *in vivo* (Seitz et al., 2000a; Seitz et al., 2000b). In the skin lesions from *Nemo*$^{D/WT}$ animals I observed a combination of hyperproliferation and increased cell death. It seems likely that the affected areas detected on the skin from *Nemo*$^{D/WT}$ mice consist of keratinocytes that lack NEMO protein because of random X inactivation and therefore cannot activate NF-κB. Proliferating cells were detected not only in the basal layer of these skin patches, but also in the suprabasal layers of the epidermis indicating abnormal keratinocyte differentiation. Failure to activate NF-κB may cause hyperproliferation, incomplete differentiation and premature cell death of NEMO-deficient keratinocytes, resulting in the macroscopic picture of verrucous scaling skin. Increased apoptosis of NEMO-deficient basal keratinocytes could lead to their progressive replacement by NEMO expressing keratinocytes and thus to the gradual clearance of the skin lesions. TNF and other cytokines that may be produced in the epidermis during the early inflammatory phase could play a role in this process by directly killing the NEMO-deficient keratinocytes. Experimental evidence showing that NF-κB inhibition *in vitro* sensitizes primary keratinocytes to apoptosis induced by TNF or Fas (Seitz et al., 2000b) further supports this hypothesis. However, although TNF-induced NF-κB activation is markedly reduced in IKK2-deficient keratinocytes, they show only mildly increased apoptosis on TNF treatment compared to controls (Pasparakis et al., 2002a). This shows, that TNF-induced killing of *Ikk2*-knockout keratinocytes does not play an important role in the pathogenesis of the inflammatory skin disease caused by epidermis-specific deletion of IKK2 (Pasparakis et al., 2002a). It has also been postulated for human IP that invasion of affected skin by normal cells takes place at the transition from the inflammatory to the verrucuous stage (Wieacker et al., 1985). Studies in mice with epidermis-specific deletion of IKK2 (*K14*-

Cre/IKK2$^{FL/FL}$) showed that IKK2 deficiency inhibited NF-κB activation in keratinocytes, but did not lead to cell-autonomous hyperproliferation or impaired differentiation. Mice lacking IKK2 specifically in the epidermis develop an inflammatory response that develops in the skin shortly after birth and leads to their death at around day 10 after birth (Pasparakis et al., 2002a). Subsequent to upregulation of cytokines in epidermis and dermis and infiltration by immune cells keratinocytes start to hyperproliferate and epidermal differentiation patterns are abrogated (Pasparakis et al., 2002a). Treatment of newborn *K14-Cre/IKK2*$^{FL/FL}$ mice with neutralizing antibodies against TNF or crossing these mice onto a TNFR1-/- genetic background completely rescued the skin-phenotype. *K14-Cre/IKK2*$^{FL/FL}$*/TNFR1-/-* mice develop normally (Pasparakis et al., 2002a). The skin phenotype is also ameliorated in *Nemo*$^{D/WT}$*/TNFR1-/-* mice, but they still develop lesions and the mortality remains high. Studies employing *K14-Cre/ Nemo*$^{FL/WT}$, *K14-Cre/Nemo*$^{FL/Y}$, *K14-Cre/Nemo*$^{FL/WT}$*/TNFR1-/-* and *K14-Cre/ Nemo*$^{FL/Y}$*/TNFR1-/-* mice will reveal whether this is due to a TNF-independent defect in other organs in *Nemo*$^{D/WT}$ mice or to the presence of NEMO-proficient and –deficient keratinocytes in the skin of these animals. These mice will also reveal whether the lack of NEMO has a more severe (and partly TNF-independent) effect on the epidermis than the lack of IKK2.

At this point it remains unclear why most *Nemo*$^{D/WT}$ females die within the first 10 days of life. The lethal effect of keratinocyte-specific inhibition of NF-κB activation in transgenic mice (Seitz et al., 1998) supports the hypothesis that the skin lesions in *Nemo*$^{D/WT}$ mice interfere with vital skin functions causing death of the animals. This view is supported by the data from Pasparakis et al., showing that deletion of IKK2 specifically in the epidermis leads to death of all animals before they are two weeks old (Pasparakis et al., 2002a). Therefore it might depend on the percentage of NEMO-deficient cells generated by X-chromosome inactivation whether an animal survives or succumbs to the disease. Indeed, the few *Nemo*$^{D/WT}$ mice that survive after day ten showed a milder phenotype from the beginning, with only a small area of the skin covered by the lesions. Early lethality does not seem to be a prominent feature in female IP patients.

The repair mechanism proposed to heal the skin defect by the replacement of NEMO-deficient with NEMO-expressing cells may apply also to other tissues. The increased number of apoptotic cells observed in the fetal liver of *Nemo*$^{D/WT}$ embryos might

represent NEMO-deficient hepatocytes whose death at this stage presumably “clears” the liver from NEMO-deficient cells. Whether a similar mechanism operates also in other tissues could be assessed by the quantitation of the percentage of NEMO-deficient cells persisting in these tissues at different developmental stages. This would uncover the importance of NEMO-mediated NF-κB activation for the survival of individual cell types *in vivo* in an ideal experimental setting. I tried to approach this question using mosaic inactivation of *Nemo* by crossing mice containing a floxed *Nemo* allele to the balancer-Cre strain (Betz et al., 1996). Unfortunately deletion with the balancer-Cre varied a lot from mouse to mouse so that it was difficult to reach clear conclusions from the results obtained in this study. Additionally I crossed the $Nemo^{D/WT}$ with mice carrying a EGFP-transgene on the X-Chromosome (Hadjantonakis et al., 1998). In the resulting $Nemo^{D/EGFP}$ offspring I planned to assess presence or absence of cells that have inactivated the X-chromosome bearing the deleted nemo allele by quantitating the proportion of GFP-expressing cells in various cell-types and tissues. Unfortunately in adult mice the EGFP-transgene was object to epigenetic silencing and therefore no conclusive results could be obtained from these experiments. In the future I will readdress these issues by using improved genetic tools, such as HPRT(X-linked)-GFP-knockin mice.

The striking similarities between the skin phenotype we observe in the $Nemo^{D/WT}$ mice and the skin lesions described in IP, which is caused by mutations in the human *NEMO* gene, indicate that these mice constitute a model for human IP. Further analysis of these mice should increase our understanding of the molecular mechanisms involved in the pathogenesis of this disease. Cell-type-specific and/or inducible inactivation of the loxP-flanked *Nemo* gene, which we have introduced into the mouse germline as part of our targeting strategy, will not only help in this context in the future, but also allow us to study the role of the NF-κB signaling pathway in other cellular compartments in the mouse.

4.3 The $ikk2\Delta K^{FL}$ Allele Produces a Kinase-dead Protein

Comparison of NF-κB activation in response to proinflammatory signals in $Ikk2\Delta K^{D/D}$ and IKK2-deficient MEFs showed a similar impairment measured by EMSA or IκBα

degradation. However, measuring induction of NF-κB-dependent gene products in response to inflammatory signals, such as TNF induced death and IL-6 production, *Ikk2*Δ*K*$^{D/D}$ cells showed lower NF-κB activity than IKK2 deficient cells. These results suggest that the expression of IKK2ΔK, even at the low levels observed, contributes to a stronger reduction of NF-κB activity than IKK2-deficiency, presumably by a dominant-negative effect.

At this stage I can only speculate how this dominant-negative effect comes about. In wild-type cells the most prevalent IKK dimer is the IKK1/2 heterodimer. Therefore it seems likely that in *Ikk2*Δ*K*$^{D/D}$ cells IKK2ΔK is preferentially integrated into the complex, even though there is a vast excess of IKK1 compared to IKK2ΔK. In addition the presence of one IKK1/IKK2ΔK dimer in the 700 – 900 kD IKK complex could disrupt the activation process, which depends on cross-phosphorylation between the kinases (Delhase et al., 1999). After liberation from IκB NF-κB can bind to DNA, but transcriptional activation is additionally regulated by further modifications of the Rel proteins, such as phosphorylation and acetylation (Ghosh and Karin, 2002). Both IKKs are implicated in this process (Sizemore et al., 2002). IKK complexes consisting of IKK1 only could be more efficient in initiating the events leading to phosphorylation of Rel proteins than IKK complexes also containing the kinase-inactive IKK2ΔK.

4.4 IKK-mediated Activation of NF-κB is Essential for Mature B Cell Maintenance

I investigated the role of IKK-induced NF-κB activity in B cells by conditional inactivation of IKK2 and NEMO. B cell specificity was achieved by crossing mice carrying conditional NEMO and IKK2 alleles (*Ikk2*$^{FL/D}$, *Ikk2*Δ*K*$^{FL/D}$ and *Nemo*$^{FL/Y}$) to CD19-Cre mice. All three mutations similarly lead to a strong reduction of B cell numbers in mutant mouse strains. *CD19-Cre*/*Ikk2*$^{FL/D}$, -*Ikk2*Δ*K*$^{FL/D}$ or -*Nemo*$^{FL/Y}$ mice have 3-4 fold reduced B cells in the spleen and at least two-fold reduced numbers in recirculating bone marrow B cells, lymph node B cells and peritoneal cavity B1 and B2 cells. Southern blot analysis of sorted B cell populations revealed that whereas deletion efficiency in IgM$^-$ bone marrow B cells is as high as reported for CD19-Cre mice and comparable to deletion observed in *CD19-Cre/Ikk2*$^{FL/WT}$ mice, IgM$^+$ bone marrow B

cells are already counterselected, most likely reflecting counterselection against recirculating B cells. In the transition from IM to FO B cells the percentage of B cells with deleted alleles is reduced, indicating that mature B cells lacking IKK activity are counter-selected. In the case of *CD19-Cre*/*Ikk2*$^{FL/D}$ and -*Ikk2*Δ*K*$^{FL/D}$ mice over 90% of the IM B cells have deleted the floxed allele, whereas in FO cells, which presumably originate from the immature transitional cells, the proportion of cells carrying the deletion ranges from 40 to 70 %, clearly demonstrating counterselection of *Ikk*$^{D/D}$- and *Ikk2*Δ*K*$^{D/D}$ B cells. In *CD19-Cre*/*Nemo*$^{FL/Y}$ mice, *Nemo*$^{D/Y}$ IM B cells are already counter-selected, as evidenced by Southern blot and cell counting. The fact that deletion of NEMO, in contrast to the deletion of IKK2, seems to lead to counter-selection of cells already within the immature B cell compartment may be explained in two ways. One explanation is that in the absence of IKK2 some IKK-induced NF-κB activation can still occur while loss of NEMO completely blocks IKK activity. Thus, in *CD19-Cre*/*Ikk2*$^{FL/D}$ mice low levels of remaining NF-κB activity could be sufficient to sustain development of B cells to the IM stage. In the *CD19-Cre*/*Nemo*$^{FL/Y}$ mice the complete absence of NF-κB activity may lead to the loss of IM B cells. Additionally or alternatively different turnover rates of IKK2 and NEMO mRNA and protein could play a role. The relatively long half-life of IKK2(Fischer et al., 1999) might ensure that most B lineage cells of *CD19-Cre*/*Ikk2*$^{FL/D}$ mice develop into FO B cells before they are devoid of this protein. The half-life of NEMO could be shorter than that of IKK2, leading to a rapid depletion of NEMO protein from IM B cells that have deleted the *nemo*^{FL} allele, resulting in the loss of cells at this stage. The fact that *CD19-Cre*/*Ikk2*Δ*K*$^{FL/D}$ mice display an intermediate phenotype with some loss of deleted IM B cells, as demonstrated by the reduction of the absolute cell numbers of IM B cells in these mice, is compatible with both hypotheses, since the production of IKK2ΔK may lead both to the earlier loss and to more complete inhibition of IKK activity in comparison to the *CD19-Cre*/*Ikk2*$^{FL/D}$ mice.

The picture seen in MZ B cells differs from that seen in FO B cells. The remaining MZ B cells of the IKK-conditional mutant mice crossed to CD19-Cre mice are nearly completely devoid of the deleted genotype, clearly demonstrating that *Ikk2*$^{D/D}$-, *Ikk2*Δ*K*$^{D/D}$ and *Nemo*$^{D/Y}$ MZ B cells cannot be generated and/or persist. Recent evidence suggests that MZ B cells represent a self-renewing separate subset of B cells

(Carvalho et al., 2001; Hao and Rajewsky, 2001). In this case cells of the deleted genotype would disappear early during the generation of this lineage and a subset of cells that have lost their ability to delete would be sustained by self-renewal. Another view is that MZ B cells are a highly antigen-selected population of B cells (Cariappa et al., 2000; Martin and Kearney, 2000). During this selection process all B cells able to undergo Cre-mediated deletion should have deleted the loxP-flanked gene and subsequently disappeared. Thus the virtual absence of MZ B cells with a deleted genotype in IKK conditional-CD19Cre mice could be due to the fact that the MZ B cell compartment is not constantly refilled with B cells that recently acquired the deleted genotype as is the follicular compartment. Alternatively, the absence of MZ B cells with deleted *nemo* or *ikk2* alleles could mean that MZ B cells are more dependent on IKK-induced NF-κB activity then other B cell populations. This explanation, which does not exclude the former, is supported by the specific loss of MZ B cells in p50 deficient mice (Cariappa et al., 2000).

Mature splenic B cells do not proliferate much (Forster et al., 1989; Fulcher and Basten, 1997; Hao and Rajewsky, 2001), so that in a BrdU incorporation experiment over the period of one week most of the BrdU-positive B cells in the spleen represent IM B cells from the BM (Forster et al., 1989). Roughly twice as many *CD19-Cre*/*Nemo*$^{FL/Y}$ splenic B cells stain positive for BrdU after one week of BrdU administration compared to control B cells. This data are consistent with a BrdU-based B cell turnover analysis in *CD19-Cre*/*Ikk2*Δ*K*$^{FL/D}$ mice (Pasparakis et al., 2002b). This means that recently generated B cells constitute a larger fraction of total splenic B cells in mutant compared to control mice despite the reduction in B cell numbers in mutant mice. Thus *CD19-Cre*/*Ikk2*Δ*K*$^{FL/D}$ mice contain a higher percentage of short-lived splenic B cells than do wild-type mice. These short-lived B cells should be cells that carry two deleted alleles and are on their way to lose their ability to signal through the IKK complex and subsequently die. When B cell influx from the bone marrow is blocked for one month by interfering with IL-7R signaling using injections of anti-IL-7R antibodies, *Ikk2*Δ*K*$^{D/D}$ B cells completely disappear from the spleens of these mice. The fact that only *Ikk2*Δ*K*$^{FL/D}$ B cells remain in these *CD19-Cre*/*Ikk2*Δ*K*$^{FL/D}$ mice shows that there must be a strong selection for cells in which Cre is either absent or cannot function. FO B cells were shown to have an average calculated half-life of 134 days in the absence of replenishment of the splenic B cell pool from the BM (Hao and

Rajewsky, 2001). Since all of the *Ikk2*Δ*K*$^{D/D}$ FO B cells disappear after one month this clearly demonstrates that IKK2 signaling is essential for the maintenance of mature B cells. We therefore conclude that mature B cells need IKK-mediated survival signals.

Based on our experimental findings we envisage the following scenario: Deletion of the conditional alleles in mice containing the CD19-Cre transgene is initiated in the bone marrow and continues throughout the later stages of B cell development. B cells that underwent Cre-mediated recombination initially retain sufficient amounts of IKK2 or NEMO protein to allow development into IM B cells and some of these cells progress further into the mature B cells compartments. B cells that escape Cre-mediated deletion develop normally into mature B cell subsets. Thus, the follicular B cell compartment of these mice consists of a mixture of cells that have already deleted and cells that retain loxP-flanked alleles. The fact that blockade of B cell development in the bone marrow for four weeks leads to the disappearance of all B cells that have deleted the *ikk2*Δ*K* floxed alleles from the spleen demonstrates that mature B cells can not survive without IKK2 activity.

It has been speculated that constitutive activation of NF-κB by signaling through the BCR is essential for B cell survival (Bendall et al., 1999; Petro and Khan, 2001). In agreement with this idea B cells die by apoptosis upon inducible deletion of the B cell receptor (BCR) (Lam et al., 1997). However, it was shown recently that while deletion of Bcl10 in mice selectively abolishes NF-κB activation by the antigen receptor in B cells, Bcl10-/- mice show normal B cell development. This argues against the possibility that NF-κB activation originating from the BCR is needed for B cell survival (Ruland et al., 2001). Therefore mature peripheral B cells seem to depend on NF-κB activating signals other than BCR crosslinking, even though a role for the BCR in this process cannot be excluded with certainty. BAFF is a TNF-family protein that is expressed mainly on myeloid cells (Hu et al., 1999a; Moore et al., 1999; Schneider et al., 1999); BAFF-deficient mice revealed a block in B cell development a the T1 to T2 transitional checkpoint, leading to loss of follicular and marginal zone B lymphocytes (Schiemann et al., 2001). It has been shown that BAFF induces processing of p100 and nuclear translocation of p52 and RelB via the BAFFR and NIK (Claudio et al., 2002; Mackall et al., 1996). This process, however, is independent of NEMO (Claudio et al., 2002) and most likely mediated by IKK1. Since IKK1-deficient B cells develop, albeit in reduced numbers, BAFF must elicit additional survival signals in B cells apart from

p100 processing. Ligation of all three receptors for BAFF (BAFFR, BCMA, TACI) (Mackay et al., 2002) induced phosphorylation of IκBα (Kayagaki et al., 2002) and treatment with BAFF was shown to induce p50/RelB complexes (Do et al., 2000). Therefore one potential survival signal initiated by BAFF could be activation of NF-κB through degradation of IκB via IKK2 and NEMO. Of course also other receptors, maybe several receptors acting in concert, could initiate the IKK2- and NEMO mediated response to keep B cells alive.

4.5 The Role of NEMO and IKK2 in Mature T Cell Development

Activation of NF-κB through degradation of IκBs is mediated by the IKK complex and activation of p52/RelB through processing of p100 depends largely on IKK1. Adoptive transfer experiments, published while this work was in progress, revealed that IKK1 is dispensable for T cell development (Kaisho et al., 2001; Senftleben et al., 2001a). Also IKK2 has no essential role in the generation of T cells, but is important for protecting thymocytes against TNF-induced apoptosis (Senftleben et al., 2001b). These data indicate that either IKK1 and 2 can compensate for each other or that T cell development occurs independently of the IKK. On the other hand, inhibition of NF-κB activation through T cell specific transgenic expression of repressors of NF-κB resulted in reduced peripheral T cell populations and CD8-SP thymocytes to varying degrees (Attar et al., 1998; Boothby et al., 1997; Esslinger et al., 1997; Ferreira et al., 1999; Hettmann et al., 1999). This shows that NF-κB is required for maintenance of normal T cell numbers, especially CD8 T cells; it also shows, however, that inhibition of NF-κB was not complete or that T cells can be generated in the absence of NF-κB activity.

Even though these studies yielded important information about the role of NF-κB in T cells no clear conclusions could be drawn concerning the dependence of T cell development on activation of NF-κB. Therefore I chose to analyze the function of the IKK complex in T cells of the adult mouse employing conditional gene targeting. Absence of NEMO leads to disruption of the IKK complex and blocks IKK-mediated activation of NF-κB. T cell-specific ablation of NEMO was achieved by crossing mice a conditional *nemo* allele ($Nemo^{FL/Y}$) to CD4-Cre mice. The complete disruption of the

IKK complex in T cells of CD4-Cre/*Nemo*$^{FLY/}$ mice was compared to the deletion of IKK2 in CD4-Cre/*Ikk2*$^{FL/D}$ mice.

In mice containing the CD4 transgene deletion of loxP-flanked alleles in T cells is consistently complete from the DP stage on (Lee et al., 2001; Wolfer et al., 2001). The data obtained from *CD4-Cre/Nemo*$^{FL/Y}$ mice unambiguously demonstrate that T cells in which the IKK has been disrupted through absence of NEMO are not viable. At this stage I cannot determine exactly when absence of IKK-mediated NF-κB activation leads to the loss of deficient T cells. In the thymus of *CD4-Cre/Nemo*$^{FL/Y}$ mice CD8-SP thymocytes are reduced compared to control mice, mainly because of a lack of more mature HSA$^{low/-}$ CD8-SP cells. In these mice CD4-SP thymocytes are found in nearly normal proportions, even though there is also a loss of CD4-SP/HSA$^{low/-}$ cells. These findings suggest that T cells with deleted *nemo* alleles start disappearing as they mature in the thymus. The presence of a small population of splenic CD4 cells with deleted *nemo* alleles indicates that some CD4 cells may survive for a short time after they exit the thymus and populate the periphery. Although different interpretations could be envisaged, I favor the hypothesis that *Nemo*$^{D/Y}$ T cells die as soon as they lose all their reserves of NEMO mRNA and protein. Deletion at the DP thymocyte stage creates *Nemo*$^{D/Y}$ cells that still contain sufficient levels of wild-type NEMO mRNA and protein to survive and get positively selected to become CD4 and CD8 single positive cells. The residual amount of remaining NEMO protein in DP and CD4-SP thymocytes from *CD4-Cre/Nemo*$^{FL/Y}$ showing more than 95% deletion at the DNA level further supports this hypothesis. As *Nemo*$^{D/Y}$ thymocytes mature, they slowly lose their mRNA and protein reserves through turnover and become deficient in IKK signaling. When IKK activity falls below a certain threshold the cells cannot be maintained anymore and die. This leads to the very small number of peripheral T cells in *CD4-Cre/Nemo*$^{FL/Y}$ mice that still contain loxP-flanked alleles, which means that they have escaped Cre-mediated recombination. A minor fraction of *Nemo*$^{D/Y}$ CD4 peripheral T cells can be detected. These are presumably cells that deleted *Nemo* late in development and still retain sufficient endogenous NEMO protein to stay alive until the protein is lost completely. Nearly all peripheral T cells in *CD4-Cre/Nemo*$^{FL/Y}$ mice are CD44^{+}. This indicates that the few T cells that escaped deletion underwent homeostatic proliferation to expand within this lymphopenic environment. During homeostatic expansion T cells acquire phenotype and functions of memory T cells (Goldrath, 2002).

T cells that lack IKK2, on the contrary, persist in the periphery, albeit in reduced numbers. Spleen and LNs of *CD4-Cre/Ikk2$^{FL/D}$* mice contain less than 50 % CD8 and around 80 % CD4 T cells of control mice in absolute numbers. More detailed analyses revealed that the lack of CD4 T cells is mostly due to T cells defined by CD25, CD44 and/or CD45Rb^{low} surface expression. CD4 T cell subsets defined by these markers have been shown to contain suppressive/regulatory (CD25$^+$, CD45Rb^{low}) and memory (CD44$^+$, CD45Rb^{low}) functions. The reduction in CD4$^+$CD25$^+$ T cells can be observed already in the thymus, where regulatory T cells are thought to be generated (Read and Powrie, 2001; Shevach, 2001). I found that in control mice CD4$^+$CD25$^+$ T cells in spleen and LNs are smaller than those in the thymus, whereas in *CD4-Cre/Ikk2$^{FL/D}$* mice the size remains constant. Since more immature cells are bigger this could indicate that peripheral CD4$^+$CD25$^+$ T cells in *CD4-Cre/Ikk2$^{FL/D}$* mice are cell that emigrated recently from the thymus and disappear before they develop into smaller, more mature T cells. However, so far I could not detect additional differences between CD4$^+$CD25$^+$ T from *CD4-Cre/Ikk2$^{FL/D}$* and those from control mice: the remaining peripheral CD4$^+$CD25$^+$ T cells in *CD4-Cre/Ikk2$^{FL/D}$* mice express constitutive CTLA-4 to the same extent as control CD4$^+$CD25$^+$ T cells and are slightly lower in CD4 as has been published for regulatory T cells (Read et al., 2000; Takahashi et al., 2000). I presently do not know whether the defect in CD4$^+$CD25$^+$, CD4$^+$CD45Rb^{low} and CD4$^+$CD44$^+$ T cells in *CD4-Cre/Ikk2$^{FL/D}$* mice reflects a true deficiency in regulatory and/or memory function.

IKK2-/-TNFR1-/- double deficient thymocytes were reported to have a complete defect in IKK activation and NF-κB DNA binding and reduced [^{3}H]thymidine uptake in response to plate-bound anti-CD3 treatment and to a lesser extent to PMA/Ionomycin or Concanavalin A treatment (Senftleben et al., 2001b). I used EMSA to measure NF-κB activation in FACS-purified *Ikk2$^{D/D}$* and control peripheral T cells upon stimulation with TNF, anti-CD3 or anti-CD3/CD28. The response of *Ikk2$^{D/D}$* T cells to these stimuli was somewhat weaker than that of control T cells, however IKK2-deficient T cells could clearly activate NF-κB to a significant extent. The composition of the induced NF-κB complexes is similar in IKK2-deficient and control T cells. It is well documented that in MEFs in the absence of IKK2 residual NF-κB activation occurs in response to proinflammatory stimuli (Li et al., 2000; Li et al., 1999b; Schmidt-Supprian et al., 2000; Tanaka et al., 1999). It seems that T cells can compensate better for the

loss of this protein. How this compensation is effected is difficult to predict. It seems possible that in the absence of IKK2 other kinases or co-activator proteins, present in T cells but not or in much lower levels in MEFs, associate with IKK1 and allow for NF-κB activation. One candidate could be IKKε (also known as IKKi), a kinase that was shown to phosphorylate IκB at one serine residue *in vitro* (Peters et al., 2000). Another possibility is that in T cells upstream activators of the IKK complex are expressed that can activate IKK1 homodimers better than those expressed in MEFs. At this point we cannot explain the obvious contradiction with the complete absence of NF-κB activation in IKK2-/-TNFR1-/- double deficient thymocytes. However, the speculations about the differences between MEFs and T cells could also apply to thymocytes and T cells. In light of the finding that NEMO-deficient T cells do not exist, it seems reasonable to argue that the ability of IKK2-deficient T cells to activate NF-κB allows their generation and persistence. Analysis of [^{3}H]thymidine incorporation in response to plate-bound anti-CD3 treatment revealed a mild defect in IKK2-deficient compared to control T cells. Using different experimental settings we observed that IKK2-deficient T cells could be induced to proliferate *in vitro* as well as control T cells in response to a whole variety of stimuli, demonstrating that these cells have no intrinsic defect impairing cell division. Similarly *Ikk2-/-* T cells can be induced to efficiently upregulate activation markers with normal kinetics. I acknowledge that these assays do not exclude potential defects of IKK2-deficient T cells to physiological responses *in vivo*. Nevertheless these data show that T cells without IKK2 can execute programs necessary for cellular functions such as proliferation and upregulation of activation markers, which are generally believed to depend to some extent on NF-κB activation. To test the function of IKK2-deficient T cells *in vivo* I immunized *CD4-Cre/Ikk2$^{FL/D}$* and control mice with the T-dependent antigen NP-CG. Measurement of NP-specific immunoglobulin concentrations in the serum during the time course of the immune response revealed that *CD4-Cre/Ikk2$^{FL/D}$* mice were able to mount an efficient, albeit delayed, anti-NP antibody response. This experiment shows that IKK2-deficient T cells are functional participants in the immune system of the mouse. Although it seems unlikely, I cannot formally exclude the rapid expansion and subsequent participation in the immune response of a minute fraction of T cells that escaped Cre-mediated deletion in *CD4-Cre/Ikk2$^{FL/D}$* mice.

In agreement with published data I show here that IKK2 is not needed for the development of mature T cells. IKK2-deficient T cells can activate NF-κB, proliferate, upregulate activation markers and participate in immune responses. It is interesting to note, however, that IKK2-deficiency leads to a reduction in peripheral T cell numbers, especially CD8 T cells. Initial data also indicate that IKK2 is essential for the generation and/or persistence of CD4 T cell subsets that contain T cells with regulatory or memory functions, defined by co-expression of CD25 or CD44.

In addition to deletion of IKK2 I analyzed the cell-autonomous role of the IKK complex in T cells through its disruption by deletion of NEMO. My results clearly show that IKK-mediated activation of NF-κB is essential for the generation of mature T cells from single-positive thymocytes. Additionally my data suggest that IKK-signaling is necessary for CD4 T cell maintenance.

5. SUMMARIES

5.1 Abstract

I generated a mouse strain harboring a conditional allele (*Nemo*^{FL}) of the X-linked gene encoding **N**F-κB **e**ssential **mo**dulator (NEMO), in order to analyze the function of the activation of the NF-κB transcription factor family via the IκB-Kinase complex (IKK) in the immune system of the mouse.

Biochemical studies using NEMO-deficient murine embryonic fibroblasts (MEFs) showed that NEMO is indispensable for NF-κB activation. Hemizygous male NEMO knockout mice die at embryonic day 11.5 displaying massive destruction of the liver. Heterozygous NEMO knockout (*Nemo*$^{D/WT}$) female mice develop a progressive inflammatory skin disease, become runted and growth-retarded and most die six to ten days after birth. Animals that survive beyond this period of time gradually recover. Detailed analysis of the histopathology of these mice revealed that an inflammatory response in the skin of *Nemo*$^{D/WT}$ mice soon after birth leads to hyperproliferation and increased apoptosis of keratinocytes. Due to random X-inactivation *Nemo*$^{D/WT}$ mice are mosaic animals, During the inflammatory response the skin is presumably cleared of keratinocytes unable to express NEMO. It seems that only mice in which initially the majority of cell have inactivated the X-chromosome harboring the *nemo*^{D}-allele can survive this period and recover. Male embryonic lethality and transient inflammatory skin lesions are characteristic of the human hereditary genodermatosis Incontinentia Pigmenti, which is caused by mutations in the human *NEMO* gene. The striking similarities between the pathology in NEMO-deficient mice and human IP suggest that the *Nemo*-knockout mice represent a mouse model for this disease.

The role of the IKK and NF-κB in B and T lymphocytes was investigated by cell-type specific deletion of *Nemo* employing CD19-Cre (B cell-specific) and CD4-Cre (T cell specific) transgenic mouse strains. *CD19-Cre/Nemo*^{FL} and *CD4-Cre/Nemo*^{FL} mice were compared in a side-by-side analysis to two mutant mouse strains, carrying either a conditional IKK2 allele (*ikk2*^{FL}) or a conditional IKK2ΔK allele (*ikk2*Δ*K*^{FL}), crossed to the same Cre-transgenic mice. In *Ikk2*Δ*K*$^{D/D}$ cells IKK2 should be replaced by a kinase-inactive version of IKK2, IKK2ΔK. Biochemical analysis of *Ikk2*Δ*K*$^{D/D}$ MEFs revealed

that the *Ikk2*ΔK^{D}-mutation leads to a more pronounced defect in transcription of pro-inflammatory NF-κB target genes than a mere lack of IKK2.

Analysis of the CD19-Cre/IKK conditional mutants showed that the maintenance of mature B cells critically depends on signals mediated by IKK2 and NEMO. Disruption of the IKK2-signaling pathway leads to loss of mature B cells. Deletion of NEMO or IKK2-activity in T cells mediated by the CD4-Cre transgene yielded a different picture: Peripheral T cells lacking NEMO cannot be generated and/or persist, whereas IKK2-deficient T cells are generated, although in reduced numbers. *CD4-Cre/IKK2*^{FL} mice have around half the number of CD8 T cells, a profound deficit in the $CD4^{+}/CD25^{+}$ regulatory T cell population and a reduction in $CD44^{+}$ memory-type T cells. Analysis of IKK2-deficient T cells showed that they can activate NF-κB to a considerable extent, upregulate activation markers, proliferate and elicit an, albeit delayed, T-dependent immune response.

5.2 Zusammenfassung

Ziel dieser Arbeit war es, die Funktion der Aktivierung der Transkriptionsfaktor-Familie NF-κB durch den IκB-Kinase Komplex (IKK) im Immunsystem der Maus zu untersuchen. Zu diesem Zweck wurde ein Mausstamm erzeugt, der ein konditionales Allel (*Nemo*^{FL}) des sich auf dem X-Chromosom befindenden *Nemo* (**N**F-κB **e**ssential **mo**dulator) Gens enthält.

Zunächst wurde die Rolle von NEMO in der Entwicklung der Maus anhand von NEMO-defizienten Mäusen (NEMO-knockout Mäuse) untersucht. Biochemische Analysen an NEMO-defizienten embryonalen Fibroblasten (MEFs) zeigten, dass ohne NEMO keine Aktivierung von NF-κB möglich ist. Hemizygote männliche NEMO-knockout Mäuse sterben an Tag 11.5 der Embryonalentwicklung und weisen eine weitgehende Degeneration der Leber auf. Heterozygote weibliche NEMO-knockout Mäuse (*Nemo*$^{D/WT}$) entwickeln eine progressive Hautkrankheit mit Anzeichen von lokalen Entzündungsreaktionen. Sie bleiben zunehmend im Wachstum zurück und die meisten sterben sechs bis zehn Tage nach Geburt. Tiere, die diese Phase überleben, erholen sich nach einigen Wochen vollständig. Anhand von detallierten histopathologischen Untersuchungen dieser Mäuse liessen sich einige Tage nach der Geburt in der Haut von *Nemo*$^{D/WT}$ Mäusen Anzeichen einer Entzündungsreaktion und hyperproliferierende und absterbende Keratinozyten nachweisen. Durch X-Inaktivierung werden *Nemo*$^{D/WT}$ Mäuse genetische Mosaike. Während der Entzündungsreaktion werden vermutlich in der Haut dieser Tiere die NEMO-defizienten Keratinozyten durch NEMO-ausprägende Keratinozyten ersetzt. Es scheint so, dass nur Mäuse, in denen während der X-Inaktivierung hauptsächlich das *nemo*^{D}-Allel inaktiviert wurde, überleben und sich erholen können. Embryonale Lethalität und eine progressive Hauterkrankung sind charakteristisch für die menschliche Erbkrankheit Incontinentia Pigmenti (IP); in 80 % der IP-Patienten wurden Mutationen im humanen *NEMO* Gen gefunden. Die starke Ähnlichkeit des Krankheitsverlaufes in NEMO-defizienten Mäusen mit Incontinentia Pigmenti zeigt, dass diese Mäuse ein Tiermodell für die menschliche Erbkrankheit Incontinentia Pigmenti (IP) darstellen.

Die Rolle des IKK Komplexes und NF-κB in Lymphozyten wurde in Mäusen analysiert, denen NEMO ausschliesslich in B oder T Zellen fehlt. Hierzu wurden *Nemo*^{FL} Mäuse mit CD19-Cre (B Zellen) oder mit CD4-Cre (T Zellen) transgenen Mäusen verkreuzt. Der zelltyp-spezifische Verlust von NEMO wurde mit dem Verlust

von IKK2 und dem Austausch von IKK2 durch eine Kinase-inaktive Variante, IKK2ΔK, verglichen. Biochemische Analysen zeigten, dass der Ersatz von IKK2 durch die inaktive Mutante IKK2ΔK einen stärkeren Effekt auf die Transkription von NF-κB-abhängigen inflammatorischen Genen hat, als das Fehlen von IKK2. Die Analyse der CD19-Cre/IKK-konditionalen Mausmutanten zeigte, dass reife B Zellen zum Überleben auf IKK2/NEMO-vermittelte Signale angewiesen sind.

Die Deletion von NEMO oder IKK2 in T Zellen anhand des CD4-Cre Transgens zeitigte ein anderes Bild: Periphere NEMO-defiziente T Zellen können nicht erzeugt oder nicht erhalten werden, während IKK2-defiziente T Zellen sich entwickeln können, wenn auch in verminderter Anzahl. *CD4-Cre/IKK2^{FL}* Mäuse haben ungefähr die Hälfte an CD8 T Zellen verglichen mit Kontrollmäusen. Zudem können sich IKK2-defiziente T Zellen nur vermindert zu $CD4^+CD25^+$ oder $CD4^+CD44^+$ T Zellen entwickeln, oder als solche überleben. Dies zeigt, dass IKK2-vermittelte Signale essentiell für die Erzeugung und/oder Erhaltung bestimmter T Zell Untergruppen sind. Weitergehende Analysen ergaben, dass T Zellen ohne IKK2 NF-κB aktivieren, Aktivierungsmarker hochregulieren, proliferieren und eine, wenn auch verzögert, T Zell-abhängige Immunantwort initiieren können.

5.3 Kurzzusammenfassung

In dieser Arbeit wurde die Rolle der NF-κB Aktivierung durch den IκB-Kinase Komplex *in vivo* untersucht. Die Erzeugung und Untersuchung von NEMO-defizienten Mäusen ergab, dass diese ein Tiermodell für die menschliche Erbkrankheit Incontinentia Pigmenti darstellen. Die Rolle des den IκB-Kinase Komplexes in B und T Lymphozyten wurde mit Hilfe von drei verschiedenen konditionalen Mausstämmen untersucht. Genetische Manipulationen in diesen Mäusen führt entweder zu Fehlen von NEMO oder IKK2, oder zum Austausch von IKK2 durch ein IKK2-Protein, das keine Kinase-Aktivität besitzt. In B Zellen sind IKK2-vermittelte Signale überlebensnotwendig. In T Zellen dagegen führt die IKK2-Defizienz zur Reduktion bestimmter T Zell Untergruppen, während das Fehlen von NEMO und damit von NF-κB Aktivierung durch den IKK Komplex nicht mit der Erzeugung und/oder Erhaltung von reifen T Zellen vereinbar ist.

6 REFERENCES

Abastado, J. P., Jaulin, C., Schutze, M. P., Langlade-Demoyen, P., Plata, F., Ozato, K., and Kourilsky, P. (1987). Fine mapping of epitopes by intradomain Kd/Dd recombinants. *J Exp Med* 166, 327-340.

Agou, F., Ye, F., Goffinont, S., Courtois, G., Yamaoka, S., Israel, A., and Veron, M. (2002). NEMO trimerizes through its coiled-coil C-terminal domain. *J Biol Chem* 277, 17464-17475.

Alcamo, E., Hacohen, N., Schulte, L. C., Rennert, P. D., Hynes, R. O., and Baltimore, D. (2002). Requirement for the NF-kappaB family member RelA in the development of secondary lymphoid organs. *J Exp Med* 195, 233-244.

Allman, D. M., Ferguson, S. E., Lentz, V. M., and Cancro, M. P. (1993). Peripheral B cell maturation. II. Heat-stable antigen(hi) splenic B cells are an immature developmental intermediate in the production of long-lived marrow-derived B cells. *J Immunol* 151, 4431-4444.

Allman, D., Lindsley, R. C., DeMuth, W., Rudd, K., Shinton, S. A., and Hardy, R. R. (2001). Resolution of three nonproliferative immature splenic B cell subsets reveals multiple selection points during peripheral B cell maturation. *J Immunol* 167, 6834-6840.

Annacker, O., Pimenta-Araujo, R., Burlen-Defranoux, O., Barbosa, T. C., Cumano, A., and Bandeira, A. (2001). CD25+ CD4+ T cells regulate the expansion of peripheral CD4 T cells through the production of IL-10. *J Immunol* 166, 3008-3018.

Annacker, O., and Powrie, F. (2002). Homeostasis of intestinal immune regulation. *Microbes Infect* 4, 567-574.

Aradhya, S., and Nelson, D. L. (2001). NF-kappaB signaling and human disease. *Curr Opin Genet Dev* 11, 300-306.

Aradhya, S., Courtois, G., Rajkovic, A., Lewis, R. A., Levy, M., Israel, A., and Nelson, D. L. (2001). Atypical forms of incontinentia pigmenti in male individuals result from mutations of a cytosine tract in exon 10 of NEMO (IKK-gamma). *Am J Hum Genet* 68, 765-771.

Aradhya, S., Woffendin, H., Jakins, T., Bardaro, T., Esposito, T., Smahi, A., Shaw, C., Levy, M., Munnich, A., D'Urso, M., *et al.* (2001). A recurrent deletion in the ubiquitously expressed NEMO (IKK-gamma) gene accounts for the vast majority of incontinentia pigmenti mutations. *Hum Mol Genet* 10, 2171-2179.

Asano, M., Toda, M., Sakaguchi, N., and Sakaguchi, S. (1996). Autoimmune disease as a consequence of developmental abnormality of a T cell subpopulation. *J Exp Med* 184, 387-396.

Attar, R. M., Macdonald-Bravo, H., Raventos-Suarez, C., Durham, S. K., and Bravo, R. (1998). Expression of constitutively active IkappaB beta in T cells of transgenic mice: persistent NF-kappaB activity is required for T-cell immune responses. *Mol Cell Biol* 18, 477-487.

Aune, T. M., Mora, A. L., Kim, S., Boothby, M., and Lichtman, A. H. (1999). Costimulation reverses the defect in IL-2 but not effector cytokine production by T cells with impaired IkappaBalpha degradation. *J Immunol* 162, 5805-5812.

Baeuerle, P. A. (1998). IkappaB-NF-kappaB structures: at the interface of inflammation control. *Cell* 95, 729-731.

Baeuerle, P. A. (1998). Pro-inflammatory signaling: last pieces in the NF-kappaB puzzle? *Curr Biol* 8, R19-22.

Baldwin, A. S., Jr. (1996). The NF-kappa B and I kappa B proteins: new discoveries and insights. *Annu Rev Immunol* 14, 649-683.

Baldwin, A. S., Jr. (2001). Series introduction: the transcription factor NF-kappaB and human disease. *J*

Clin Invest 107, 3-6.

Baniyash, M., and Eshhar, Z. (1984). Inhibition of IgE binding to mast cells and basophils by monoclonal antibodies to murine IgE. *Eur J Immunol* 14, 799-807.

Barkett, M., and Gilmore, T. D. (1999). Control of apoptosis by Rel/NF-kappaB transcription factors. *Oncogene* 18, 6910-6924.

Barton, D., HogenEsch, H., and Weih, F. (2000). Mice lacking the transcription factor RelB develop T cell-dependent skin lesions similar to human atopic dermatitis. *Eur J Immunol* 30, 2323-2332.

Baumhackel, H., Liesegang, B., Radbruch, A., Rajewsky, K., and Sablitzky, F. (1982). Switch from NP-specific IgG3 to IgG1 in the mouse hybridoma cell line S24/63/63. *J Immunol* 128, 1217-1220.

Beg, A. A., Sha, W. C., Bronson, R. T., Ghosh, S., and Baltimore, D. (1995). Embryonic lethality and liver degeneration in mice lacking the RelA component of NF-kappa B. *Nature* 376, 167-170.

Bendall, H. H., Sikes, M. L., Ballard, D. W., and Oltz, E. M. (1999). An intact NF-kappa B signaling pathway is required for maintenance of mature B cell subsets. *Mol Immunol* 36, 187-195.

Bendall, H. H., Sikes, M. L., and Oltz, E. M. (2001). Transcription factor NF-kappa B regulates Ig lambda light chain gene rearrangement. *J Immunol* 167, 264-269.

Betz, U. A., Vosshenrich, C. A., Rajewsky, K., and Muller, W. (1996). Bypass of lethality with mosaic mice generated by Cre-loxP-mediated recombination. *Curr Biol* 6, 1307-1316.

Bhattacharya, A., Dorf, M. E., and Springer, T. A. (1981). A shared alloantigenic determinant on Ia antigens encoded by the I-A and I-E subregions: evidence for I region gene duplication. *J Immunol* 127, 2488-2495.

Bigos, M., Baumgarth, N., Jager, G. C., Herman, O. C., Nozaki, T., Stovel, R. T., Parks, D. R., and Herzenberg, L. A. (1999). Nine color eleven parameter immunophenotyping using three laser flow cytometry. *Cytometry* 36, 36-45.

Birnboim, H. C. (1983). A rapid alkaline extraction method for the isolation of plasmid DNA. *Methods Enzymol* 100, 243-255.

Bonnard, M., Mirtsos, C., Suzuki, S., Graham, K., Huang, J., Ng, M., Itie, A., Wakeham, A., Shahinian, A., Henzel, W. J., *et al.* (2000). Deficiency of T2K leads to apoptotic liver degeneration and impaired NF-kappaB-dependent gene transcription. *Embo J* 19, 4976-4985.

Boone, D. L., Lee, E. G., Libby, S., Gibson, P. J., Chien, M., Chan, F., Madonia, M., Burkett, P. R., and Ma, A. (2002). Recent advances in understanding NF-kappaB regulation. *Inflamm Bowel Dis* 8, 201-212.

Boothby, M. R., Mora, A. L., Scherer, D. C., Brockman, J. A., and Ballard, D. W. (1997). Perturbation of the T lymphocyte lineage in transgenic mice expressing a constitutive repressor of nuclear factor (NF)-kappaB. *J Exp Med* 185, 1897-1907.

Bottomly, K., Luqman, M., Greenbaum, L., Carding, S., West, J., Pasqualini, T., and Murphy, D. B. (1989). A monoclonal antibody to murine CD45R distinguishes CD4 T cell populations that produce different cytokines. *Eur J Immunol* 19, 617-623.

Buchholz, F., Angrand, P. O., and Stewart, A. F. (1998). Improved properties of FLP recombinase evolved by cycling mutagenesis. *Nat Biotechnol* 16, 657-662.

Bunting, M., Bernstein, K. E., Greer, J. M., Capecchi, M. R., and Thomas, K. R. (1999). Targeting genes for self-excision in the germ line. *Genes Dev* 13, 1524-1528.

Bureau, F., Vanderplasschen, A., Jaspar, F., Minner, F., Pastoret, P. P., Merville, M. P., Bours, V., and Lekeux, P. (2002). Constitutive nuclear factor-kappaB activity preserves homeostasis of quiescent

mature lymphocytes and granulocytes by controlling the expression of distinct Bcl-2 family proteins. *Blood* 99, 3683-3691.

Caamano, J., and Hunter, C. A. (2002). NF-kappaB family of transcription factors: central regulators of innate and adaptive immune functions. *Clin Microbiol Rev* 15, 414-429.

Cao, Y., Bonizzi, G., Seagroves, T. N., Greten, F. R., Johnson, R., Schmidt, E. V., and Karin, M. (2001). IKKalpha provides an essential link between RANK signaling and cyclin D1 expression during mammary gland development. *Cell* 107, 763-775.

Cariappa, A., Liou, H. C., Horwitz, B. H., and Pillai, S. (2000). Nuclear factor kappa B is required for the development of marginal zone B lymphocytes. *J Exp Med* 192, 1175-1182.

Cariappa, A., Tang, M., Parng, C., Nebelitskiy, E., Carroll, M., Georgopoulos, K., and Pillai, S. (2001). The follicular versus marginal zone B lymphocyte cell fate decision is regulated by Aiolos, Btk, and CD21. *Immunity* 14, 603-615.

Carney, R. G. (1976). Incontinentia pigmenti. A world statistical analysis. *Arch Dermatol* 112, 535-542.

Carvalho, T. L., Mota-Santos, T., Cumano, A., Demengeot, J., and Vieira, P. (2001). Arrested B lymphopoiesis and persistence of activated B cells in adult interleukin 7(-/)- mice. *J Exp Med* 194, 1141-1150.

Cazac, B. B., and Roes, J. (2000). TGF-beta receptor controls B cell responsiveness and induction of IgA in vivo. *Immunity* 13, 443-451.

Chomczynski, P., and Qasba, P. K. (1984). Alkaline transfer of DNA to plastic membrane. *Biochem Biophys Res Commun* 122, 340-344.

Claudio, E., Brown, K., Park, S., Wang, H., and Siebenlist, U. (2002). BAFF-induced NEMO-independent processing of NF-kappa B2 in maturing B cells. *Nat Immunol* 3, 958-965.

Coffman, R. L. (1982). Surface antigen expression and immunoglobulin gene rearrangement during mouse pre-B cell development. *Immunol Rev* 69, 5-23.

Cooke, E. L., Uings, I. J., Xia, C. L., Woo, P., and Ray, K. P. (2001). Functional analysis of the interleukin-1-receptor-associated kinase (IRAK-1) in interleukin-1 beta-stimulated nuclear factor kappa B (NF-kappa B) pathway activation: IRAK-1 associates with the NF-kappa B essential modulator (NEMO) upon receptor stimulation. *Biochem J* 359, 403-410.

Coope, H. J., Atkinson, P. G., Huhse, B., Belich, M., Janzen, J., Holman, M. J., Klaus, G. G., Johnston, L. H., and Ley, S. C. (2002). CD40 regulates the processing of NF-kappaB2 p100 to p52. *Embo J* 21, 5375-5385.

Cooper, M. D., Mulvaney, D., Coutinho, A., and Cazenave, P. A. (1986). A novel cell surface molecule on early B-lineage cells. *Nature* 321, 616-618.

Courtois, G., and Israel, A. (2000). NF-kappaB defects in humans: the NEMO/incontinentia pigmenti connection. *Sci STKE* 2000, E1.

Courtois, G., Smahi, A., and Israel, A. (2001). NEMO/IKK gamma: linking NF-kappa B to human disease. *Trends Mol Med* 7, 427-430.

Cumano, A., and Rajewsky, K. (1985). Structure of primary anti-(4-hydroxy-3-nitrophenyl)acetyl (NP) antibodies in normal and idiotypically suppressed C57BL/6 mice. *Eur J Immunol* 15, 512-520.

Cumano, A., and Rajewsky, K. (1986). Clonal recruitment and somatic mutation in the generation of immunological memory to the hapten NP. *Embo J* 5, 2459-2468.

Curotto de Lafaille, M. A., and Lafaille, J. J. (2002). CD4(+) regulatory T cells in autoimmunity and

allergy. *Curr Opin Immunol* 14, 771-778.

Davis, R. E., Brown, K. D., Siebenlist, U., and Staudt, L. M. (2001). Constitutive nuclear factor kappaB activity is required for survival of activated B cell-like diffuse large B cell lymphoma cells. *J Exp Med* 194, 1861-1874.

Dejardin, E., Droin, N. M., Delhase, M., Haas, E., Cao, Y., Makris, C., Li, Z. W., Karin, M., Ware, C. F., and Green, D. R. (2002). The Lymphotoxin-beta Receptor Induces Different Patterns of Gene Expression via Two NF-kappaB Pathways. *Immunity* 17, 525.

DeKoning, J., DiMolfetto, L., Reilly, C., Wei, Q., Havran, W. L., and Lo, D. (1997). Thymic cortical epithelium is sufficient for the development of mature T cells in relB-deficient mice. *J Immunol* 158, 2558-2566.

Delhase, M., Hayakawa, M., Chen, Y., and Karin, M. (1999). Positive and negative regulation of IkappaB kinase activity through IKKbeta subunit phosphorylation. *Science* 284, 309-313.

Denk, A., Wirth, T., and Baumann, B. (2000). NF-kappaB transcription factors: critical regulators of hematopoiesis and neuronal survival. *Cytokine Growth Factor Rev* 11, 303-320.

Devin, A., Cook, A., Lin, Y., Rodriguez, Y., Kelliher, M., and Liu, Z. (2000). The distinct roles of TRAF2 and RIP in IKK activation by TNF-R1: TRAF2 recruits IKK to TNF-R1 while RIP mediates IKK activation. *Immunity* 12, 419-429.
Devin, A., Lin, Y., Yamaoka, S., Li, Z., Karin, M., and Liu, Z. (2001). The alpha and beta subunits of IkappaB kinase (IKK) mediate TRAF2-dependent IKK recruitment to tumor necrosis factor (TNF) receptor 1 in response to TNF. *Mol Cell Biol* 21, 3986-3994.

Dialynas, D. P., Quan, Z. S., Wall, K. A., Pierres, A., Quintans, J., Loken, M. R., Pierres, M., and Fitch, F. W. (1983). Characterization of the murine T cell surface molecule, designated L3T4, identified by monoclonal antibody GK1.5: similarity of L3T4 to the human Leu-3/T4 molecule. *J Immunol* 131, 2445-2451.

DiDonato, J. A. (2001). IKK alpha on center stage. *Sci STKE* 2001, E1.

Dixit, V., and Mak, T. W. (2002). NF-kappaB signaling. Many roads lead to madrid. *Cell* 111, 615-619.

Do, R. K., Hatada, E., Lee, H., Tourigny, M. R., Hilbert, D., and Chen-Kiang, S. (2000). Attenuation of apoptosis underlies B lymphocyte stimulator enhancement of humoral immune response. *J Exp Med* 192, 953-964.

Do, R. K., and Chen-Kiang, S. (2002). Mechanism of BLyS action in B cell immunity. *Cytokine Growth Factor Rev* 13, 19-25.

Doerre, S., and Corley, R. B. (1999). Constitutive nuclear translocation of NF-kappa B in B cells in the absence of I kappa B degradation. *J Immunol* 163, 269-277.

Doi, T. S., Takahashi, T., Taguchi, O., Azuma, T., and Obata, Y. (1997). NF-kappa B RelA-deficient lymphocytes: normal development of T cells and B cells, impaired production of IgA and IgG1 and reduced proliferative responses. *J Exp Med* 185, 953-961.

Dudley, E., Hornung, F., Zheng, L., Scherer, D., Ballard, D., and Lenardo, M. (1999). NF-kappaB regulates Fas/APO-1/CD95- and TCR- mediated apoptosis of T lymphocytes. *Eur J Immunol* 29, 878-886.

Esslinger, C. W., Wilson, A., Sordat, B., Beermann, F., and Jongeneel, C. V. (1997). Abnormal T lymphocyte development induced by targeted overexpression of IkappaB alpha. *J Immunol* 158, 5075-5078.

Esslinger, C. W., Jongeneel, C. V., and MacDonald, H. R. (1998). Survival-independent function of NF-kappaB/Rel during late stages of thymocyte differentiation. *Mol Immunol* 35, 847-852.

Fagarasan, S., Watanabe, N., and Honjo, T. (2000). Generation, expansion, migration and activation of mouse B1 cells. *Immunol Rev* 176, 205-215.

Feinberg, A. P., and Vogelstein, B. (1984). "A technique for radiolabeling DNA restriction endonuclease fragments to high specific activity". Addendum. *Anal Biochem* 137, 266-267.

Ferreira, V., Sidenius, N., Tarantino, N., Hubert, P., Chatenoud, L., Blasi, F., and Korner, M. (1999). In vivo inhibition of NF-kappa B in T-lineage cells leads to a dramatic decrease in cell proliferation and cytokine production and to increased cell apoptosis in response to mitogenic stimuli, but not to abnormal thymopoiesis. *J Immunol* 162, 6442-6450.

Feuillard, J., Memet, S., Goudeau, B., Lilienbaum, A., Schmidt-Ullrich, R., Raphael, M., and Israel, A. (2000). In vivo identification of lymphocyte subsets exhibiting transcriptionally active NF-kappaB/Rel complexes. *Int Immunol* 12, 613-621.

Fields, E. R., Seufzer, B. J., Oltz, E. M., and Miyamoto, S. (2000). A switch in distinct I kappa B alpha degradation mechanisms mediates constitutive NF-kappa B activation in mature B cells. *J Immunol* 164, 4762-4767.

Finn, P. W., Stone, J. R., Boothby, M. R., and Perkins, D. L. (2001). Inhibition of NF-kappaB-dependent T cell activation abrogates acute allograft rejection. *J Immunol* 167, 5994-6001.

Fiorini, E., Schmitz, I., Marissen, W. E., Osborn, S. L., Touma, M., Sasada, T., Reche, P. A., Tibaldi, E. V., Hussey, R. E., Kruisbeek, A. M., *et al.* (2002). Peptide-induced negative selection of thymocytes activates transcription of an NF-kappa B inhibitor. *Mol Cell* 9, 637-648.

Fischer, C., Page, S., Weber, M., Eisele, T., Neumeier, D., and Brand, K. (1999). Differential effects of lipopolysaccharide and tumor necrosis factor on monocytic IkappaB kinase signalsome activation and IkappaB proteolysis. *J Biol Chem* 274, 24625-24632.

Fleming, T. J., Fleming, M. L., and Malek, T. R. (1993). Selective expression of Ly-6G on myeloid lineage cells in mouse bone marrow. RB6-8C5 mAb to granulocyte-differentiation antigen (Gr-1) detects members of the Ly-6 family. *J Immunol* 151, 2399-2408.

Forster, I., Vieira, P., and Rajewsky, K. (1989). Flow cytometric analysis of cell proliferation dynamics in the B cell compartment of the mouse. *Int Immunol* 1, 321-331.

Forster, I., and Rajewsky, K. (1990). The bulk of the peripheral B-cell pool in mice is stable and not rapidly renewed from the bone marrow. *Proc Natl Acad Sci U S A* 87, 4781-4784.

Franzoso, G., Carlson, L., Xing, L., Poljak, L., Shores, E. W., Brown, K. D., Leonardi, A., Tran, T., Boyce, B. F., and Siebenlist, U. (1997). Requirement for NF-kappaB in osteoclast and B-cell development. *Genes Dev* 11, 3482-3496.

Franzoso, G., Carlson, L., Poljak, L., Shores, E. W., Epstein, S., Leonardi, A., Grinberg, A., Tran, T., Scharton-Kersten, T., Anver, M., *et al.* (1998). Mice deficient in nuclear factor (NF)-kappa B/p52 present with defects in humoral responses, germinal center reactions, and splenic microarchitecture. *J Exp Med* 187, 147-159.

Friedman, R., and Hughes, A. L. (2002). Molecular evolution of the NF-kappaB signaling system. *Immunogenetics* 53, 964-974.

Fuchs, E. (1993). Epidermal differentiation and keratin gene expression. *J Cell Sci Suppl* 17, 197-208.

Fulcher, D. A., and Basten, A. (1997). B cell life span: a review. *Immunol Cell Biol* 75, 446-455.

Fulcher, D. A., and Basten, A. (1997). Influences on the lifespan of B cell subpopulations defined by

different phenotypes. *Eur J Immunol* 27, 1188-1199.

Furtado, G. C., Olivares-Villagomez, D., Curotto de Lafaille, M. A., Wensky, A. K., Latkowski, J. A., and Lafaille, J. J. (2001). Regulatory T cells in spontaneous autoimmune encephalomyelitis. *Immunol Rev* 182, 122-134.

Gabor, M. J., Godfrey, D. I., and Scollay, R. (1997). Recent thymic emigrants are distinct from most medullary thymocytes. *Eur J Immunol* 27, 2010-2015.

Gabor, M. J., Scollay, R., and Godfrey, D. I. (1997). Thymic T cell export is not influenced by the peripheral T cell pool. *Eur J Immunol* 27, 2986-2993.

Galgoczy, P., Rosenthal, A., and Platzer, M. (2001). Human-mouse comparative sequence analysis of the NEMO gene reveals an alternative promoter within the neighboring G6PD gene. *Gene* 271, 93-98.

Gallatin, W. M., Weissman, I. L., and Butcher, E. C. (1983). A cell-surface molecule involved in organ-specific homing of lymphocytes. *Nature* 304, 30-34.

Gavin, M. A., Clarke, S. R., Negrou, E., Gallegos, A., and Rudensky, A. (2002). Homeostasis and anergy of CD4(+)CD25(+) suppressor T cells in vivo. *Nat Immunol* 3, 33-41.

Ge, Q., Hu, H., Eisen, H. N., and Chen, J. (2002). Different contributions of thymopoiesis and homeostasis-driven proliferation to the reconstitution of naive and memory T cell compartments. *Proc Natl Acad Sci U S A* 99, 2989-2994.

Ge, Q., Palliser, D., Eisen, H. N., and Chen, J. (2002). Homeostatic T cell proliferation in a T cell-dendritic cell coculture system. *Proc Natl Acad Sci U S A* 99, 2983-2988.

Germain, R. N. (2002). T-cell development and the CD4-CD8 lineage decision. *Nat Rev Immunol* 2, 309-322.

Gerondakis, S., Grumont, R., Rourke, I., and Grossmann, M. (1998). The regulation and roles of Rel/NF-kappa B transcription factors during lymphocyte activation. *Curr Opin Immunol* 10, 353-359.

Gerondakis, S., Grossmann, M., Nakamura, Y., Pohl, T., and Grumont, R. (1999). Genetic approaches in mice to understand Rel/NF-kappaB and IkappaB function: transgenics and knockouts. *Oncogene* 18, 6888-6895.

Ghosh, S., May, M. J., and Kopp, E. B. (1998). NF-kappa B and Rel proteins: evolutionarily conserved mediators of immune responses. *Annu Rev Immunol* 16, 225-260.

Ghosh, S. (1999). Regulation of inducible gene expression by the transcription factor NF-kappaB. *Immunol Res* 19, 183-189.

Ghosh, S., and Karin, M. (2002). Missing pieces in the NF-kappaB puzzle. *Cell* 109 Suppl, S81-96.

Gilmore, T. D. (1999). The Rel/NF-kappaB signal transduction pathway: introduction. *Oncogene* 18, 6842-6844.

Goldrath, A. W., Bogatzki, L. Y., and Bevan, M. J. (2000). Naive T cells transiently acquire a memory-like phenotype during homeostasis-driven proliferation. *J Exp Med* 192, 557-564.

Goldrath, A. W. (2002). Maintaining the status quo: T-cell homeostasis. *Microbes Infect* 4, 539-545.

Gray, D. (1988). Population kinetics of rat peripheral B cells. *J Exp Med* 167, 805-816.

Grossmann, M., Metcalf, D., Merryfull, J., Beg, A., Baltimore, D., and Gerondakis, S. (1999). The combined absence of the transcription factors Rel and RelA leads to multiple hemopoietic cell defects. *Proc Natl Acad Sci U S A* 96, 11848-11853.

Grossmann, M., Nakamura, Y., Grumont, R., and Gerondakis, S. (1999). New insights into the roles of ReL/NF-kappa B transcription factors in immune function, hemopoiesis and human disease. *Int J Biochem Cell Biol* 31, 1209-1219.

Grossmann, M., O'Reilly, L. A., Gugasyan, R., Strasser, A., Adams, J. M., and Gerondakis, S. (2000). The anti-apoptotic activities of Rel and RelA required during B-cell maturation involve the regulation of Bcl-2 expression. *Embo J* 19, 6351-6360.

Gruetzman, R. (1981) Vergleichende Idiotypische Analyse von Rezeptoren mit Spezifitaet fuer Histokompatibilitaetsantigene, PhD, Cologne, Cologne.

Grumont, R. J., and Gerondakis, S. (1994). The subunit composition of NF-kappa B complexes changes during B-cell development. *Cell Growth Differ* 5, 1321-1331.

Grumont, R. J., Rourke, I. J., O'Reilly, L. A., Strasser, A., Miyake, K., Sha, W., and Gerondakis, S. (1998). B lymphocytes differentially use the Rel and nuclear factor kappaB1 (NF-kappaB1) transcription factors to regulate cell cycle progression and apoptosis in quiescent and mitogen-activated cells. *J Exp Med* 187, 663-674.

Grumont, R. J., Rourke, I. J., and Gerondakis, S. (1999). Rel-dependent induction of A1 transcription is required to protect B cells from antigen receptor ligation-induced apoptosis. *Genes Dev* 13, 400-411.

Gu, H., Marth, J. D., Orban, P. C., Mossmann, H., and Rajewsky, K. (1994). Deletion of a DNA polymerase beta gene segment in T cells using cell type-specific gene targeting. *Science* 265, 103-106.

Guermonprez, P., Valladeau, J., Zitvogel, L., Thery, C., and Amigorena, S. (2002). Antigen presentation and T cell stimulation by dendritic cells. *Annu Rev Immunol* 20, 621-667.

Gugasyan, R., Grumont, R., Grossmann, M., Nakamura, Y., Pohl, T., Nesic, D., and Gerondakis, S. (2000). Rel/NF-kappaB transcription factors: key mediators of B-cell activation. *Immunol Rev* 176, 134-140.

Gulley, M. L., Ogata, L. C., Thorson, J. A., Dailey, M. O., and Kemp, J. D. (1988). Identification of a murine pan-T cell antigen which is also expressed during the terminal phases of B cell differentiation. *J Immunol* 140, 3751-3757.

Hadjantonakis, A. K., Gertsenstein, M., Ikawa, M., Okabe, M., and Nagy, A. (1998). Generating green fluorescent mice by germline transmission of green fluorescent ES cells. *Mech Dev* 76, 79-90.

Hao, Z., and Rajewsky, K. (2001). Homeostasis of peripheral B cells in the absence of B cell influx from the bone marrow. *J Exp Med* 194, 1151-1164.

Happle, R. (1985). Lyonization and the lines of Blaschko. *Hum Genet* 70, 200-206.

Harhaj, E. W., Good, L., Xiao, G., Uhlik, M., Cvijic, M. E., Rivera-Walsh, I., and Sun, S. C. (2000). Somatic mutagenesis studies of NF-kappa B signaling in human T cells: evidence for an essential role of IKK gamma in NF-kappa B activation by T-cell costimulatory signals and HTLV-I Tax protein. *Oncogene* 19, 1448-1456.

Harlin, H., Hwang, K. W., Palucki, D. A., Kim, O., Thompson, C. B., Boothby, M., and Alegre, M. L. (2002). CTLA-4 engagement regulates NF-kappaB activation in vivo. *Eur J Immunol* 32, 2095-2104.

Hatada, E. N., Krappmann, D., and Scheidereit, C. (2000). NF-kappaB and the innate immune response. *Curr Opin Immunol* 12, 52-58.

Herzenberg, L. A., and Black, S. J. (1980). Regulatory circuits and antibody responses. *Eur J Immunol* 10, 1-11.

Hettmann, T., DiDonato, J., Karin, M., and Leiden, J. M. (1999). An essential role for nuclear factor kappaB in promoting double positive thymocyte apoptosis. *J Exp Med* 189, 145-158.

Hettmann, T., and Leiden, J. M. (2000). NF-kappa B is required for the positive selection of CD8+ thymocytes. *J Immunol* 165, 5004-5010.

Heyninck, K., and Beyaert, R. (2001). Crosstalk between NF-kappaB-activating and apoptosis-inducing proteins of the TNF-receptor complex. *Mol Cell Biol Res Commun* 4, 259-265.

Hoeflich, K. P., Luo, J., Rubie, E. A., Tsao, M. S., Jin, O., and Woodgett, J. R. (2000). Requirement for glycogen synthase kinase-3beta in cell survival and NF-kappaB activation. *Nature* 406, 86-90.

Hoffmann, P., Ermann, J., Edinger, M., Fathman, C. G., and Strober, S. (2002). Donor-type CD4(+)CD25(+) regulatory T cells suppress lethal acute graft-versus-host disease after allogeneic bone marrow transplantation. *J Exp Med* 196, 389-399.

Hogan, B., Constantini, F., and Lacy, I. (1987). Manuipulating the mouse embryo, Cold Spring Harbor Laboratory Press).

Horcher, M., Souabni, A., and Busslinger, M. (2001). Pax5/BSAP maintains the identity of B cells in late B lymphopoiesis. *Immunity* 14, 779-790.

Horwitz, B. H., Scott, M. L., Cherry, S. R., Bronson, R. T., and Baltimore, D. (1997). Failure of lymphopoiesis after adoptive transfer of NF-kappaB-deficient fetal liver cells. *Immunity* 6, 765-772.

Horwitz, B. H., Zelazowski, P., Shen, Y., Wolcott, K. M., Scott, M. L., Baltimore, D., and Snapper, C. M. (1999). The p65 subunit of NF-kappa B is redundant with p50 during B cell proliferative responses, and is required for germline CH transcription and class switching to IgG3. *J Immunol* 162, 1941-1946.

Howard, T., Balogh, R., Overbeek, P., and Bernstein, K. E. (1993). Sperm-specific expression of angiotensin-converting enzyme (ACE) is mediated by a 91-base-pair promoter containing a CRE-like element. *Mol Cell Biol* 13, 18-27.

Hsu, B. L., Harless, S. M., Lindsley, R. C., Hilbert, D. M., and Cancro, M. P. (2002). Cutting edge: BLyS enables survival of transitional and mature B cells through distinct mediators. *J Immunol* 168, 5993-5996.

Hu, Y., Baud, V., Delhase, M., Zhang, P., Deerinck, T., Ellisman, M., Johnson, R., and Karin, M. (1999). Abnormal morphogenesis but intact IKK activation in mice lacking the IKKalpha subunit of IkappaB kinase. *Science* 284, 316-320.

Hu, S., Tamada, K., Ni, J., Vincenz, C., and Chen, L. (1999). Characterization of TNFRSF19, a novel member of the tumor necrosis factor receptor superfamily. *Genomics* 62, 103-107.

Hu, Y., Baud, V., Oga, T., Kim, K. I., Yoshida, K., and Karin, M. (2001). IKKalpha controls formation of the epidermis independently of NF-kappaB. *Nature* 410, 710-714.

Huang, T. T., Feinberg, S. L., Suryanarayanan, S., and Miyamoto, S. (2002). The zinc finger domain of NEMO is selectively required for NF-kappa B activation by UV radiation and topoisomerase inhibitors. *Mol Cell Biol* 22, 5813-5825.

Huleatt, J. W., and Lefrancois, L. (1995). Antigen-driven induction of CD11c on intestinal intraepithelial lymphocytes and CD8+ T cells in vivo. *J Immunol* 154, 5684-5693.

Inaba, K., Witmer-Pack, M., Inaba, M., Hathcock, K. S., Sakuta, H., Azuma, M., Yagita, H., Okumura, K., Linsley, P. S., Ikehara, S., and et al. (1994). The tissue distribution of the B7-2 costimulator in mice: abundant expression on dendritic cells in situ and during maturation in vitro. *J Exp Med* 180, 1849-1860.

Inoue, H., Nojima, H., and Okayama, H. (1990). High efficiency transformation of Escherichia coli with plasmids. *Gene* 96, 23-28.

Inui, S., Maeda, K., Hua, D. R., Yamashita, T., Yamamoto, H., Miyamoto, E., Aizawa, S., and Sakaguchi, N. (2002). BCR signal through alpha4 is involved in S6 kinase activation and required for B cell maturation including isotype switching and V region somatic hypermutation. *Int Immunol* 14, 177-187.

Israel, A. (2000). The IKK complex: an integrator of all signals that activate NF-kappaB? *Trends Cell Biol* 10, 129-133.

Itoh, M., Takahashi, T., Sakaguchi, N., Kuniyasu, Y., Shimizu, J., Otsuka, F., and Sakaguchi, S. (1999). Thymus and autoimmunity: production of CD25+CD4+ naturally anergic and suppressive T cells as a key function of the thymus in maintaining immunologic self-tolerance. *J Immunol* 162, 5317-5326.

Jain, A., Ma, C. A., Liu, S., Brown, M., Cohen, J., and Strober, W. (2001). Specific missense mutations in NEMO result in hyper-IgM syndrome with hypohydrotic ectodermal dysplasia. *Nat Immunol* 2, 223-228.

Jin, D. Y., and Jeang, K. T. (1999). Isolation of full-length cDNA and chromosomal localization of human NF-kappaB modulator NEMO to Xq28. *J Biomed Sci* 6, 115-120.

Jordan, M. S., Boesteanu, A., Reed, A. J., Petrone, A. L., Holenbeck, A. E., Lerman, M. A., Naji, A., and Caton, A. J. (2001). Thymic selection of CD4+CD25+ regulatory T cells induced by an agonist self-peptide. *Nat Immunol* 2, 301-306.

Joyce, D., Albanese, C., Steer, J., Fu, M., Bouzahzah, B., and Pestell, R. G. (2001). NF-kappaB and cell-cycle regulation: the cyclin connection. *Cytokine Growth Factor Rev* 12, 73-90.

Kaisho, T., Takeda, K., Tsujimura, T., Kawai, T., Nomura, F., Terada, N., and Akira, S. (2001). IkappaB kinase alpha is essential for mature B cell development and function. *J Exp Med* 193, 417-426.

Kane, L. P., Lin, J., and Weiss, A. (2002). It's all Rel-ative: NF-kappaB and CD28 costimulation of T-cell activation. *Trends Immunol* 23, 413-420.

Kanegae, Y., Tavares, A. T., Izpisua Belmonte, J. C., and Verma, I. M. (1998). Role of Rel/NF-kappaB transcription factors during the outgrowth of the vertebrate limb. *Nature* 392, 611-614.

Karin, M. (1999). How NF-kappaB is activated: the role of the IkappaB kinase (IKK) complex. *Oncogene* 18, 6867-6874.

Karin, M. (1999). The beginning of the end: IkappaB kinase (IKK) and NF-kappaB activation. *J Biol Chem* 274, 27339-27342.

Karin, M., and Ben-Neriah, Y. (2000). Phosphorylation meets ubiquitination: the control of NF-[kappa]B activity. *Annu Rev Immunol* 18, 621-663.

Karin, M., and Lin, A. (2002). NF-kappaB at the crossroads of life and death. *Nat Immunol* 3, 221-227.

Karin, M., Cao, Y., Greten, F. R., and Li, Z. W. (2002). NF-kappaB in cancer: from innocent bystander to major culprit. *Nat Rev Cancer* 2, 301-310.

Kaufman, C. K., and Fuchs, E. (2000). It's got you covered. NF-kappaB in the epidermis. *J Cell Biol* 149, 999-1004.

Kayagaki, N., Yan, M., Seshasayee, D., Wang, H., Lee, W., French, D. M., Grewal, I. S., Cochran, A. G., Gordon, N. C., Yin, J., *et al.* (2002). BAFF/BLyS receptor 3 binds the B cell survival factor BAFF ligand through a discrete surface loop and promotes processing of NF-kappaB2. *Immunity* 17, 515-524.

Kendall, C., Ionescu-Matiu, I., and Dreesman, G. R. (1983). Utilization of the biotin/avidin system to

amplify the sensitivity of the enzyme-linked immunosorbent assay (ELISA). *J Immunol Methods* 56, 329-339.

Khoshnan, A., Kempiak, S. J., Bennett, B. L., Bae, D., Xu, W., Manning, A. M., June, C. H., and Nel, A. E. (1999). Primary human CD4+ T cells contain heterogeneous I kappa B kinase complexes: role in activation of the IL-2 promoter. *J Immunol* 163, 5444-5452.

Khoshnan, A., Tindell, C., Laux, I., Bae, D., Bennett, B., and Nel, A. E. (2000). The NF-kappa B cascade is important in Bcl-xL expression and for the anti-apoptotic effects of the CD28 receptor in primary human CD4+ lymphocytes. *J Immunol* 165, 1743-1754.

Khoshnan, A., Bae, D., Tindell, C. A., and Nel, A. E. (2000). The physical association of protein kinase C theta with a lipid raft-associated inhibitor of kappa B factor kinase (IKK) complex plays a role in the activation of the NF-kappa B cascade by TCR and CD28. *J Immunol* 165, 6933-6940.

Kieper, W. C., and Jameson, S. C. (1999). Homeostatic expansion and phenotypic conversion of naive T cells in response to self peptide/MHC ligands. *Proc Natl Acad Sci U S A* 96, 13306-13311.

Kilshaw, P. J., and Baker, K. C. (1988). A unique surface antigen on intraepithelial lymphocytes in the mouse. *Immunol Lett* 18, 149-154.

Kingsley, C. I., Karim, M., Bushell, A. R., and Wood, K. J. (2002). CD25+CD4+ regulatory T cells prevent graft rejection: CTLA-4- and IL-10-dependent immunoregulation of alloresponses. *J Immunol* 168, 1080-1086.

Kinoshita, T., Takeda, J., Hong, K., Kozono, H., Sakai, H., and Inoue, K. (1988). Monoclonal antibodies to mouse complement receptor type 1 (CR1). Their use in a distribution study showing that mouse erythrocytes and platelets are CR1-negative. *J Immunol* 140, 3066-3072.

Kistler, B., Rolink, A., Marienfeld, R., Neumann, M., and Wirth, T. (1998). Induction of nuclear factor-kappa B during primary B cell differentiation. *J Immunol* 160, 2308-2317.

Kontgen, F., Suss, G., Stewart, C., Steinmetz, M., and Bluethmann, H. (1993). Targeted disruption of the MHC class II Aa gene in C57BL/6 mice. *Int Immunol* 5, 957-964.

Krappmann, D., Patke, A., Heissmeyer, V., and Scheidereit, C. (2001). B-cell receptor- and phorbol ester-induced NF-kappaB and c-Jun N-terminal kinase activation in B cells requires novel protein kinase C's. *Mol Cell Biol* 21, 6640-6650.

Kraus, M. (2001) Functional Studies on the B Cell Antigen Receptor Signaling Subunit Igaplpha by Conditional Gene Targeting in Mice, PhD, Cologne, Cologne.

Krop, I., Shaffer, A. L., Fearon, D. T., and Schlissel, M. S. (1996). The signaling activity of murine CD19 is regulated during cell development. *J Immunol* 157, 48-56.

Kubo, R. T., Born, W., Kappler, J. W., Marrack, P., and Pigeon, M. (1989). Characterization of a monoclonal antibody which detects all murine alpha beta T cell receptors. *J Immunol* 142, 2736-2742.

Kuhn, R., Schwenk, F., Aguet, M., and Rajewsky, K. (1995). Inducible gene targeting in mice. *Science* 269, 1427-1429.

Kuhn, R., and Torres, R. M. (2002). Cre/loxP recombination system and gene targeting. *Methods Mol Biol* 180, 175-204.

Kuniyasu, Y., Takahashi, T., Itoh, M., Shimizu, J., Toda, G., and Sakaguchi, S. (2000). Naturally anergic and suppressive CD25(+)CD4(+) T cells as a functionally and phenotypically distinct immunoregulatory T cell subpopulation. *Int Immunol* 12, 1145-1155.

Kupfer, R., and Scheinman, R. I. (2002). Measurement of IKK activity in primary rat T cells: rapid activation and inactivation. *J Immunol Methods* 266, 155-164.

Lam, K. P., Kuhn, R., and Rajewsky, K. (1997). In vivo ablation of surface immunoglobulin on mature B cells by inducible gene targeting results in rapid cell death. *Cell* 90, 1073-1083.

Landy, S. J., and Donnai, D. (1993). Incontinentia pigmenti (Bloch-Sulzberger syndrome). *J Med Genet* 30, 53-59.

Laurie, K. L., Van Driel, I. R., and Gleeson, P. A. (2002). The role of CD4+CD25+ immunoregulatory T cells in the induction of autoimmune gastritis. *Immunol Cell Biol* 80, 567-573.

Ledbetter, J. A., and Herzenberg, L. A. (1979). Xenogeneic monoclonal antibodies to mouse lymphoid differentiation antigens. *Immunol Rev* 47, 63-90.

Lee, P. P., Fitzpatrick, D. R., Beard, C., Jessup, H. K., Lehar, S., Makar, K. W., Perez-Melgosa, M., Sweetser, M. T., Schlissel, M. S., Nguyen, S., *et al.* (2001). A critical role for Dnmt1 and DNA methylation in T cell development, function, and survival. *Immunity* 15, 763-774.

Lehmann, J., Huehn, J., de la Rosa, M., Maszyna, F., Kretschmer, U., Krenn, V., Brunner, M., Scheffold, A., and Hamann, A. (2002). Expression of the integrin alpha Ebeta 7 identifies unique subsets of CD25+ as well as CD25- regulatory T cells. *Proc Natl Acad Sci U S A* 99, 13031-13036.

Leitges, M., Sanz, L., Martin, P., Duran, A., Braun, U., Garcia, J. F., Camacho, F., Diaz-Meco, M. T., Rennert, P. D., and Moscat, J. (2001). Targeted disruption of the zetaPKC gene results in the impairment of the NF-kappaB pathway. *Mol Cell* 8, 771-780.

Leo, O., Foo, M., Sachs, D. H., Samelson, L. E., and Bluestone, J. A. (1987). Identification of a monoclonal antibody specific for a murine T3 polypeptide. *Proc Natl Acad Sci U S A* 84, 1374-1378.

Leptin, M., Potash, M. J., Grutzmann, R., Heusser, C., Shulman, M., Kohler, G., and Melchers, F. (1984). Monoclonal antibodies specific for murine IgM I. Characterization of antigenic determinants on the four constant domains of the mu heavy chain. *Eur J Immunol* 14, 534-542.

Leptin, M. (1985). Monoclonal antibodies specific for murine IgM. II. Activation of B lymphocytes by monoclonal antibodies specific for the four constant domains of IgM. *Eur J Immunol* 15, 131-137.

Li, Z. W., Chu, W., Hu, Y., Delhase, M., Deerinck, T., Ellisman, M., Johnson, R., and Karin, M. (1999). The IKKbeta subunit of IkappaB kinase (IKK) is essential for nuclear factor kappaB activation and prevention of apoptosis. *J Exp Med* 189, 1839-1845.

Li, Q., Van Antwerp, D., Mercurio, F., Lee, K. F., and Verma, I. M. (1999). Severe liver degeneration in mice lacking the IkappaB kinase 2 gene. *Science* 284, 321-325.

Li, Q., Lu, Q., Hwang, J. Y., Buscher, D., Lee, K. F., Izpisua-Belmonte, J. C., and Verma, I. M. (1999). IKK1-deficient mice exhibit abnormal development of skin and skeleton. *Genes Dev* 13, 1322-1328.

Li, Q., Estepa, G., Memet, S., Israel, A., and Verma, I. M. (2000). Complete lack of NF-kappaB activity in IKK1 and IKK2 double-deficient mice: additional defect in neurulation. *Genes Dev* 14, 1729-1733.

Li, J., Peet, G. W., Balzarano, D., Li, X., Massa, P., Barton, R. W., and Marcu, K. B. (2001). Novel NEMO/IkappaB kinase and NF-kappa B target genes at the pre-B to immature B cell transition. *J Biol Chem* 276, 18579-18590.

Li, X. H., Fang, X., and Gaynor, R. B. (2001). Role of IKKgamma/nemo in assembly of the Ikappa B kinase complex. *J Biol Chem* 276, 4494-4500.

Li, Q., and Verma, I. M. (2002). NF-kappaB regulation in the immune system. *Nat Rev Immunol* 2, 725-734.

Li, X., Massa, P. E., Hanidu, A., Peet, G. W., Aro, P., Savitt, A., Mische, S., Li, J., and Marcu, K. B.

(2002). IKKalpha, IKKbeta, and NEMO/IKKgamma are each required for the NF-kappa B-mediated inflammatory response program. *J Biol Chem* 277, 45129-45140.

Liou, H. C., Jin, Z., Tumang, J., Andjelic, S., Smith, K. A., and Liou, M. L. (1999). c-Rel is crucial for lymphocyte proliferation but dispensable for T cell effector function. *Int Immunol* 11, 361-371.
Loken, M. R., and Stall, A. M. (1982). Flow cytometry as an analytical and preparative tool in immunology. *J Immunol Methods* 50, R85-112.

Lucas, B., Vasseur, F., and Penit, C. (1994). Production, selection, and maturation of thymocytes with high surface density of TCR. *J Immunol* 153, 53-62.

Lyons, A. B., and Parish, C. R. (1994). Determination of lymphocyte division by flow cytometry. *J Immunol Methods* 171, 131-137.

Mackall, C. L., Bare, C. V., Granger, L. A., Sharrow, S. O., Titus, J. A., and Gress, R. E. (1996). Thymic-independent T cell regeneration occurs via antigen-driven expansion of peripheral T cells resulting in a repertoire that is limited in diversity and prone to skewing. *J Immunol* 156, 4609-4616.

Mackay, F., Schneider, P., Rennert, P., and Browning, J. (2002). BAFF and APRIL: A Tutorial on B Cell Survival. *Annu Rev Immunol*.

Mackay, F., and Browning, J. L. (2002). BAFF: a fundamental survival factor for B cells. *Nat Rev Immunol* 2, 465-475.

Mak, T. W., and Yeh, W. C. (2002). Signaling for survival and apoptosis in the immune system. *Arthritis Res* 4 Suppl 3, S243-252.

Makris, C., Godfrey, V. L., Krahn-Senftleben, G., Takahashi, T., Roberts, J. L., Schwarz, T., Feng, L., Johnson, R. S., and Karin, M. (2000). Female mice heterozygous for IKK gamma/NEMO deficiencies develop a dermatopathy similar to the human X-linked disorder incontinentia pigmenti. *Mol Cell* 5, 969-979.

Malek, T. R., Robb, R. J., and Shevach, E. M. (1983). Identification and initial characterization of a rat monoclonal antibody reactive with the murine interleukin 2 receptor-ligand complex. *Proc Natl Acad Sci U S A* 80, 5694-5698.

Malek, T. R., Yu, A., Vincek, V., Scibelli, P., and Kong, L. (2002). CD4 regulatory T cells prevent lethal autoimmunity in IL-2Rbeta-deficient mice. Implications for the nonredundant function of IL-2. *Immunity* 17, 167-178.

Martin, F., and Kearney, J. F. (1999). CD21high IgMhigh splenic B cells enriched in the marginal zone: distinct phenotypes and functions. *Curr Top Microbiol Immunol* 246, 45-50.

Martin, F., and Kearney, J. F. (2000). B-cell subsets and the mature preimmune repertoire. Marginal zone and B1 B cells as part of a "natural immune memory". *Immunol Rev* 175, 70-79.

Martin, F., and Kearney, J. F. (2000). Positive selection from newly formed to marginal zone B cells depends on the rate of clonal production, CD19, and btk. *Immunity* 12, 39-49.

Martin, F., Oliver, A. M., and Kearney, J. F. (2001). Marginal zone and B1 B cells unite in the early response against T- independent blood-borne particulate antigens. *Immunity* 14, 617-629.

Mason, N., Aliberti, J., Caamano, J. C., Liou, H. C., and Hunter, C. A. (2002). Cutting edge: identification of c-Rel-dependent and -independent pathways of IL-12 production during infectious and inflammatory stimuli. *J Immunol* 168, 2590-2594.

May, M. J., and Ghosh, S. (1997). Rel/NF-kappa B and I kappa B proteins: an overview. *Semin Cancer Biol* 8, 63-73.

May, M. J., and Ghosh, S. (1998). Signal transduction through NF-kappa B. *Immunol Today* 19, 80-88.

May, M. J., and Ghosh, S. (1999). IkappaB kinases: kinsmen with different crafts. *Science* 284, 271-273.

McAllister-Lucas, L. M., Inohara, N., Lucas, P. C., Ruland, J., Benito, A., Li, Q., Chen, S., Chen, F. F., Yamaoka, S., Verma, I. M., *et al.* (2001). Bimp1, a MAGUK family member linking protein kinase C activation to Bcl10-mediated NF-kappaB induction. *J Biol Chem* 276, 30589-30597.

McHugh, R. S., Whitters, M. J., Piccirillo, C. A., Young, D. A., Shevach, E. M., Collins, M., and Byrne, M. C. (2002). CD4(+)CD25(+) immunoregulatory T cells: gene expression analysis reveals a functional role for the glucocorticoid-induced TNF receptor. *Immunity* 16, 311-323.

McHugh, R. S., and Shevach, E. M. (2002). Cutting edge: depletion of CD4+CD25+ regulatory T cells is necessary, but not sufficient, for induction of organ-specific autoimmune disease. *J Immunol* 168, 5979-5983.

McHugh, R. S., and Shevach, E. M. (2002). The role of suppressor T cells in regulation of immune responses. *J Allergy Clin Immunol* 110, 693-702.

Mercurio, F., Zhu, H., Murray, B. W., Shevchenko, A., Bennett, B. L., Li, J., Young, D. B., Barbosa, M., Mann, M., Manning, A., and Rao, A. (1997). IKK-1 and IKK-2: cytokine-activated IkappaB kinases essential for NF-kappaB activation. *Science* 278, 860-866.

Mercurio, F., and Manning, A. M. (1999). NF-kappaB as a primary regulator of the stress response. *Oncogene* 18, 6163-6171.

Mercurio, F., Murray, B. W., Shevchenko, A., Bennett, B. L., Young, D. B., Li, J. W., Pascual, G., Motiwala, A., Zhu, H., Mann, M., and Manning, A. M. (1999). IkappaB kinase (IKK)-associated protein 1, a common component of the heterogeneous IKK complex. *Mol Cell Biol* 19, 1526-1538.

Miller, S. A., Dykes, D. D., and Polesky, H. F. (1988). A simple salting out procedure for extracting DNA from human nucleated cells. *Nucleic Acids Res* 16, 1215.

Miltenyi, S., Muller, W., Weichel, W., and Radbruch, A. (1990). High gradient magnetic cell separation with MACS. *Cytometry* 11, 231-238.

Miyake, K., Medina, K. L., Hayashi, S., Ono, S., Hamaoka, T., and Kincade, P. W. (1990). Monoclonal antibodies to Pgp-1/CD44 block lympho-hemopoiesis in long-term bone marrow cultures. *J Exp Med* 171, 477-488.

Moore, N. C., Girdlestone, J., Anderson, G., Owen, J. J., and Jenkinson, E. J. (1995). Stimulation of thymocytes before and after positive selection results in the induction of different NF-kappa B/Rel protein complexes. *J Immunol* 155, 4653-4660.

Moore, P. A., Belvedere, O., Orr, A., Pieri, K., LaFleur, D. W., Feng, P., Soppet, D., Charters, M., Gentz, R., Parmelee, D., *et al.* (1999). BLyS: member of the tumor necrosis factor family and B lymphocyte stimulator. *Science* 285, 260-263.

Mora, A. L., Stanley, S., Armistead, W., Chan, A. C., and Boothby, M. (2001). Inefficient ZAP-70 phosphorylation and decreased thymic selection in vivo result from inhibition of NF-kappaB/Rel. *J Immunol* 167, 5628-5635.

Mullis, K. B., and Faloona, F. A. (1987). Specific synthesis of DNA in vitro via a polymerase-catalyzed chain reaction. *Methods Enzymol* 155, 335-350.

Nakamura, K., Kitani, A., and Strober, W. (2001). Cell contact-dependent immunosuppression by CD4(+)CD25(+) regulatory T cells is mediated by cell surface-bound transforming growth factor beta. *J Exp Med* 194, 629-644.

Nelson, G., Paraoan, L., Spiller, D. G., Wilde, G. J., Browne, M. A., Djali, P. K., Unitt, J. F., Sullivan, E., Floettmann, E., and White, M. R. (2002). Multi-parameter analysis of the kinetics of NF-kappaB

signalling and transcription in single living cells. *J Cell Sci* 115, 1137-1148.

Nishikawa, S., Sasaki, Y., Kina, T., Amagai, T., and Katsura, Y. (1986). A monoclonal antibody against Igh6-4 determinant. *Immunogenetics* 23, 137-139.

O'Neill, L. A., and Kaltschmidt, C. (1997). NF-kappa B: a crucial transcription factor for glial and neuronal cell function. *Trends Neurosci* 20, 252-258.

Opitz, H. G., Opitz, U., Hewlett, G., and Schlumberger, H. D. (1982). A new model for investigations of T-cell functions in mice: differential immunosuppressive effects of two monoclonal anti-Thy-1.2 antibodies. *Immunobiology* 160, 438-453.

Orange, J. S., Brodeur, S. R., Jain, A., Bonilla, F. A., Schneider, L. C., Kretschmer, R., Nurko, S., Rasmussen, W. L., Kohler, J. R., Gellis, S. E., *et al.* (2002). Deficient natural killer cell cytotoxicity in patients with IKK-gamma/NEMO mutations. *J Clin Invest* 109, 1501-1509.

Orban, P. C., Chui, D., and Marth, J. D. (1992). Tissue- and site-specific DNA recombination in transgenic mice. *Proc Natl Acad Sci U S A* 89, 6861-6865.

Ouaaz, F., Li, M., and Beg, A. A. (1999). A critical role for the RelA subunit of nuclear factor kappaB in regulation of multiple immune-response genes and in Fas-induced cell death. *J Exp Med* 189, 999-1004.

Ouaaz, F., Arron, J., Zheng, Y., Choi, Y., and Beg, A. A. (2002). Dendritic cell development and survival require distinct NF-kappaB subunits. *Immunity* 16, 257-270.

Parrish, J. E., Scheuerle, A. E., Lewis, R. A., Levy, M. L., and Nelson, D. L. (1996). Selection against mutant alleles in blood leukocytes is a consistent feature in Incontinentia Pigmenti type 2. *Hum Mol Genet* 5, 1777-1783.

Pasparakis, M., and Kollias, G. (1995). Production of cytokine transgenic and knockout mice. In Cytokines: A Practical Approach, F. R. Balkwill, ed. (Oxford, Oxford University Press), pp. 297-324.

Pasparakis, M., Schmidt-Supprian, M., and Rajewsky, K. (2002). IkappaB kinase signaling is essential for maintenance of mature B cells. *J Exp Med* 196, 743-752.

Pasparakis, M., Courtois, G., Hafner, M., Schmidt-Supprian, M., Nenci, A., Toksoy, A., Krampert, M., Goebeler, M., Gillitzer, R., Israel, A., *et al.* (2002). TNF-mediated inflammatory skin disease in mice with epidermis-specific deletion of IKK2. *Nature* 417, 861-866.
Peters, R. T., Liao, S. M., and Maniatis, T. (2000). IKKepsilon is part of a novel PMA-inducible IkappaB kinase complex. *Mol Cell* 5, 513-522.

Petro, J. B., and Khan, W. N. (2001). Phospholipase C-gamma 2 couples Bruton's tyrosine kinase to the NF-kappaB signaling pathway in B lymphocytes. *J Biol Chem* 276, 1715-1719.

Piccirillo, C. A., and Shevach, E. M. (2001). Cutting edge: control of CD8+ T cell activation by CD4+CD25+ immunoregulatory cells. *J Immunol* 167, 1137-1140.

Piccirillo, C. A., Letterio, J. J., Thornton, A. M., McHugh, R. S., Mamura, M., Mizuhara, H., and Shevach, E. M. (2002). CD4(+)CD25(+) regulatory T cells can mediate suppressor function in the absence of transforming growth factor beta1 production and responsiveness. *J Exp Med* 196, 237-246.

Pohl, T., Gugasyan, R., Grumont, R. J., Strasser, A., Metcalf, D., Tarlinton, D., Sha, W., Baltimore, D., and Gerondakis, S. (2002). The combined absence of NF-kappa B1 and c-Rel reveals that overlapping roles for these transcription factors in the B cell lineage are restricted to the activation and function of mature cells. *Proc Natl Acad Sci U S A* 99, 4514-4519.

Pomerantz, J. L., Denny, E. M., and Baltimore, D. (2002). CARD11 mediates factor-specific activation of NF-kappaB by the T cell receptor complex. *Embo J* 21, 5184-5194.

Pomerantz, J. L., and Baltimore, D. (2002). Two pathways to NF-kappaB. *Mol Cell* 10, 693-695.

Powrie, F., Leach, M. W., Mauze, S., Caddle, L. B., and Coffman, R. L. (1993). Phenotypically distinct subsets of CD4+ T cells induce or protect from chronic intestinal inflammation in C. B-17 scid mice. *Int Immunol* 5, 1461-1471.

Poyet, J. L., Srinivasula, S. M., Lin, J. H., Fernandes-Alnemri, T., Yamaoka, S., Tsichlis, P. N., and Alnemri, E. S. (2000). Activation of the Ikappa B kinases by RIP via IKKgamma /NEMO-mediated oligomerization. *J Biol Chem* 275, 37966-37977.

Prajapati, S., and Gaynor, R. B. (2002). Regulation of Ikappa B kinase (IKK)gamma /NEMO function by IKKbeta -mediated phosphorylation. *J Biol Chem* 277, 24331-24339.

Rajewsky, K., Gu, H., Kuhn, R., Betz, U. A., Muller, W., Roes, J., and Schwenk, F. (1996). Conditional gene targeting. *J Clin Invest* 98, 600-603.

Rao, M., Lee, W. T., and Conrad, D. H. (1987). Characterization of a monoclonal antibody directed against the murine B lymphocyte receptor for IgE. *J Immunol* 138, 1845-1851.

Read, S., Malmstrom, V., and Powrie, F. (2000). Cytotoxic T lymphocyte-associated antigen 4 plays an essential role in the function of CD25(+)CD4(+) regulatory cells that control intestinal inflammation. *J Exp Med* 192, 295-302.

Read, S., and Powrie, F. (2001). CD4(+) regulatory T cells. *Curr Opin Immunol* 13, 644-649.

Ren, H., Schmalstieg, A., Yuan, D., and Gaynor, R. B. (2002). I-kappaB Kinase beta Is Critical for B Cell Proliferation and Antibody Response. *J Immunol* 168, 577-587.

Ren, H., Schmalstieg, A., van Oers, N. S., and Gaynor, R. B. (2002). I-kappa B kinases alpha and beta have distinct roles in regulating murine T cell function. *J Immunol* 168, 3721-3731.
Reth, M. (1981) Charakterisierung individueller Antikoerper und Idiotope des NP^b Idiotyps., Cologne, Cologne.

Rickert, R. C., Rajewsky, K., and Roes, J. (1995). Impairment of T-cell-dependent B-cell responses and B-1 cell development in CD19-deficient mice. *Nature* 376, 352-355.

Rickert, R. C., Roes, J., and Rajewsky, K. (1997). B lymphocyte-specific, Cre-mediated mutagenesis in mice. *Nucleic Acids Res* 25, 1317-1318.

Rodriguez, C. I., Buchholz, F., Galloway, J., Sequerra, R., Kasper, J., Ayala, R., Stewart, A. F., and Dymecki, S. M. (2000). High-efficiency deleter mice show that FLPe is an alternative to Cre-loxP. *Nat Genet* 25, 139-140.

Roes, J., and Rajewsky, K. (1993). Immunoglobulin D (IgD)-deficient mice reveal an auxiliary receptor function for IgD in antigen-mediated recruitment of B cells. *J Exp Med* 177, 45-55.

Roes, J., Muller, W., and Rajewsky, K. (1995). Mouse anti-mouse IgD monoclonal antibodies generated in IgD-deficient mice. *J Immunol Methods* 183, 231-237.

Rolink, A. G., Tschopp, J., Schneider, P., and Melchers, F. (2002). BAFF is a survival and maturation factor for mouse B cells. *Eur J Immunol* 32, 2004-2010.

Rothwarf, D. M., Zandi, E., Natoli, G., and Karin, M. (1998). IKK-gamma is an essential regulatory subunit of the IkappaB kinase complex. *Nature* 395, 297-300.

Rothwarf, D. M., and Karin, M. (1999). The NF-{kappa}B Activation Pathway: A Paradigm in Information Transfer from Membrane to Nucleus. *Sci STKE* 1999, RE1.

Rudolph, D., Yeh, W. C., Wakeham, A., Rudolph, B., Nallainathan, D., Potter, J., Elia, A. J., and Mak, T. W. (2000). Severe liver degeneration and lack of NF-kappaB activation in NEMO/IKKgamma-deficient mice. *Genes Dev* 14, 854-862.

Ruland, J., Duncan, G. S., Elia, A., del Barco Barrantes, I., Nguyen, L., Plyte, S., Millar, D. G., Bouchard, D., Wakeham, A., Ohashi, P. S., and Mak, T. W. (2001). Bcl10 is a positive regulator of antigen receptor-induced activation of NF-kappaB and neural tube closure. *Cell* 104, 33-42.

Saiki, R. K., Scharf, S., Faloona, F., Mullis, K. B., Horn, G. T., Erlich, H. A., and Arnheim, N. (1985). Enzymatic amplification of beta-globin genomic sequences and restriction site analysis for diagnosis of sickle cell anemia. *Science* 230, 1350-1354.

Saitoh, T., Nakano, H., Yamamoto, N., and Yamaoka, S. (2002). Lymphotoxin-beta receptor mediates NEMO-independent NF-kappaB activation. *FEBS Lett* 532, 45-51.

Salomon, B., Lenschow, D. J., Rhee, L., Ashourian, N., Singh, B., Sharpe, A., and Bluestone, J. A. (2000). B7/CD28 costimulation is essential for the homeostasis of the CD4+CD25+ immunoregulatory T cells that control autoimmune diabetes. *Immunity* 12, 431-440.

Sambrook, J., E.F., F., and Maniatis, T. (1989). Molecular Cloning, Cold Spring Harbor Laboratory Press).
Sanger, F., Nicklen, S., and Coulson, A. R. (1977). DNA sequencing with chain-terminating inhibitors. *Proc Natl Acad Sci U S A* 74, 5463-5467.

Sauer, B., and Henderson, N. (1988). Site-specific DNA recombination in mammalian cells by the Cre recombinase of bacteriophage P1. *Proc Natl Acad Sci U S A* 85, 5166-5170.

Sauer, B., and Henderson, N. (1989). Cre-stimulated recombination at loxP-containing DNA sequences placed into the mammalian genome. *Nucleic Acids Res* 17, 147-161.

Schamburg-Lever, G., and Lever, W. F. (1973). Electron microscopy of incontinentia pigmenti. *J Invest Dermatol* 61, 151-158.

Scherer, D. C., Brockman, J. A., Bendall, H. H., Zhang, G. M., Ballard, D. W., and Oltz, E. M. (1996). Corepression of RelA and c-rel inhibits immunoglobulin kappa gene transcription and rearrangement in precursor B lymphocytes. *Immunity* 5, 563-574.

Scheuerle, A. E. (1998). Male cases of incontinentia pigmenti: case report and review. *Am J Med Genet* 77, 201-218.

Schiemann, B., Gommerman, J. L., Vora, K., Cachero, T. G., Shulga-Morskaya, S., Dobles, M., Frew, E., and Scott, M. L. (2001). An essential role for BAFF in the normal development of B cells through a BCMA-independent pathway. *Science* 293, 2111-2114.

Schmidt-Supprian, M., Bloch, W., Courtois, G., Addicks, K., Israel, A., Rajewsky, K., and Pasparakis, M. (2000). NEMO/IKK gamma-deficient mice model incontinentia pigmenti. *Mol Cell* 5, 981-992.

Schneider, P., MacKay, F., Steiner, V., Hofmann, K., Bodmer, J. L., Holler, N., Ambrose, C., Lawton, P., Bixler, S., Acha-Orbea, H., *et al.* (1999). BAFF, a novel ligand of the tumor necrosis factor family, stimulates B cell growth. *J Exp Med* 189, 1747-1756.

Schwabe, R. F., and Brenner, D. A. (2002). Role of glycogen synthase kinase-3 in TNF-alpha-induced NF-kappaB activation and apoptosis in hepatocytes. *Am J Physiol Gastrointest Liver Physiol* 283, G204-211.

Schwenk, F., Baron, U., and Rajewsky, K. (1995). A cre-transgenic mouse strain for the ubiquitous deletion of loxP- flanked gene segments including deletion in germ cells. *Nucleic Acids Res* 23, 5080-5081.

Seitz, C. S., Lin, Q., Deng, H., and Khavari, P. A. (1998). Alterations in NF-kappaB function in transgenic epithelial tissue demonstrate a growth inhibitory role for NF-kappaB. *Proc Natl Acad Sci U S*

A 95, 2307-2312.

Seitz, C. S., Deng, H., Hinata, K., Lin, Q., and Khavari, P. A. (2000). Nuclear factor kappaB subunits induce epithelial cell growth arrest. *Cancer Res* 60, 4085-4092.
Seitz, C. S., Freiberg, R. A., Hinata, K., and Khavari, P. A. (2000). NF-kappaB determines localization and features of cell death in epidermis. *J Clin Invest* 105, 253-260.

Seitz, C., Muller, P., Krieg, R. C., Mannel, D. N., and Hehlgans, T. (2001). A novel p75TNF receptor isoform mediating NFkappa B activation. *J Biol Chem* 276, 19390-19395.

Sen, R., and Baltimore, D. (1986). Multiple nuclear factors interact with the immunoglobulin enhancer sequences. *Cell* 46, 705-716.

Senftleben, U., Cao, Y., Xiao, G., Greten, F. R., Krahn, G., Bonizzi, G., Chen, Y., Hu, Y., Fong, A., Sun, S. C., and Karin, M. (2001). Activation by IKKalpha of a second, evolutionary conserved, NF-kappa B signaling pathway. *Science* 293, 1495-1499.

Senftleben, U., Li, Z. W., Baud, V., and Karin, M. (2001). IKKbeta is essential for protecting T cells from TNFalpha-induced apoptosis. *Immunity* 14, 217-230.

Senftleben, U., and Karin, M. (2002). The IKK/NF-kappaB pathway. *Crit Care Med* 30, S18-26.

Sha, W. C. (1998). Regulation of immune responses by NF-kappa B/Rel transcription factor. *J Exp Med* 187, 143-146.

Shevach, E. M. (2001). Certified professionals: CD4(+)CD25(+) suppressor T cells. *J Exp Med* 193, F41-46.

Shevach, E. M., McHugh, R. S., Piccirillo, C. A., and Thornton, A. M. (2001). Control of T-cell activation by CD4+ CD25+ suppressor T cells. *Immunol Rev* 182, 58-67.

Shevach, E. M. (2002). CD4+ CD25+ suppressor T cells: more questions than answers. *Nat Rev Immunol* 2, 389-400.

Shortman, K., Wilson, A., Egerton, M., Pearse, M., and Scollay, R. (1988). Immature CD4- CD8+ murine thymocytes. *Cell Immunol* 113, 462-479.

Silver, L. M. (1995). Mouse genetics: concepts and practice, Oxford University Press).

Silverman, N., and Maniatis, T. (2001). NF-kappaB signaling pathways in mammalian and insect innate immunity. *Genes Dev* 15, 2321-2342.

Singh, B., Read, S., Asseman, C., Malmstrom, V., Mottet, C., Stephens, L. A., Stepankova, R., Tlaskalova, H., and Powrie, F. (2001). Control of intestinal inflammation by regulatory T cells. *Immunol Rev* 182, 190-200.

Sizemore, N., Leung, S., and Stark, G. R. (1999). Activation of phosphatidylinositol 3-kinase in response to interleukin-1 leads to phosphorylation and activation of the NF-kappaB p65/RelA subunit. *Mol Cell Biol* 19, 4798-4805.

Sizemore, N., Lerner, N., Dombrowski, N., Sakurai, H., and Stark, G. R. (2002). Distinct roles of the Ikappa B kinase alpha and beta subunits in liberating nuclear factor kappa B (NF-kappa B) from Ikappa B and in phosphorylating the p65 subunit of NF-kappa B. *J Biol Chem* 277, 3863-3869.

Smahi, A., Courtois, G., Vabres, P., Yamaoka, S., Heuertz, S., Munnich, A., Israel, A., Heiss, N. S., Klauck, S. M., Kioschis, P., *et al.* (2000). Genomic rearrangement in NEMO impairs NF-kappaB activation and is a cause of incontinentia pigmenti. The International Incontinentia Pigmenti (IP) Consortium. *Nature* 405, 466-472.

Smahi, A., Courtois, G., Rabia, S. H., Doffinger, R., Bodemer, C., Munnich, A., Casanova, J. L., and Israel, A. (2002). The NF-kappaB signalling pathway in human diseases: from incontinentia pigmenti to ectodermal dysplasias and immune-deficiency syndromes. *Hum Mol Genet* 11, 2371-2375.

Solan, N. J., Miyoshi, H., Carmona, E. M., Bren, G. D., and Paya, C. V. (2002). RelB cellular regulation and transcriptional activity are regulated by p100. *J Biol Chem* 277, 1405-1418.

Speirs, K., Caamano, J., Goldschmidt, M. H., Hunter, C. A., and Scott, P. (2002). NF-kappa B2 is required for optimal CD40-induced IL-12 production but dispensable for Th1 cell Differentiation. *J Immunol* 168, 4406-4413.

Springer, T., Galfre, G., Secher, D. S., and Milstein, C. (1979). Mac-1: a macrophage differentiation antigen identified by monoclonal antibody. *Eur J Immunol* 9, 301-306.

Sudo, T., Nishikawa, S., Ohno, N., Akiyama, N., Tamakoshi, M., and Yoshida, H. (1993). Expression and function of the interleukin 7 receptor in murine lymphocytes. *Proc Natl Acad Sci U S A* 90, 9125-9129.

Sun, Z., Arendt, C. W., Ellmeier, W., Schaeffer, E. M., Sunshine, M. J., Gandhi, L., Annes, J., Petrzilka, D., Kupfer, A., Schwartzberg, P. L., and Littman, D. R. (2000). PKC-theta is required for TCR-induced NF-kappaB activation in mature but not immature T lymphocytes. *Nature* 404, 402-407.

Surh, C. D., and Sprent, J. (2000). Homeostatic T cell proliferation: how far can T cells be activated to self-ligands? *J Exp Med* 192, F9-F14.

Suri-Payer, E., Amar, A. Z., Thornton, A. M., and Shevach, E. M. (1998). CD4+CD25+ T cells inhibit both the induction and effector function of autoreactive T cells and represent a unique lineage of immunoregulatory cells. *J Immunol* 160, 1212-1218.

Suto, A., Nakajima, H., Ikeda, K., Kubo, S., Nakayama, T., Taniguchi, M., Saito, Y., and Iwamoto, I. (2002). CD4(+)CD25(+) T-cell development is regulated by at least 2 distinct mechanisms. *Blood* 99, 555-560.

Symington, F. W., Subbarao, B., Mosier, D. E., and Sprent, J. (1982). Lyb-8.2: A new B cell antigen defined and characterized with a monoclonal antibody. *Immunogenetics* 16, 381-391.

Takahashi, T., Kuniyasu, Y., Toda, M., Sakaguchi, N., Itoh, M., Iwata, M., Shimizu, J., and Sakaguchi, S. (1998). Immunologic self-tolerance maintained by CD25+CD4+ naturally anergic and suppressive T cells: induction of autoimmune disease by breaking their anergic/suppressive state. *Int Immunol* 10, 1969-1980.

Takahashi, T., Tagami, T., Yamazaki, S., Uede, T., Shimizu, J., Sakaguchi, N., Mak, T. W., and Sakaguchi, S. (2000). Immunologic self-tolerance maintained by CD25(+)CD4(+) regulatory T cells constitutively expressing cytotoxic T lymphocyte-associated antigen 4. *J Exp Med* 192, 303-310.

Takeda, K., Takeuchi, O., Tsujimura, T., Itami, S., Adachi, O., Kawai, T., Sanjo, H., Yoshikawa, K., Terada, N., and Akira, S. (1999). Limb and skin abnormalities in mice lacking IKKalpha. *Science* 284, 313-316.

Tam, W. F., Wang, W., and Sen, R. (2001). Cell-specific association and shuttling of IkappaBalpha provides a mechanism for nuclear NF-kappaB in B lymphocytes. *Mol Cell Biol* 21, 4837-4846.

Tan, S. S., Williams, E. A., and Tam, P. P. (1993). X-chromosome inactivation occurs at different times in different tissues of the post-implantation mouse embryo. *Nat Genet* 3, 170-174.

Tanaka, M., Fuentes, M. E., Yamaguchi, K., Durnin, M. H., Dalrymple, S. A., Hardy, K. L., and Goeddel, D. V. (1999). Embryonic lethality, liver degeneration, and impaired NF-kappa B activation in IKK-beta-deficient mice. *Immunity* 10, 421-429.

Teixeiro, E., Garcia-Sahuquillo, A., Alarcon, B., and Bragado, R. (1999). Apoptosis-resistant T cells have a deficiency in NF-kappaB-mediated induction of Fas ligand transcription. *Eur J Immunol* 29, 745-754.

Thomas, K. R., and Capecchi, M. R. (1987). Site-directed mutagenesis by gene targeting in mouse embryo-derived stem cells. *Cell* 51, 503-512.

Thompson, J. S., Bixler, S. A., Qian, F., Vora, K., Scott, M. L., Cachero, T. G., Hession, C., Schneider, P., Sizing, I. D., Mullen, C., *et al.* (2001). BAFF-R, a newly identified TNF receptor that specifically interacts with BAFF. *Science* 293, 2108-2111.

Thornton, A. M., and Shevach, E. M. (1998). CD4+CD25+ immunoregulatory T cells suppress polyclonal T cell activation in vitro by inhibiting interleukin 2 production. *J Exp Med* 188, 287-296.

Thornton, A. M., and Shevach, E. M. (2000). Suppressor effector function of CD4+CD25+ immunoregulatory T cells is antigen nonspecific. *J Immunol* 164, 183-190.

Tian, W. N., Braunstein, L. D., Pang, J., Stuhlmeier, K. M., Xi, Q. C., Tian, X., and Stanton, R. C. (1998). Importance of glucose-6-phosphate dehydrogenase activity for cell growth. *J Biol Chem* 273, 10609-10617.

Tian, W. N., Braunstein, L. D., Apse, K., Pang, J., Rose, M., Tian, X., and Stanton, R. C. (1999). Importance of glucose-6-phosphate dehydrogenase activity in cell death. *Am J Physiol* 276, C1121-1131.

Tian, T., Zhang, J., Gao, L., Qian, X. P., and Chen, W. F. (2001). Heterogeneity within medullary-type TCRalphabeta(+)CD3(+)CD4(-)CD8(+) thymocytes in normal mouse thymus. *Int Immunol* 13, 313-320.

Ting, A. Y., and Endy, D. (2002). Signal transduction. Decoding NF-kappaB signaling. *Science* 298, 1189-1190.

Tivol, E. A., Borriello, F., Schweitzer, A. N., Lynch, W. P., Bluestone, J. A., and Sharpe, A. H. (1995). Loss of CTLA-4 leads to massive lymphoproliferation and fatal multiorgan tissue destruction, revealing a critical negative regulatory role of CTLA-4. *Immunity* 3, 541-547.

Toniolo, D., Filippi, M., Dono, R., Lettieri, T., and Martini, G. (1991). The CpG island in the 5' region of the G6PD gene of man and mouse. *Gene* 102, 197-203.

Torres, R. M., and Kuehn, R. (1997). Laboratory Protocols for Conditional Gene Targeting (Oxford, Oxford University Press).

Tough, D. F., and Sprent, J. (1995). Lifespan of lymphocytes. *Immunol Res* 14, 1-12.

Trushin, S. A., Pennington, K. N., Algeciras-Schimnich, A., and Paya, C. V. (1999). Protein kinase C and calcineurin synergize to activate IkappaB kinase and NF-kappaB in T lymphocytes. *J Biol Chem* 274, 22923-22931.

Van Antwerp, D. J., Martin, S. J., Verma, I. M., and Green, D. R. (1998). Inhibition of TNF-induced apoptosis by NF-kappa B. *Trends Cell Biol* 8, 107-111.

Vaux, D. L. (2002). The buzz about BAFF. *J Clin Invest* 109, 17-18.

Verma, I. M., Stevenson, J. K., Schwarz, E. M., Van Antwerp, D., and Miyamoto, S. (1995). Rel/NF-kappa B/I kappa B family: intimate tales of association and dissociation. *Genes Dev* 9, 2723-2735.

Wall, K. A., Lorber, M. I., Loken, M. R., McClatchey, S., and Fitch, F. W. (1983). Inhibition of proliferation of MIs- and Ia-reactive cloned T cells by a monoclonal antibody against a determinant shared by I-A and I-E. *J Immunol* 131, 1056-1064.

Wang, W., Wykrzykowska, J., Johnson, T., Sen, R., and Sen, J. (1999). A NF-kappa B/c-myc-dependent survival pathway is targeted by corticosteroids in immature thymocytes. *J Immunol* 162, 314-322.

Wang, Y., Cui, H., Schroering, A., Ding, J. L., Lane, W. S., McGill, G., Fisher, D. E., and Ding, H. F. (2002). NF-kappaB2 p100 is a pro-apoptotic protein with anti-oncogenic function. *Nat Cell Biol* 4, 888-893.

Weih, F., Carrasco, D., Durham, S. K., Barton, D. S., Rizzo, C. A., Ryseck, R. P., Lira, S. A., and Bravo, R. (1995). Multiorgan inflammation and hematopoietic abnormalities in mice with a targeted disruption of RelB, a member of the NF-kappa B/Rel family. *Cell* 80, 331-340.

Weih, F., Durham, S. K., Barton, D. S., Sha, W. C., Baltimore, D., and Bravo, R. (1996). Both multiorgan inflammation and myeloid hyperplasia in RelB-deficient mice are T cell dependent. *J Immunol* 157, 3974-3979.

Weih, F., Warr, G., Yang, H., and Bravo, R. (1997). Multifocal defects in immune responses in RelB-deficient mice. *J Immunol* 158, 5211-5218.

Weih, F., Durham, S. K., Barton, D. S., Sha, W. C., Baltimore, D., and Bravo, R. (1997). p50-NF-kappaB complexes partially compensate for the absence of RelB: severely increased pathology in p50(-/-)relB(-/-) double-knockout mice. *J Exp Med* 185, 1359-1370.

Weiss, U., and Rajewsky, K. (1990). The repertoire of somatic antibody mutants accumulating in the memory compartment after primary immunization is restricted through affinity maturation and mirrors that expressed in the secondary response. *J Exp Med* 172, 1681-1689.

Wieacker, P., Zimmer, J., and Ropers, H. H. (1985). X inactivation patterns in two syndromes with probable X-linked dominant, male lethal inheritance. *Clin Genet* 28, 238-242.

Williams, B. R. (1991). Transcriptional regulation of interferon-stimulated genes. *Eur J Biochem* 200, 1-11.

Wilson, A., Day, L. M., Scollay, R., and Shortman, K. (1988). Subpopulations of mature murine thymocytes: properties of CD4-CD8+ and CD4+CD8- thymocytes lacking the heat-stable antigen. *Cell Immunol* 117, 312-326.

Wolfer, A., Bakker, T., Wilson, A., Nicolas, M., Ioannidis, V., Littman, D. R., Lee, P. P., Wilson, C. B., Held, W., MacDonald, H. R., and Radtke, F. (2001). Inactivation of Notch 1 in immature thymocytes does not perturb CD4 or CD8T cell development. *Nat Immunol* 2, 235-241.

Wu, A. J., Hua, H., Munson, S. H., and McDevitt, H. O. (2002). Tumor necrosis factor-alpha regulation of CD4+CD25+ T cell levels in NOD mice. *Proc Natl Acad Sci U S A* 99, 12287-12292.

Yamamoto, Y., and Gaynor, R. B. (2001). Role of the NF-kappaB pathway in the pathogenesis of human disease states. *Curr Mol Med* 1, 287-296.

Yamaoka, S., Courtois, G., Bessia, C., Whiteside, S. T., Weil, R., Agou, F., Kirk, H. E., Kay, R. J., and Israel, A. (1998). Complementation cloning of NEMO, a component of the IkappaB kinase complex essential for NF-kappaB activation. *Cell* 93, 1231-1240.

Yan, M., Brady, J. R., Chan, B., Lee, W. P., Hsu, B., Harless, S., Cancro, M., Grewal, I. S., and Dixit, V. M. (2001). Identification of a novel receptor for B lymphocyte stimulator that is mutated in a mouse strain with severe B cell deficiency. *Curr Biol* 11, 1547-1552.

Yokoyama, W. M., Koning, F., Kehn, P. J., Pereira, G. M., Stingl, G., Coligan, J. E., and Shevach, E. M. (1988). Characterization of a cell surface-expressed disulfide-linked dimer involved in murine T cell activation. *J Immunol* 141, 369-376.

Zandi, E., and Karin, M. (1999). Bridging the gap: composition, regulation, and physiological function of

the IkappaB kinase complex. *Mol Cell Biol* 19, 4547-4551.

Zhang, G., and Ghosh, S. (2000). Molecular mechanisms of NF-kappaB activation induced by bacterial lipopolysaccharide through Toll-like receptors. *J Endotoxin Res* 6, 453-457.

Zheng, Y., Ouaaz, F., Bruzzo, P., Singh, V., Gerondakis, S., and Beg, A. A. (2001). NF-kappa B RelA (p65) is essential for TNF-alpha-induced fas expression but dispensable for both TCR-induced expression and activation-induced cell death. *J Immunol* 166, 4949-4957.

Zhong, H., Voll, R. E., and Ghosh, S. (1998). Phosphorylation of NF-kappa B p65 by PKA stimulates transcriptional activity by promoting a novel bivalent interaction with the coactivator CBP/p300. *Mol Cell* 1, 661-671.

Zhou, C., Yang, Y., and Jong, A. Y. (1990). Mini-prep in ten minutes. *Biotechniques* 8, 172-173.

Zhou, D., Yu, T., Chen, G., Brown, S. A., Yu, Z., Mattson, M. P., and Thompson, J. S. (2001). Effects of NF-kappaB1 (p50) targeted gene disruption on ionizing radiation-induced NF-kappaB activation and TNFalpha, IL-1alpha, IL-1beta and IL-6 mRNA expression in vivo. Int J Radiat Biol 77, 763-772

Zhou, J., Zhang, J., Lichtenheld, M. G., and Meadows, G. G. (2002). A role for NF-kappa B activation in perforin expression of NK cells upon IL-2 receptor signaling. *J Immunol* 169, 1319-1325.

Zillikens, D., Mehringer, A., Lechner, W., and Burg, G. (1991). Hypo- and hyperpigmented areas in incontinentia pigmenti. Light and electron microscopic studies. *Am J Dermatopathol* 13, 57-62.

Zonana, J., Elder, M. E., Schneider, L. C., Orlow, S. J., Moss, C., Golabi, M., Shapira, S. K., Farndon, P. A., Wara, D. W., Emmal, S. A., and Ferguson, B. M. (2000). A novel X-linked disorder of immune deficiency and hypohidrotic ectodermal dysplasia is allelic to incontinentia pigmenti and due to mutations in IKK-gamma (NEMO). *Am J Hum Genet* 67, 1555-1562.

7 **ACKNOWLEDGEMENTS**

I would like to thank the people who contributed to this work.

First of all Manolis Pasparakis for teaching me a lot of things, for supervision, help and support during these years.

I thank Klaus Rajewsky for the opportunity to join his research group and for his supervision of my thesis in various ways. I am indebted to Gilles Courtois, Wilhelm Bloch, Yoshiteru Sasaki and Jane Tian for our collaborations and their help. Gilles Courtois provided rabbit serum against NEMO, various plasmids, invaluable informations, help, advice and enthusiasm. I wish to express my gratefulness to Tatiana Novobrantseva for help and advice.

I am grateful to Angela Egert and Anke Roth for blastocyst injections and mouse work, Brigitte Hampel for cutting sections, Claudia Uthoff-Hachenberg for performing ELISAs, Christoph Göttlinger for cell sorting, Simone Wilms for sequencing and Victoria Dreier for mouse work. I am indebted to Asmae Smahi, Christine Bodemer and Sylvie Fraitag for histological slides from skin sections of human IP patients and to Exelixis for sequencing part of the *Nemo* locus. I thank Charo Robles, Dominik Schenten and Kevin Otipoby for proof-reading parts of my thesis. I thank Teresa, Kristina, Thomas, Ari and Thorsten for helping with a beaurocratic problem. Thanks to Marat Alimzhanov for providing pEasyFlox.

Klaus Rajewsky, Jürgen Dohmen, Martin Scheffner and Ursula Lichtenberg agreed to form my thesis committee.

On a more personal note I would like to express my sincere gratitude to all the members of the Rajewsky laboratories in Köln and Boston for creating a friendly environment and for help in various ways. I acknowledge Chryssa, Dominik, Philipp, Thomas and others for being a great outgoing crowd and I acknowledge Flann O'Brien and various Spelunken in Cologne.

I thank my friends, Charito my love, I owe my family everything.

8 **VERSICHERUNG**

Ich versichere, daß ich die von mir vorgelegte Dissertation selbständig angefertigt, die benutzten Quellen und Hilfsmittel vollständig angegeben und die Stellen der Arbeit - einschließlich Tabellen, Karten und Abbildungen -, die anderen Werken im Wortlaut oder dem Sinn nach entnommen sind, in jedem Einzelfall als Entlehnung kenntlich gemacht habe; daß diese Dissertation noch keiner anderen Fakultät oder Universität zur Prüfung vorgelegen hat; daß sie - abgesehen von unten angegebenen Teilpublikationen - noch nicht veröffentlicht worden ist sowie, daß ich eine solche Veröffentlichung vor Abschluß des Promotionsverfahrens nicht vornehmen werde. Die Bestimmungen dieser Promotionsordnung sind mir bekannt. Die von mir vorgelegte Dissertation ist von Prof. Dr. Klaus Rajewsky betreut worden.

Köln, im Dezember 2001

Marc Schmidt-Supprian

Teilpublikationen:

Schmidt-Supprian M, Courtois G, Tian J, Israel A, Rajewsky K, Pasparakis M. Mature T cell development depends on signaling through the IKK complex; submitted

Pasparakis M*, Schmidt-Supprian M*, Rajewsky K (2002). IκB Kinase Signaling is Essential for Maintenance of Mature B Cells. *J Exp Med* 196(6), 743-752

*Equal contribution

Marc Schmidt-Supprian**,** Wilhelm Bloch, Gilles Courtois, Klaus Addicks, Alain Israel, Klaus Rajewsky, and Manolis Pasparakis (2000). NEMO/IKKγ-Deficient Mice Model Incontinentia Pigmenti. *Mol. Cell* 5, 981-992

9 LEBENSLAUF

Name:	Marc Schmidt-Supprian
Geburtsdatum:	06.07.1972
Geburtsort:	Rotterdam, Holland
Staatsangehörigkeit:	Deutsch
Familienstand:	Ledig

Schulbildung:

1979-1983	Grundschule Ottobrunn, München
1983-1986	Gymnasium Ottobrunn, München
1986-1992	Deutsche Schule Helsinki, Helsinki, Finnland
Mai 1992	Abitur

Studienverlauf:

Oktober 1992	Immatrikulation an der Universitaet Würzburg Studium der Chemie (Diplom)
September 1994	Diplom-Vorpruefung in Chemie
Oktober 1994 – Dezember 1998	Studium der Biochemie (Diplom) an der Universität Tübingen
April 1995	Diplom-Vorpruefung in Biochemie, Teil I
Oktober 1995	Diplom-Vorpruefung in Biochemie, Teil II
September 1996-September 1997	Studium der Biochemie und der Genetik am Trinity College Dublin, Irland B.A. (Mod.) Thesis: Factor V Leiden, prevalence and association with thrombotic diseases
Juni 1997	Bachelor of Arts, Trinity College Dublin, Ireland
März1998	Diplom-Hauptprüfung in Biochemie
Mai 1997 - Dezember 1998	Diplomarbeit: Universität Tübingen, St James's Hospital and Trinity College und Fraunhofer Institut Stuttgart "Protein C – Structure and anti-inflammatory mechanisms"

März 1999 - Dezember 2002	Doktorarbeit am Institut für Genetik Universität zu Köln
Mai 2001 -	Center for Blood Research, Harvard Medical School, Boston, USA